THE UNIVERSITY
of EDINBURGH

Redox regulation of plant *S*-nitrosylation

Tao-Ho Chang

Doctor of Philosophy

THE UNIVERSITY
of EDINBURGH

2016

Declaration

I hereby declare that the work presented here is my own and has not been submitted in any form for any degree at this or any other university. Any contribution made by other parties is clearly acknowledged.

Tao-Ho Chang

Abstract

Nitric oxide (NO), a diffusible gas molecule, is a major signal molecule in both plants and animals and regulates a plethora of biological processes. *S*-nitrosylation, a post-translation modification, is conducted by NO, which covalently attaches protein cysteine thiols and forms an *S*-nitroso thiol. *S*-nitrosylation plays an important role in plant development and plant immune systems. In *Arabidopsis thaliana, S*-nitrosoglutathione (GSNO) is the major NO donor for *S*-nitrosylation, and GSNO reductase (GSNOR) indirectly controls the *S*-nitrosylation level by turning over the GSNO. An *A. thaliana* T-DNA insertion mutant *gsnor1-3* shows the loss of GSNOR activity and increases the *S*-nitrosylation level, resulting in loss of apical dominance, reduction of SA accumulation, increased hypersensitive response (HR) cell death and reduced disease resistance against virulence, avirulence and non-host pathogens. Interestingly, loss of GSNOR in *Drosophila melanogaster*, an animal model system, reduces the resistance against gram-positive and fungal pathogens.

Catalase is an antioxidant enzyme and regulates the redox environment through scavenging the hydrogen peroxide (H_2O_2) to oxygen and water. Previous work in our lab had discovered two *gsnor1-3* suppressor mutants, *gsnor1-3 spl7* and *gsnor1-3 spl8*, which restore the loss of apical dominance and partially restore disease resistance. These two suppressor mutants were then identified as the point mutation in *CAT3*. *CAT3*, one of the three *CAT* genes in *Arabidopsis*, expresses catalase specifically in vascular tissues. To further extend the suppression of *cat3* in *gsnor1-3*, the mutations in *CAT3* and its paralogs *CAT2* and *CAT1*, as well as other redox-related genes in *gsnor1-3* background, were generated. In the developmental phenotype, only the *gsnor1-3 cat3* showed significant changes compared with *gsnor1-3*. The disease susceptibility and HR cell death in *gsnor1-3 cat3* were less than *gsnor1-3* and similar to wild-type. Moreover, the redox-related genes and *CAT3* paralog mutations in

gsnor1-3 background showed no significant changes in disease resistance against virulence pathogen compared with *gsnor1-3* plant. Meanwhile, an SA-dependent (salicylic acid) defence-related gene (*PR1*, pathogenesis-related gene 1) showed the early expression in *gsnor1-3 cat3* plant compared with *gsnor1-3* plant. Results of developmental and disease-related phenotypes suggest the suppression effects which turn-over the malfunction in *gsnor1-3* are highly specific to *CAT3*.

The previous report demonstrates that the hydroxyl radical, a reactive oxygen species by-product from H_2O_2, decomposes GSNO to oxidised glutathione *in vitro*. The interaction of GSNO and hydroxyl radical may be the possible mechanism of how *cat3* suppresses *gsnor1-3*. Therefore, we speculated less amount of GSNO in *gsnor1-3 cat3* plant than in *gsnor1-3* plant and lower level of hydroxyl radicals in *gsnor1-3 cat3* plant than in *cat3* plant. To evaluate our hypothesis, the content hydroxyl and GSNO were analysed in wild-type, *gsnor1-3, cat3* and *gsnor1-3 cat3* plants. The total *S*-nitrosylated protein, which indicates the GSNO content *in vivo*, was less in *gsnor1-3 cat3* than in *gsnor1-3*. Furthermore, the level of hydroxyl radical in *gsnor1-3 cat3* was lower than *cat3*. Accordingly, the reduction of hydroxyl radical in *gsnor1-3 cat3* may occur due to the reaction with GSNO and vice versa.

Similar to what has been found in *Arabidopsis*, *D. melanogaster* also reported partial restoration of the immunodeficiency phenotypes of *gsnor* knock-out flies with an additional mutation in *CAT* gene. Interestingly, the content of hydroxyl radical in $gsnor^{-/-}$ $cat^{-/-}$ line was less than $cat^{+/-}$. Collectively, our results suggest an interaction of hydroxyl radical and GSNO may happen both in *Arabidopsis* and *Drosophila*. Further research is needed to clarify the interaction between hydroxyl radical and GSNO in *Arabidopsis* as well as in *Drosophila*.

Lay summary

S-nitrosylation is an important protein modification and regulates most of the biological processes including development and immune system. A mutation of *GSNOR1* (*S*-nitrosoglutathione (GSNO) reductase, *gsnor1-3*) in the model plant *Arabidopsis thaliana* increases the cellular *S*-nitrosylation by regulating the level of GSNO, a NO donor for *S*-nitrosylation. The *gsnor1-3* plant has shown a loss of apical dominance and a reduction in pathogen resistance. Interestingly, the absence of *CAT3* (catalase 3) in *gsnor1-3* background suppresses the development and disease resistance of *gsnor1-3*. *CAT3* expresses a redox-related enzyme catalase which scavenges H_2O_2. Thus, mutations in redox-related genes and *CAT3* paralogs were introduced in *gsnor1-3* background to investigate other candidates in the regulation of *S*-nitrosylation. However, the *cat3* mutation was the only mutation that significantly turns over the developmental and disease-related phenotype in *gsnor1-3* background. The results suggest the suppression of excessive *S*-nitrosylation is highly specific to *CAT3*. Previous research had suggested GSNO decomposes by the H_2O_2 by-product, hydroxyl radical, *in vitro*. We hypothesise the mechanism that *cat3* suppresses *gsnor1-3* may be the cause of the interaction of GSNO and hydroxyl radical. As we speculated, the content of GSNO and hydroxyl radical in *gsnor1-3 cat3* were lower than in *gsnor1-3* plant and in *cat3* plant, respectively. The results confirmed that the interaction of GSNO and hydroxyl radical might lead to regulation of *S*-nitrosylation. Similar to what have found in *Arabidopsis*, *Drosophila. melanogaster* also reported *CAT* mutation restores the disease resistance of *GSNOR* knock-out mutant. The level of hydroxyl radical in the *gsnor cat* double mutant was also lower than in the *cat* mutant. Collectively, our results suggest the interaction of GSNO and hydroxyl radical may be the mechanism of how missing *cat* suppresses excessive *S*-nitrosylation. Our work gives a new insight of *S*-nitrosylation regulation across kingdoms, but more research is needed to uncover the mechanism fully.

Acknowledgement

I would like to thank my family for supporting my PhD life here in Edinburgh; it was a fantastic adventure for me to accomplish this PhD, and their support was invaluable.

Special thanks must also made to my supervisor Prof. Gary Loake for providing many valuable suggestions about my PhD project. Many thanks to Dr. Colin Campbell and Dr. Mark Miller for their advice and help with biochemistry equipment.

I would also like to thank the people who were formerly involved in this project; Kirsti Sorhagen isolated the suppressor mutants for the start of this project, as well as Kerstin Brezezek, Adil Hussain and Rafael Augusto Homem who all provided a well-established foundation for me to continue the project.

Thanks to my colleagues in Loake Lab for having a friendly and delightful work environment. Special thanks to Nurun Nahar Fancy for her generous help and creative ideas.

Lastly, I would like to thank all my friends in Edinburgh, especially those I met from volleyball (Big thanks to Dr. Scott Stetkiewicz). I will never forget the amazing experiences as an EUVC volleyball player in Scotland.

Rice, Tao-Ho Chang

Contents

List of figures

Abbreviations

3-AT	3-Amino-1,2,4-triazole
4-POBN	α-(4-Pyridyl N-oxide)-N-tert-butylnitrone
ABA	Abscisic acid
AFB	Auxin signalling F-box
ANP1	MAP kinase kinase kinase 1
APS	Ammonium persulfate
APX	Ascorbate peroxidase
ARF-GEF	ADP ribosylation factor hydrolyzing guanidine triphosphate
ASK1	Arabidopsis SKP1
Avr	Avirulence factor
BCA	Bicinchoninic acid assay for protein concentration
Bgt	*Blumeria graminis* f. sp. *tritici*
Biotin–HPDP	N-[6-(biotinamido)hexyl]-3'-(2'-pyridyldithio) propionamide
BSA	Bovine serum albumin
BST	Biotin-switch technique
CAB2	Chlorophyll binding protein 2
CaM	Calmaldulin
CAT	Catalase
CBP60g	CaM binding protein
CC	Coiled coil
cDNA	Complementary DNA
CFU	Colony forming unit
CK	Cytokinin
CMV	*Cucumber mosaic virus*
COI1	Coronatine-insensitive protein 1
CPK	Calcium-dependent protein kinase
CTAB	Cetyltrimethylammonium bromide
Cys	Cysteine
CysNO	*S*-nitrosocysteine
CUL	Cullin, component of ubiquitin E3 ligase
DEPC	Diethylpyrocarbonate

E2	Ubiquitin-conjugating enzyme
EDS1	Enhanced Disease Susceptibility 1
EMS	Ethyl methane sulfonate
EDTA	Ethylenediaminetetraacetic acid
eNOS	endothelial NOS
EPR	Electron paramagnetic resonance
ET	Ethylene
ETI	Effector triggered immunity
ETS	Effector triggered susceptibility
FIT	FER-like iron deficiency induced transcription factor
Foc	*Fusarium oxysporum* f. sp. *cicero*
FRO2	Ferric-chelate reductase oxidase
GAPDH	Glyceraldehyde 3-phosphate dehydrogenase
GPX	Glutathione peroxidase
GSH	Reduced glutathione
GSNO	*S*-nitrosoglutathione
GSNHOH	Glutathione *S*-hydroxysulfenamide
GSNOR	GSNO reductase
GSSG	Oxidised glutathione
GUS	β-glucosidase
Hb	Haemoglobin
HDA	Histone deacetylase
HEN	Buffer contains HEPES, EDTA, Neocuproine
HEPES	4-(2-hydroxyethyl)-1-piperazineethanesulfonic acid
HopM	Hrp-dependent outer protein
HR	Hypersensitive response
ICS1	Isochorismate synthase 1
iNOS	Inducible NOS
IRT1	Iron-regulated transporter
JA	Jasmonic acid
JA-Ile	Jasmonoyl-isoleucine
JAZ	Jasmonate-ZIM domain
LB	Lysogeny broth medium
LC-MS	Liquid chromatography mass spectrometry

LOL1	LSD-One-Like 1
LRR	Leucine rich repeat
LSD1	Lesions simulating disease 1
MAMP	Microbe associate molecular pattern
MAPK	Mitogen-activated protein kinase
MALDI-TOF	matrix assisted laser desorption ionization-time of flight
MC	Metacaspase
MED25	Mediator 25
Me-JA	Methyl JA
MIN7	HopM interactor 7
MOS	Modifier of *snc1*
MS	Murashige and Skoog medium
MYC2	bHLH zip transcription factor
NADPH	Reduced nicotinamide adenine dinucleotide phosphate
NB	Nucleotide binding site
NEM	*N*-Ethylmaleimide
NINJA	Novel interactor of JAZ
nNOS	Neuronal NOS
NO	Nitric oxide
NOA1	Nitric oxide associated 1
NOS	NO synthase
NOX	NADPH oxidase
NPR1	Non-expressor of *PR* gene 1
NR	Nitrate reductase
OxyR	Hydrogen peroxide inducible gene activator
pad2	Phytoalexin deficiency 2
PAL	Phenylalanine ammonia lyase
PAMP	Pathogen associate molecular pattern
PBS	Phosphate-buffered saline
PBST	PBS contains TWEEN®20
PCD	Programme cell death
PCR	Polymerase chain reaction
PR	Pathogenicity related protein
PRR	Membrane-anchored pattern recognition receptors

Prx	Peroxidase
PSH	Persephone
PS	Plastid photosystem
Pst	*Pseudomonas syringae* pv. *tomato*
PTI	PAMP-triggered immunity
R	Resistant factor
RbohD	NADPH oxidase
RBX	RING-H2 protein
RIN	RPM1 interaction protein
RNI	Reactive nitrogen intermediates
ROS	Reactive oxygen species
RPM1	Resistance to *Pst* 1 protein
RT-PCR	Reverse transcription polymerase chain reaction
SA	Salicylic acid
SCF	Complex of SKP1, CUL1 and F-box promoter
SDS-PAGE	Sodium dodecyl sulfate polyacrylamide gel electrophoresis
Ser	Serine
Siah1	Seven in Absentia Homolog 1, E3 Ubiquitin-Protein Ligase
SKP1	S-phase kinase-associated protein 1
SNC1	Suppressor of *npr1-1* constitutive1
SNI1	Suppressor of *npr1-1* inducible 1
SNO	*S*-nitrosothiol
SOD	Superoxide dismutase
SPE	Spatzle-Processing Enzyme
spl	SNO plough
T-DNA	Transfer DNA
TCA	Trichloroacetic acid
TIR	Toll/mammalian interleukin-1 receptors
TOC1	Timing of CAB2 1
TPL	Topless protein
TRX	Thioredoxin
TTSS	Type three secretion system
VPE	Vacuolar processing enzyme
vtc	Vitamin C mutant

XOR	Xanthine oxidoreductase

Chapter-1 Introduction

1.1 Plant immunity

1.1.1 Overview

Plants have evolved a defence system which immediately reacts with constantly present microbes or pathogens. In order to successfully colonise in plants, a pathogen needs to go through a physical barrier such as the waxy leaf surface or rigid cell wall. While breaking through these structural defences, the pathogen's microbe- or pathogen- associated molecular pattern (MAMP or PAMP) is then recognised by the membrane-anchored pattern recognition receptors (PRRs). The MAMPs/PAMPs are consistent epitopes from pathogen molecules such as flagellins, chitin or other polysaccharides (Bent and Mackey, 2007). The interaction of MAMPs/PAMPs and PRR activates a pattern-triggered immune response (PTI). This reaction provides broad spectrum protection against whole classes of pathogens including the generation of oxidative burst, the alteration of signal transduction and the activation of defence-related genes (Moore et al., 2011). However, some pathogens have evolved to stop or avoid the PTI by secreting effectors or avirulence (Avr) proteins (Bardoel et al., 2011). The basal defences of PTI in the plant are then inadequate to prevent further progress of the disease. Additionally, plants have developed resistance (R) proteins to recognise the Avr proteins or effectors from their pathogens, activating the effector-triggered immune (ETI) responses (Jones and Dangl, 2006). Pathogens counteract the ETI responses by losing their Avr proteins to avoid R protein recognition or acquiring another effector to suppress the immune responses. As more studies accumulate, the zigzag model (Fig. 1.1) has now been proposed to address the

ongoing coevolution of plant-pathogen interactions (Jones and Dangl, 2006). More details will be described in the following paragraphs.

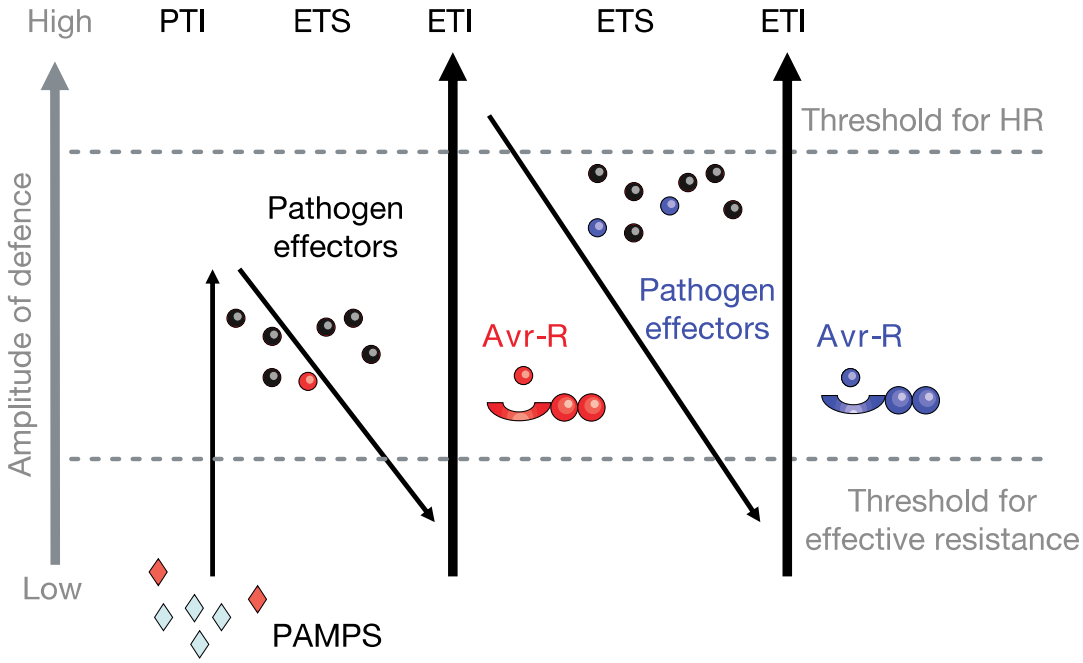

Figure 1.1. Zigzag model of the plant immune system.
In phase 1, plants detect MAMPs/ PAMPs (red diamonds) via PRRs to trigger PAMP-triggered immunity (PTI). In phase 2, pathogens deliver effectors that interfere with PTI resulting in effector-triggered susceptibility (ETS). In phase 3, one effector (red) is recognised by Resistance (R) protein activating effector-triggered immunity (ETI), an amplified version of PTI. In phase 4, pathogen gains new effectors through horizontal gene flow (blue) and suppress ETI. (Jones and Dangl, 2006).

1.1.2 Plant immune system: *Arabidopsis-Pseudomonas* pathosystem

The interaction between *Pseudomonas syringae* pv. *tomato* (*Pst*) and their host plant *Arabidopsis thaliana* is a model for plant-pathogen interactions (Katagiri et al., 2002). Following the zigzag model (Fig. 1.1), the conserved domain 22-amino-acid peptide (flg22) of *Pst* flagellin can bind to *Arabidopsis* leucine rich repeat (LRR) protein kinase FLS2 and induces PAMP-triggered immunity (PTI) which activates at least 1100 *Arabidopsis* genes in the first phase of a given plant-pathogen interaction (Zipfel et al., 2004). PAMP-triggered

immunity (PTI) induces mitogen-activated protein kinase (MAPK) cascades (MAPKKK, MAPKK, MAPK) and results in transcriptional activation of defence genes by specific transcription factors such as members of the WRKY superfamily (Panstruga et al., 2009). The first layer of defence relies on the exocytosis pathway to transport the defence-related proteins including pathogen-related protein 1 (PR1) and small molecules to the apoplast (Van Loon and Van Strien, 1999). Another defence in PTI stage is the production of the reactive oxygen species (ROS) by membrane-localised NADPH oxidases (RbohD) (Torres and Dangl, 2005).

The second phase of the zigzag model predicts pathogen driven effector-triggered susceptibility (ETS) (Fig. 1.1). The type III secretion systems (TTSS) help gram-negative phytopathogens deliver around 15-30 effectors into the plant cytosol (Collmer et al., 2002). Effectors like *Pst* HopM target ADP ribosylation factor hydrolyzing guanidine triphosphate (ARF-GEF) protein which are involved in cell vesicle trafficking. HopM binds to MIN7 (HopM interactor 7, an ARF-GEF protein) of *Arabidopsis* leading to ubiquitination-dependent proteolysis of MIN7 and consequently blocks the movement of immune-related compounds to apoplast or cell membrane (Nomura et al., 2006). Effectors like AvrPto or AvrPtoB contribute to *Pst* virulence by inhibiting the early step of the MAPK cascade kinase, MAPKKK. Interestingly, the *Pst* effector AvrPtoB C-terminal domain folds into an active E3 ligase and suggests its function is involved in host protein degradation (Göhre et al., 2008). *Pst* also can also produce small molecule effectors such as coronatine, a jasmonic acid mimic, which suppresses salicylic-acid-dependent defence against biotrophic pathogens (Katagiri et al., 2002). These effectors can help pathogens to overcome the host plants PTI.

However, these effectors which overcome PTI can be recognised by specific disease resistance (*R*) genes. The plant *R* genes encode R proteins which detect pathogen effectors directly or indirectly (Jones and Dangl, 2006). The recognition of effectors by R proteins triggers the third phase of the zigzag model, effector-triggered immunity (ETI). Like PTI, ETI

induces reactive species production and defence gene activation and is normally accompanied by host programmed cell death (PCD) at the site of attempted invasion (Mur et al., 2008). These R proteins normally contain a central nucleotide binding site (NB) and a C-terminal leucine rich repeat (LRR) domain (Panstruga et al., 2009). Based on the structure of the N-terminal domain, the NB-LRR proteins can be divided into two groups (Panstruga et al., 2009). Two of the N-terminal domain structures are a putative coiled coil (CC) and a *Drosophila* Toll/mammalian interleukin-1 receptors (TIR) domain. *A. thaliana* CC-NB-LRR R protein RPM1 (Resistance to *Pst* 1) interacts and recognises *Pst* effector AvrB and AvrRpm1 through RPM1 interaction protein 4 (RIN4). RIN4 is a protein which guards the interaction between pathogen effectors and host plant R protein (Abramovitch et al., 2006). RIN4 activates the RPM1 R protein through phosphorylation which is induced by AvrB and AvrRpm1. Consequently, the activated RPM1 protein induces the downstream defence responses like hypersensitive response (HR) cell death (Mackey et al., 2002).

1.1.3 Signalling in plant immunity

Plant hormones are key signals involved in the plant immune system. The major defence related hormones are salicylic acid (SA) and jasmonic acid (JA) (Denancé, 2013). With the growing research on plant defence responses, other hormones such as ethylene (ET) (Berrocal-Lobo and Molina, 2004), abscisic acid (ABA) (Ton et al., 2009), cytokinins (CK) (Choi et al., 2011) and auxins (Kidd et al., 2011) have also been implicated in the plant immune system. These plant hormones enable antagonistic or synergistic cross talk between each hormone.

The SA signalling pathway regulates the defence response normally against biotrophic or hemibiotrophic pathogens. Through pathogen *Pseudomonas syringae* DC3000 challenge with *A. thaliana*, the shikimate pathway which is related to SA synthesis in plants is strongly induced (Truman et al., 2006). In *Pseudomonas-Arabidopsis* interaction, chorismate from the

pathway is then synthesised to SA by Isochorismate synthase 1 (ICS1) (Seyfferth and Tsuda, 2014). As an important signalling molecule, SA induces a complex genetic regulatory network which is related to plant defences (Fig 1.2) (Vlot et al., 2009). Accumulation of SA during pathogen challenge has been reported to induce MAPK cascades which are key to signal transduction (Zhang and Klessig, 2001). Ca^{2+} and calmaldulin (CaM) regulate SA-dependent gene expression through various processes (Buchanan Wollaston et al., 2005). Transcription factor SR1 binds Ca^{2+}/CaM and represses the expression of *EDS1* (Enhanced Disease Susceptibility 1) which is required for SA accumulation during ETI (Du et al., 2009). The combination of CaM and CaM binding protein (CBP60g) increases SA accumulation and plant pathogen resistance (Wan et al., 2012).

Nonexpressor of PR (pathogenesis-related) gene 1 (NPR1) plays a central role in SA signalling gene expression (Dong, 2004). NPR1 is a transcriptional coactivator of many *PR* genes expression (Pieterse and Van Loon, 2004). NPR1 is chiefly present as an oligomer in the cytosol, while SA induces redox changes and leads to NPR1 oligomer monomerization and the subsequent transfer of the NPR1 monomer into the nucleus (Tada et al., 2008). The NPR1 monomer then interacts with TGA transcription factors and enhances the SA-dependent defence genes expression (Gatz, 2013). The fine tuning of NPR1 induction of disease resistance genes is regulated by SA accumulation and cooperation with NPR3 and NPR4 (Fu et al., 2012). NPR3 and NPR4 are Cullin ubiquitin E3 ligase (CUL3) adaptors that lead the NPR1 degradation (Fu et al., 2012). A high concentration of SA induces the NPR3-NPR1 interaction and results in NPR1 degradation. Meanwhile, an intermediate level of SA disrupts the NPR4-NPR1 interaction and results in NPR1 accumulation (Fu et al., 2012).

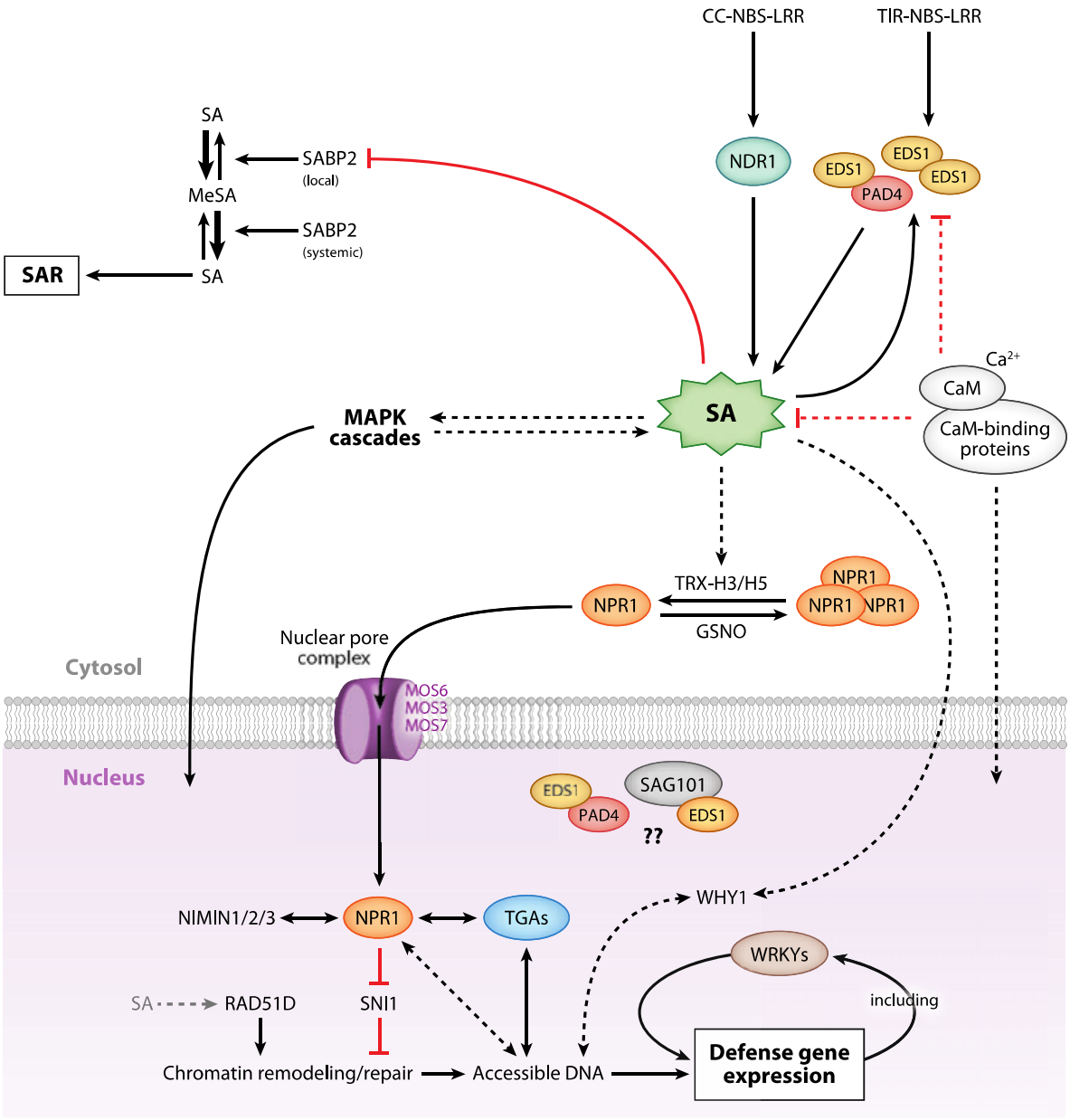

Figure 1.2. An overview of SA signaling in disease resistance.
Arrows demonstrate enzyme activation, the induction of compounds or gene expression and the compound passage from cytosol to nucleus. Double-headed arrows indicate physical protein-protein or protein-DNA interactions. Red lines indicate the inhibition of enzyme activity or the accumulation of compounds. Solid lines indicate established interactions; dashed lines represent hypothesized or less well characterized interactions. The grey dashed line indicates a direct or indirect activation of RAD51D, a DNA repair protein, by SA (Vlot et al., 2009). EDS1: enhanced disease susceptibility protein 1; PAD4: phytoalexin deficient 4; NDR1: nonspecific disease resistance 1; MOS: modifier of *snc1* (suppressor of *npr1-1* constitutive1); NPR1; non-expressor of pathogenesis-related gene 1; TRX: thioredoxins; CaM: calmodulin; SABP: SA-binding protein; SNI1: suppressor of *npr1-1* inducible 1.

The JA signalling pathway, on the other hand, induces the defence response against necrotrophic and insect herbivores. JA is synthesised through the oxylipin synthetic pathway (Kombrink, 2012). In normal status, JA is metabolised to stable conjugates such as methyl JA (Me-JA) (Seo et al., 2001) and bioactive jasmonoyl-isoleucine (JA-Ile) (Fonseca et al., 2009). Attempted infection by necrotrophic pathogens or insect herbivores will induce the accumulation of JA and result in defence signal transduction (Wasternack and Parthier, 1997). JA-induced gene expression is regulated by a JAZ-COI1 complex and the regulation mechanism is illustrated in Fig. 1.3 (Wasternack and Hause, 2013). During the resting state, the transcription factor MYC2 which binds the G-box of JA-dependent gene promoters is repressed by ZIM domain proteins (JAZs) (Chini et al., 2009). The JAZ co-repressor, novel interactor of JAZ (NINJA), links JAZ proteins to the repression of transcription through histone deacetylase 6 (HDA6) and HDA9 with the interaction of topless (TPL) (Pauwels et al., 2010). In the course of JA signal transduction, JAZs are then recruited by COI1 which combine with the SCF complex and result in the degradation of JAZs (Santner and Estelle, 2010). Following the degradation of JAZ proteins, MYC2 can cooperate with MED25 and drive the transcription of the JA-dependent gene expression including the synthesis of JAZ and MYC2 (Chen et al., 2012).

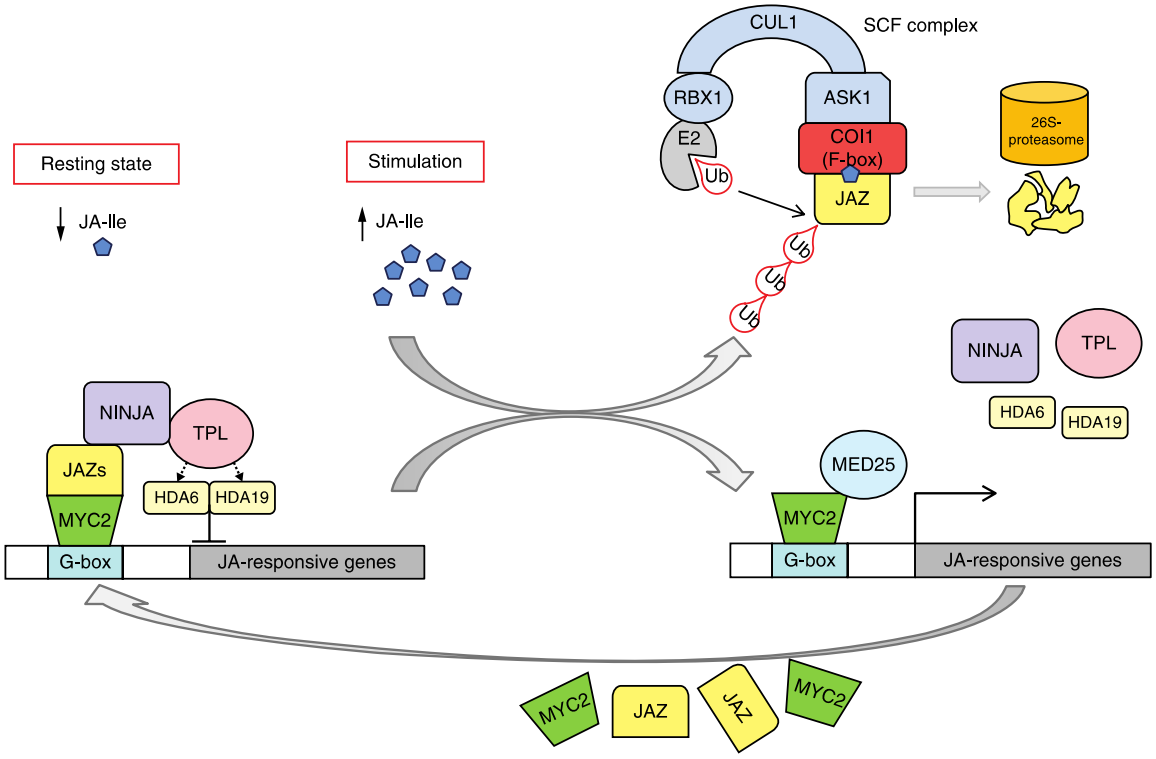

Figure 1.3. Scheme of Jasmonic acid (JA) signalling via the COI1–JAZ co-receptor complex.
In the resting state (low JA-Ile level), the complex of MYC2 and JAZ binds to a G-box in the promoter of JA-responsive genes. Novel Interactor of JAZ (NINJA) binds to JA and recruits TOPLESS (TPL) which represses transcription via HISTONE DEACETYLASE 6 (HDA6) and HDA19. Following an increase in JA-Ile levels, JAZ proteins are recruited by COI1 and subjected to ubiquitinylation and subsequent degradation by the 26S proteasome. Subsequently, MYC2 can activate transcription of early JA-responsive genes, mediated by the subunit 25 of mediator complex (MED25). ASK1: *Arabidopsis* SKP1 (S-phase kinase-associated protein 1) homologue; CUL: CULLIN, a component of E3 ubiquitin ligase; E2: ubiquitin-conjugating enzyme; MYC2: bHLHzip transcription factor; RBX: RING-H2 protein; SCF-complex: complex consisting of SKP1, CUL1 and F-box protein (COI1); Ub, ubiquitin; JAZ: JASMONATE-ZIM domain; MED25: mediator 25 (Wasternack and Hause, 2013).

SA suppresses the JA-dependent genes *PDF1.2* and *VPS2*, and this suppression can occur even after the engagement of JA-responsive gene expression (Leon-Reyes et al., 2009). SA-JA cross talk had been reported and showed most of SA-JA interactions are antagonized, while there are few examples showing a neutral or synergetic effect (Mur et al., 2006b). The SA-JA cross talk is regulated by multiple proteins such as transcription factors, redox regulators and MAPK proteins (Pieterse et al., 2012). SA is involved in transcription factor NPR1 monomerization and the NPR1 monomer in the cytosol inhibits the JA signalling pathway

(Pieterse et al., 2012). The SA-dependent signalling pathway accompanies the induction of the redox regulator peptide glutathione while JA decreases the amount of GSH (Spoel and Loake, 2011). SA increases GSH and suppresses the JA signalling pathway, suggesting the redox status alteration of the SA pathway is important in regulating JA-dependent gene expression (Koornneef et al., 2008). JA-SA cross talk also occurs at the level of MAPK cascades where *Arabidopsis* MAP Kinase 4 (MAPK4) serves as a negative regulator of the SA pathway but a positive regulator of JA pathway (Petersen et al., 2000).

1.1.4 Hypersensitive response

Plant cell death is one of the most important phenotypes in plant interactions with their pathogens. The role of cell death in plant immunity remains vague. The study of cell death at the molecular level was first undertaken in animals, and the types of cell death are classified into four types: apoptosis, autophagy, cornification and necrosis (Kroemer et al., 2008). This classification of cell death is based on morphological appearance, enzymological criteria, functional aspects or immunological characteristics. Like animal cells, plant cells also have similar types of cell death such as programmed cell death. Van Doorn et al. (2011) categorised plant programmed cell death (PCD) into two types: vacuolar cell death and necrosis, based on their morphological criteria. The phenomenon of vacuolar cell death often occurs with a decrease in the volume of the cytoplasm and an increase in the volume of the lytic vacuole (Filonova et al., 2000). Separately, the phenomenon of necrosis always comes with protoplast shrinkage and dysfunction of the cell organelles (Heath, 2000).

In plant-pathogen interactions, PCD is related to plant host resistance or susceptibility against their pathogens. HR cell death is one of the phenomena of PCD during the ETI responses which is induced by plant R proteins (Coll et al., 2011). The occurrence of HR cell death is thought to be a strategy to limit the nutrient supply for biotrophic pathogens. In the

early phase of HR, *Arabidopsis* has been reported to increase the cytosolic Ca^{2+} which is related to ETI responses (Levine et al., 1996). In the later stage, chloroplasts mediate many important defence signals including contributing to the production of the plant hormones JA and SA, reactive oxygen species (ROS) and reactive nitrogen oxide intermediates (RNI) (Delledonne et al., 2001). These defence signals are required for the activation of HR response in ETI responses and some of the molecules are also the signals related to PTI responses (Coll et al., 2011). The overlap of signal transduction in PTI and ETI suggest the fine-tuning of defence responses (Coll et al., 2011). Beside JA-SA cross talk, a balance between ROS and RNI is thought to be required for HR cell death (Delledonne et al., 2001).

VPE (vacuolar processing enzyme) is thought to be an important component of cell death responses (Hara-Nishimura et al., 1991). Overexpressing the vacuolar γ-VPE in *Arabidopsis* increases ion leakage that relates to HR cell death (Rojo et al., 2004). Plant metacaspase is a protease related to caspase proteases in animals and its function is linked to cell death (Vercammen et al., 2004). In *Arabidopsis*, an N-terminal zinc finger domain in the type I metacaspase (AtMC1-3) interacts with LSD1 (lesions simulating disease 1) which is required in HR cell death responses (Coll et al., 2010). *Arabidopsis* LSD1 is a nucleocytoplasmic shuttling transcription factor which was discovered by a forward screen for cell phenotypes; plants containing mutations in LSD1 exhibit a runaway cell death trait (Aviv et al., 2002). LSD1 has three LSD1-like zinc finger motifs which operate in protein-protein interactions (Coll et al., 2011). In yeast-two hybrid studies, LSD1 physically interacts with catalase *in vitro* (Li et al., 2013). LSD1 also up-regulates Cu/Zn superoxidase (SOD) which directly detoxifies superoxide during attempted pathogen infection (Kliebenstein et al., 2007). LSD1 also interacts with and suppresses the transcription factor LSD-One-Like 1 (LOL1) and AtbZIP10 which are enhancers of HR related gene expression (Kaminaka et al., 2006). Other than transcription

factors, a double mutant of the ROS generating NADPH oxidases, *AtRbohD* and *AtRbohF* also shows less HR (Torres et al., 2002).

1.2 Reactive oxygen species

1.2.1 Overview

Aerobic metabolic processes such as respiration and photosynthesis induce the production of reactive oxygen species (ROS) in various cell organelles (Apel and Hirt, 2004). These ROS are mostly toxic to the cell due to the impact on its redox capacity and cause damage to different molecules such as proteins, DNA and lipids. Plants have evolved both nonenzymatic and enzymatic strategies to detoxify these ROS which are constantly produced during the ground state of metabolic activities. However, ROS have also been found to function as signal molecules during plant development and the plant responses to biotic and abiotic stresses (Suzuki et al., 2012).

Moreover, drastic redox environment changes arise during a pathogen challenge as a result of the accumulation of ROS (Yu et al., 2012). The oxidative burst triggered by attempted microbial infection is one of the most rapid responses during plant-pathogen interactions (Apostol et al., 1989). The first report of the oxidative burst was found on a potato tuber inoculated with an avirulent strain of *Phytophthora infestans* (Doke, 1985). In the *Arabidopsis-Pseudomonas* pathosystem, the recognition of *Pst* AvrB protein with *Arabidopsis*'s R protein triggers the oxidative burst generated chiefly by the NADPH oxidase RbohD which generates superoxide (Panstruga et al., 2009). Besides the pathogen invasion, wounding caused by herbivore insect feeding also induces ROS generation in plants (Maffei et al., 2007). For

example, Lima beans have shown higher production of H_2O_2 after insect infestation (Maffei and Bossi, 2006).

Plant cells rapidly and simultaneously produce and scavenge various forms of ROS to maintain redox homeostasis (Mittler et al., 2011). ROS signals are tightly controlled over the subcellular location of the cell, making the accumulation of ROS highly specific. For example, oscillating ROS signals in *Arabidopsis* root hairs have demonstrated that the activation and production of ROS are located at the growth point of the root hair (Monshausen et al., 2007; Takeda et al., 2008). Further, ROS can be employed as rapid long distance signals throughout the plant. Since each cell has an ROS production mechanism, ROS-triggered ROS generation can travel over a long distance. Recent research suggests that ROS signals can propagate at the rate of up to 8.4 cm/min in *Arabidopsis* (Miller et al., 2009). Lastly, various forms of ROS have specific properties which makes their signal network diversified. For example, superoxide, a charged oxygen molecule, is unable to transfer across membranes; however, it can easily convert into H_2O_2 and cross the membrane through an aquaporin (Miller et al., 2010).

1.2.2 Regulation of ROS in plants

ROS are byproducts continuously generated by various metabolic pathways which are located in different organelles (Suzuki et al., 2012). ROS originate from the triplet molecular oxygen with serial energy transfer or electron transfer reactions (Fig. 1.4) (Apel and Hirt, 2004). Energy transfer leads to the formation of singlet oxygen while electron transfer forms superoxide, H_2O_2 and the hydroxyl radical (Klotz, 2002). In plants, H_2O_2 is relatively stable with a cellular half-life of 1 ms while other ROS like superoxide have half-lives of 2 to 4 µs (Gechev et al., 2006). There are more than 289 genes related to the production and scavenging of ROS (Gechev et al., 2006).

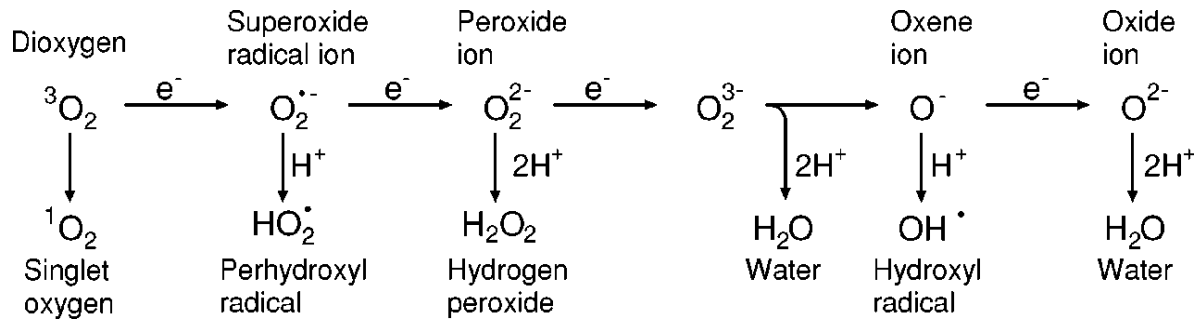

Figure 1.4. Generation of different ROS by energy transfer or sequential univalent reduction of ground state triplet oxygen (Apel and Hirt, 2004).

In the plant cell, various organelles are involved in ROS production and scavenging. The chloroplast is the major site of ROS generation. In the chloroplast, singlet oxygen is produced in plastid photosystem II (PSII, P680), while superoxide anion synthesis occurs through PSI (Asada, 2006). Besides the chloroplast, the peroxisome is also an important site generating ROS during photorespiration and fatty acid oxidation (del Río et al., 2006). The ROS in mitochondria are thought to regulate stress responses, PCD and other cellular processes (Robson and Vanlerberghe, 2002). In the apoplast, ROS generation induces cellular oxidative burst which consequently results in PCD (Gechev et al., 2006; Torres et al., 2002).

Plants have evolved a protective system that largely prevents damage from ROS through various enzymes or small redox molecules. The enzymatic mechanisms to detoxify ROS include superoxide dismutase (SOD), ascorbate peroxidase (APX), glutathione peroxidase (GPX), and catalase (CAT). SOD dismutates superoxide to H_2O_2 and is the front line of defence against ROS (Apel and Hirt, 2004). APX, GPX and CAT function as scavengers of H_2O_2. In contrast to CAT, APX and GPX require the presence of ascorbate, glutathione and their cycling system to reduce H_2O_2 to H_2O (Dat et al., 2000). Ascorbate and glutathione are two major redox buffers which help maintain cell redox homoeostasis (Noctor and Foyer, 1998). Besides the two major redox buffers, molecules such as tocopherol, flavonoids, alkaloids and

carotenoids also have antioxidant ability that can regulate the level of ROS in the cell (Apel and Hirt, 2004).

1.2.3 ROS signalling

Engagement of the oxidative burst triggers downstream immune activity. Besides the toxic properties of ROS against pathogens, ROS also function as important signal molecules which are sensed by various signal pathways (Fig 1.5).

In prokaryotes and fungi, two-component histidine kinases serve as sensors for ROS signals from outside of the cell (Apel and Hirt, 2004). The two-component systems include a transmembrane kinase which autophosphorylates a histidine residue while sensing the environment stimulus. The phosphate group is transferred from histidine to an aspartate residue and triggers a conformation change of the response regulator which drives DNA binding and gene expression. A range of two-component histidine kinases has been found in plants (Hwang et al., 2002).

Rice and *Arabidopsis* DNA sequence analysis reveals remarkable complexity in MAPK signalling: there are more than 100 MAPK, MAPKK and MAPKKK genes involved in these signal pathways (Apel and Hirt, 2004). In *Arabidopsis*, H_2O_2 activates the MAPKs, MAPK3 and MAPK6 through a MPKKK, ANP1 (Kovtun et al., 2000). Constitutively expressing the tobacco ANP1 orthologue, NPK1 enhanced the tolerance to broadly oxidative stresses such as heat, drought, and cold (Kovtun et al., 2000). H_2O_2 also increases the expression of nucleoside diphosphate kinase 2 (NDPK2) which mediates a MAPK cascade during abiotic stresses such as cold and salt (Moon et al., 2003). These strands of evidence suggest that ROS-mediated MAPK cascades are important in responses to multiple stresses.

H_2O_2 is a moderate ROS which is less active compared with other ROS and it can modify proteins through oxidation of thiol groups. In *Arabidopsis*, a protein tyrosine phosphatase (PTP)

activates MPK6 and is reversibly inactivated via oxidation by H_2O_2 (Gupta and Luan, 2003). Besides the phosphatase, direct modification of transcription factors has been reported in prokaryotes and fungi. In *Escherichia coli*, the transcription factor OxyR serves as a sensor of oxidative stress and leads to the activation of stress-related gene expression (Zheng et al., 1998). Meanwhile, the transcription factor Yap1 in budding yeast has a similar function as OxyR. In contrast, plants appear to utilize MAPK cascades which can regulate downstream gene expression. Transcription factors directly responsive to ROS have not yet been identified (Apel and Hirt, 2004).

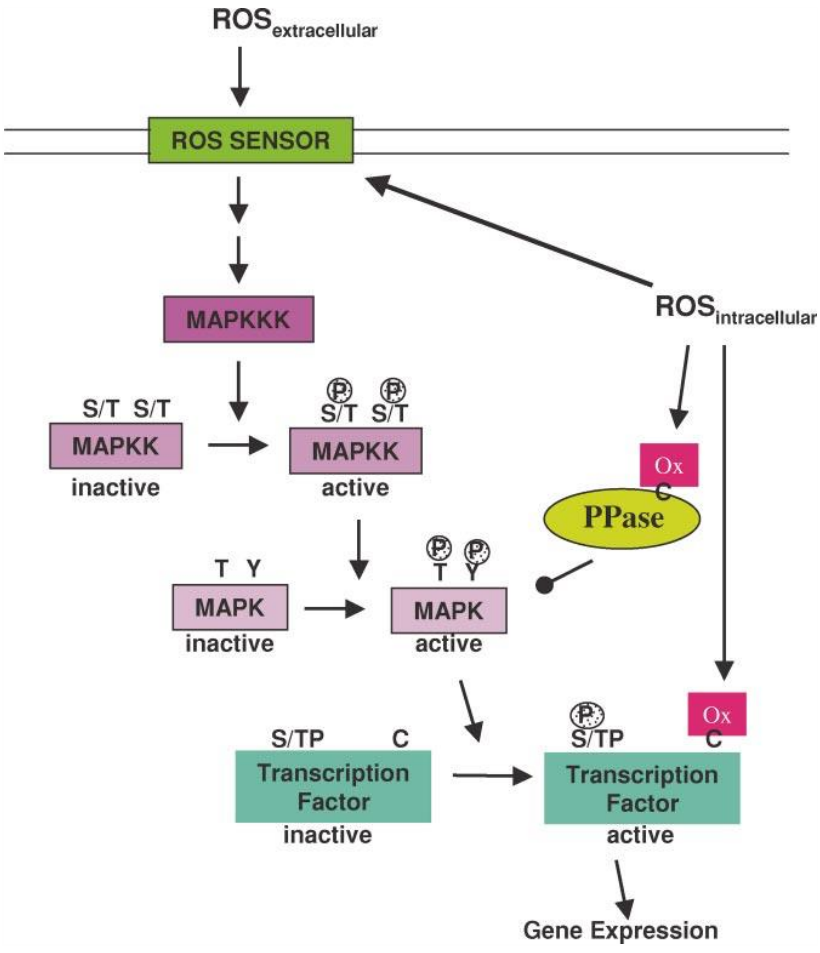

Figure 1.5. Schematic depiction of cellular ROS sensing and signalling mechanisms. ROS sensors such as membrane-localized histidine kinases can sense extracellular and intracellular ROS. Intracellular ROS can also influence ROS-induced mitogen-activated protein kinase (MAPK) signalling pathways through inhibition of MAPK phosphatases (PPases) or downstream transcription factors. Whereas MAP kinases regulate gene expression by altering transcription factor activity through phosphorylation of serine and threonine residues, ROS regulation occurs by oxidation (Ox) of cysteine residues (Apel and Hirt, 2004)

1.3 *S*-nitrosylation

1.3.1 Reactive nitrogen species and S-nitrosylation

Nitric oxide (NO) is a small and highly diffusible signalling molecule that regulates many biological features. NO is a lipophilic diatomic gas and has a relatively small Stokes radius. In addition to NO's neutral charge, these properties mediate rapid membrane diffusion (Goretski and Hollocher, 1988). NO with its unpaired electrons also facilitates a high reactivity with oxygen, superoxide, transition metals and thiol residues which are massively involved in cellular processes (Ma et al., 2016). Moreover, removal of the unpaired electron forms the nitrosonium cation (NO^+) and the addition of an electron forms the nitroxyl anion (NO^-) (Stamler et al., 1992).

The production of NO in animals is well established. NO is generated by a family of nitric oxide synthase (NOS) enzymes which convert L-arginine to citrulline (Palmer et al., 1993). Mammals have three different types of NOS which exhibit tissue specificity and Ca^{2+} requirements. These NOS enzymes include the Ca^{2+}-dependent constitutive neuronal NOS (nNOS) and endothelial NOS (eNOS) and Ca^{2+}-independent inducible NOS (iNOS) (Nathan and Xie, 1994). NOS has been identified in *Drosophila melanogaster* (Regulski and Tully, 1995) and in *Neurospora crassa* (Ninnemann and Maier, 1996).

In plants, the major mechanism that contributes to NO production remains unclear. However, genes such as nitric oxide associated 1 (*NOA1*) links to the NO generation (Crawford et al., 2006; Guo, 2003). Loss of *NOA1* function reduced *in vivo* NO levels in response to abscisic acid (Guo, 2003) and compromised the nitrosative burst in response to bacterial lipopolysaccharide (LPS) (Zeidler et al., 2004). Nitrate reductase (NR) drives not only the reduction of nitrate to nitrite but also the reduction of nitrite to NO (Yamasaki and Sakihama,

2000; Modolo et al., 2005). However, NR is unlikely to be a major factor in NO generation (Hong et al., 2008). Apart from this pathway, other sources of NO have been reported. For example, the xanthine oxidoreductase (XOR) might also contribute to NO generation (Wang et al., 2010). Additionally, other studies suggest NO production through chemical reactions in specific subcellular compartments. In apoplast of barley aleurone layers, NO is synthesised by the chemical reduction of nitrite under acidic condition (Bethke et al., 2004). In tobacco leaves, the mitochondrial electron transportation process NO synthesis via reduction of nitrite (Planchet et al., 2005).

One of the most important biological processes associated with NO is protein *S*-nitrosylation. *S*-nitrosylation is the covalent attachment of NO to protein Cysteine (Cys) residues forming an *S*-nitrosothiol. Protein *S*-nitrosylation has a ubiquitous influence on cellular signal transduction and previous research suggests this process plays a pivotal role in both physiology and disease resistance (Astier et al., 2012; Foster et al., 2009). Three major pathways result in *S*-nitrosylation: direct nitrosylation, metal-mediated nitrosylation and trans-nitrosylation (Zaffagnini et al., 2016). In plants and animals, *S*-nitrosoglutathione (GSNO) is the major NO reservoir. The GSNO content is in equilibrium with *S*-nitrosylated proteins (Feechan et al., 2005; Liu et al., 2004a). GSNO is not directly uptake by cells; however, it may transfer their NO to cysteine and form *S*-nitrosocysteine (CysNO) (Broniowska et al., 2013). The CysNO then uptake by the cell membrane amino acid transporter system and transfer the nitroso function group to other protein targets (Broniowska et al., 2013). The enzyme GSNO reductase (GSNOR) indirectly denitrosylates SNO-proteins while it reduces GSNO into oxidised glutathione (GSSG) and NH_3 (Feechan et al., 2005).

1.3.2 *S*-nitrosylation in animal diseases

Accumulating evidence suggests that *S*-nitrosylation plays an important role in animal health and disease (Foster et al., 2003). Aberrant protein *S*-nitrosylation has been reported in relation to human neurodegenerative diseases including Alzheimer's and Parkinson's (Nakamura et al., 2013). *S*-nitrosylation, as a protein modification process, can trigger protein conformation changes, activate or inhibit protein activity, alter protein-protein interactions, affect protein aggregation and influence protein localisation (Nakamura et al., 2013). These changes can affect cell signal transduction and neuronal function (Shi et al., 2013). For example, Parkin, an E3 ubiquitin ligase, has multiple cysteine residues that could be *S*-nitrosylated and alter the E3 ligase activity of this protein (Chung et al., 2004; Yao et al., 2004). Consequently, the alteration of Parkin E3 ligase activity impairs the ubiquitination and degradation of target proteins and leads to neuronal cell injury or death. GAPDH, an important glycolytic enzyme, can be *S*-nitrosylated at Cys-150 which initiates apoptotic cell death. In mammals, SNO-GAPDH increases the binding of GADPH to Siah1, an E3 ubiquitin ligase and results in translocation of the GADPH/Siah1 complex to the nucleus where it mediates apoptosis (Hara et al., 2005).

Recent work in the Loake lab suggests that *S*-nitrosylation also affects the innate immune system in flies (*Drosophila melanogaster*). *Drosophila* is widely used in research as a model system due to the highly conserved immune system compared with mammals. The absence of the *S*-nitrosylation regulator GSNOR in *D. melanogaster* reduces disease resistance against the entomopathogenic fungus *Beauveria bassiana* (Kanchanawatee, 2013). Flies without GSNOR activity show decreased expression of Toll pathway immune response marker genes which encode antimicrobial peptides (Homem, 2016). Interestingly, two CLIP-domain serine proteases associated with the Toll signalling pathway, Persephone (PSH) and Spatzle-Processing Enzyme (SPE), can be *S*-nitrosylated *in vitro* and *in vivo*. These observations

suggest *S*-nitrosylation interferes with the Toll immune system and this might be a novel mechanism of NO-mediated immune regulation.

1.3.3 *S*-nitrosylation in the plant immune system

S-nitrosylation is an important pathway that controls the resistance mechanism of plant immunity. Research has demonstrated that S-nitrosylation seriously affects *Arabidopsis* host and non-host resistance. A knockout mutant, *gsnor1-3*, which increases global S-nitrosylation shows increased susceptibility to the bacterial pathogen *Pseudomonas syringae* pv. *tomato* (*Pst* DC3000) and the fungal pathogens *Blumeria graminis* f. sp. *tritici* (*Bgt*) and *Hyaloperonospora parasitica* (Feechan et al., 2005). In contrast, *Arabidopsis* with higher GSNOR activity displayed enhanced resistance against *Pst* DC3000 and *H. parasitica* (Feechan et al., 2005). Moreover, accumulating evidence suggests a wide variety of proteins are targeted by *S*-nitrosylation (Astier et al., 2012). In plant cell culture, GSNO treatment resulted in the formation of 63 *S*-nitrosylated proteins, while treatment with NO resulted in 52 *S*-nitrosylated proteins (Lindermayr, 2005). *Arabidopsis* challenged with avirulent or virulent pathogens resulted in 112 *S*-nitrosylated proteins (Maldonado-Alconada et al., 2011).

Several regulatory proteins integral to the plant immune response have been found to be *S*-nitrosylated. Five cysteine residues (Cys-82, Cys-150, Cys-155, Cys160 and Cys-216) of the SA-dependent transcription co-factor NPR1 are S-nitrosylated which drive conformation changes which regulate the translocation from cytosol to nucleus (Mou et al., 2003). *S*-nitrosylation of NPR1 promotes NPR1 oligomerization, preventing NPR1 from translocating to the nucleus, thereby blocking the expression of SA-dependent genes (Tada et al., 2008). Other than NPR1, the transcription factor TGA1 has also been reported to be *S*-nitrosylated and co-regulate SA-dependent gene expression with NPR1 (Lindermayr, 2005). TGA1 has four cysteine residues, and pairs (Cys-260/Cys-266 and Cys-172/Cys-287) of them form disulphide

bonds. An increase in the cellular oxidation state result in suppression of the binding activity of TGA1 to target genes. *S*-nitrosylation of TGA1 Cys-172 and Cys-287 prevents disulphide bond formation and enhances the interaction between TGA1 and NPR1, which leads to gene expression.

NADPH oxidase RBOHD is also specifically *S*-nitrosylated at Cys890 *in vitro* when exposed to GSNO or CysNO and *in vivo* during inoculation with *Pst* (Yun et al., 2011). The *S*-nitrosylation of RBOHD abolishes NADPH oxidase activity and decreases cell death which is triggered by ROS. Peroxiredoxins (Prx) are a group of thiol-based reductase which function in detoxification of various peroxides. PrxII E possesses an $ONOO^-$ reductase activity and was shown to go through *S*-nitrosylation during attempted *Pst* infection in *Arabidopsis* (Romero-Puertas et al., 2007). The *S*-nitrosylation of PrxII E Cys121 active site inhibits both the peroxidase and the reductase activity and modulates peroxynitrite-mediated tyrosine nitration. Catalase is the most abundant antioxidant enzyme which exists in the peroxisome, a single-membrane-bounded organelle, and plays a key role during abiotic and biotic stresses (Mhamdi et al., 2010a). In pea plants, catalase in the peroxisome was identified to be *S*-nitrosylated and this lead to inhibition of enzyme activity, during abiotic stress (Ortega-Galisteo et al., 2012).

S-nitrosylation is also related with cell death processes. Increased cellular *S*-nitrosylation increases cell death intensity of *A. thaliana* during the interaction with avirulence pathogens (Feechan et al., 2005). Plant metacaspases (MC) are cysteine-dependent proteases and are related to the plant hypersensitive response PCD. *A. thaliana* MC 9 (AtMC9) zymogens are *S*-nitrosylated on their active site, Cys-147, and this protein modification suppresses the property of AtMC9 autoprocessing and proteolytic activity (Belenghi et al., 2007).

1.4 Reactive oxygen and reactive nitrogen species cross talk

1.4.1 Redox environment and redox state of the cell

The redox environment of the cell controls a plethora of different biological processes. The redox environment and the linkage of the half-cell reduction potential and the reducing capacity of the redox couple are described as the redox state. The redox environment is the summation of the reduction potential and the reducing capacity of the linked redox couples which are found in a biological fluid, organelle, cell or tissue (Schafer and Buettner, 2001). In any natural cellular state, the redox environment can drive electron transfer and control cellular function by regulating the oxidation state of relevant molecules such as proteins and lipids (Liu, 2005). Schafer and Buettner (2001) proposed that the redox potential of nano-switches trigger cell necrosis.

Redox-state controls various biological processes from the basic physiological changes to the gene expression regulation. The redox state is regulated by a cascade of redox couples including reduced glutathione (GSH)-glutathione disulphide (GSSG), reduced ascorbate (Asc)–dehydroascorbate (DHA) and NADPH-$NADP^+$ (Kocsy et al., 2013). Changes in the ratio and amount of the reduced and oxidised form of these redox couples mediate the redox potential of the cell and consequently alter cellular processes through the transcripts of redox responsive proteins (Birtić et al., 2011; Kolbe et al., 2006). In the flowering process, GSH/GSSG and Asc/DHA are highly involved in the control of flower meristem initiation (Barth et al., 2006; Ogawa et al., 2001). Protein cysteine residues, on the other hand, formulate a highly reactive thiolate group in response to the redox changes (Spoel and van Ooijen, 2014). In response to the redox fluctuation, cysteine thiolates are subject to modification with the increase of the oxidative state from *S*-nitrosylation to *S*-sulfonation (Fig. 1.6) (Spoel and van

Ooijen, 2014). These cysteine modifications provide a redox-link between plant hormone signalling pathways and their downstream responses. For example, *S*-nitrosylation of the histidine phosphotransfer protein (AHP1) compromises cytokinin signalling (Feng et. al 2013).

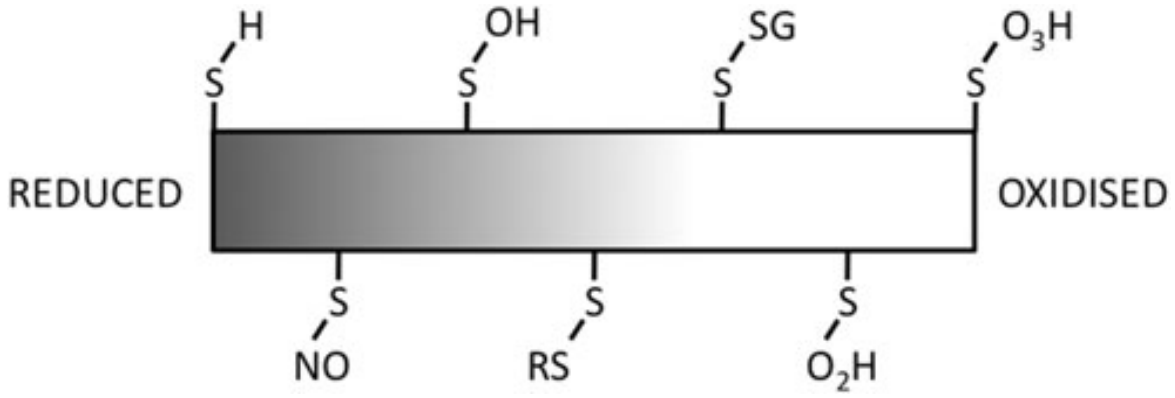

Figure 1. 6. Cysteine modifications.
Modifications of the cysteine are based on the reduced (left) and oxidized states (right). Protein cysteine thiols (-SH) are reversibly modified by attachment of nitric oxide (*S*-nitrosylation, -SNO), thiol hydroxylation (*S*-sulphenation, -SOH), disulphide bridge formation (*S*-thiolation, -S-SR where R is the Rest group). Further oxidations are covalent attachment of glutathione (*S*-glutathionylation, -S-SG), and oxidation of sulphenic -SOH groups to the sulphinic (-SO2H) and sulphonic (-SO3H) acids (Spoel and van Ooijen, 2014).

1.4.2 RNI and ROS cross talk

Reactive nitrogen intermediates (RNI) have been recognised as fundamental molecules which interact with ROS in various ways (Zaninotto et al., 2006). NO has been reported to be a signal which induces HR cell death in *Arabidopsis* and rice cell cultures (Clarke et al., 2000; Hu et al., 2003). Moreover, NO and H_2O_2 both cause cytochrome C release and a caspase-like signalling cascade during HR cell death (Mur et al., 2006a). These findings suggest RNI and ROS both contribute to the HR cell death process. During programmed cell death, NO, O_2^- and H_2O_2 have been reported to mediate the HR cell death response (Fig. 1.7) (Delledonne et al., 2001). In the previous context, the balance of NO-O_2^- modulates the NO and H_2O_2 interaction that induces the HR cell death. If the balance is in favour of O_2^-, NO will scavenge with O_2^-

before it interacts with H_2O_2. If the balance is in favour of NO, O_2^- will likely dismutate to H_2O_2 by superoxide dismutase and induce the HR cell death.

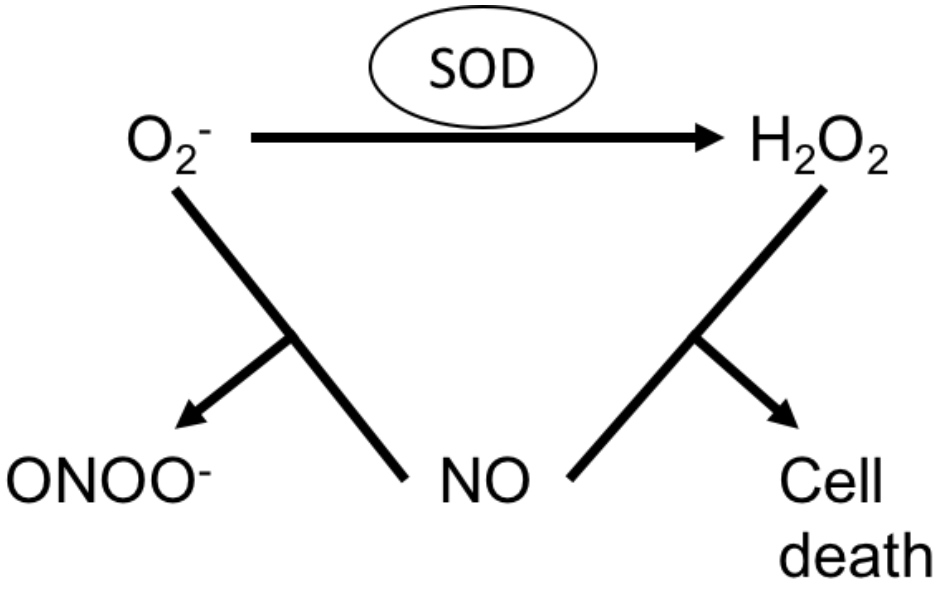

Figure 1.7. Model of the balance of NO, O_2^- and H_2O_2 in regulation of cell death.
The hypersensitive response (HR) cell death triggered by the cooperation of H_2O_2 and NO. However, the ratio of NO/O_2^- is the major factor which control the HR cell death. SOD stands for superoxide dismutase (Delledonne et al., 2001).

The molecular interaction between RNI and ROS urgently require more clarification. Studies have suggested that the regulation of RNI and ROS production are cross-linked in various ways. In tobacco, antioxidant enzymes such as catalase or ascorbate peroxidase were inhibited by the application of NO (Clark et al., 2000). By contrast, a reduced NO level mutant (*nos1*, stands for NO synthetase 1 now known as *NOA1*) increases the level of ROS content (H_2O_2, superoxide anion, oxidised lipid and oxidised protein) (Guo and Crawford, 2005). NO treatment also delays the gibberellic acid–induced PCD that is regulated by ROS in the barley aleurone layers (Beligni et al., 2002). Therefore, NO functions as an antioxidant which reduces ROS dependent cell damage and senescence.

Beside these direct chemical interactions, RNI and ROS have complementary effects on gene expression and often have similar targets for protein modification. Altering the NO

content in plants triggers a broad range of gene expression changes such as *PAL* (phenylalanine ammonia lyase) and *PR1* which are also altered by ROS (Grün et al., 2006). Further, NO has been shown to mediate overlapping gene expression changes to that of H_2O_2 (Zago et al., 2006). Proteomic approaches such as 2-D electrophoresis and MALDI-TOF MS (matrix assisted laser desorption ionization-time of flight mass spectrometry) identified *Arabidopsis* proteins which are targets of H_2O_2 (Hancock et al., 2005). The most prominent target in this study is glyceraldehyde 3-phosphate dehydrogenase (GAPDH) which enzymatically involves in the glycolysis pathway. Interestingly, GAPDH enzyme activity is inhibited by H_2O_2 and suggested to play a role in ROS signalling (Hancock et al., 2005). GAPDH enzyme activity is also inhibited by NO-dependent *S*-nitrosylation (Lindermayr, 2005). Accordingly, these discoveries suggest the potential cross-talk between ROS and RNI.

1.5 Identification of *gsnor1-3* suppressors

Suppressor screening of *gsnor1-3* has identified two suppressors *snowplough7* (*spl7*) and *spl8* which recover the developmental phenotype of *gsnor1-3* plants from loss of apical dominance to wild type (Fig. 1.8) (Sorhagen, 2011). These suppressors were generated by ethyl methane sulfonate (EMS) which generates point mutations.

The suppressor mutants have restored apical dominance, show mostly wild-type phenotype and have partially restored disease resistance against avirulent pathogens. This result suggested the *spl7* and *spl8* may ameliorate the impact of an enhanced level of *S*-nitrosylation found in *gsnor1-3* plants.

Map-based cloning was used to uncover *spl7* and *spl8* (Lukowitz et al., 2000). *spl7* and *spl8* were identified as alleles located on the left arm of chromosome 1 (Fig. 1.9) (Brezezek, 2013). Further analysis demonstrated that *spl7* and *spl8* are point mutations in *CAT3*. While *spl7* was a G to A base change and resulted in an amino acid change from arginine to lysine, *spl8* was a C to T base change and lead to amino acid change from arginine to cysteine (Fig. 1.10 and Fig. 1.11) (Brezezek, 2013).

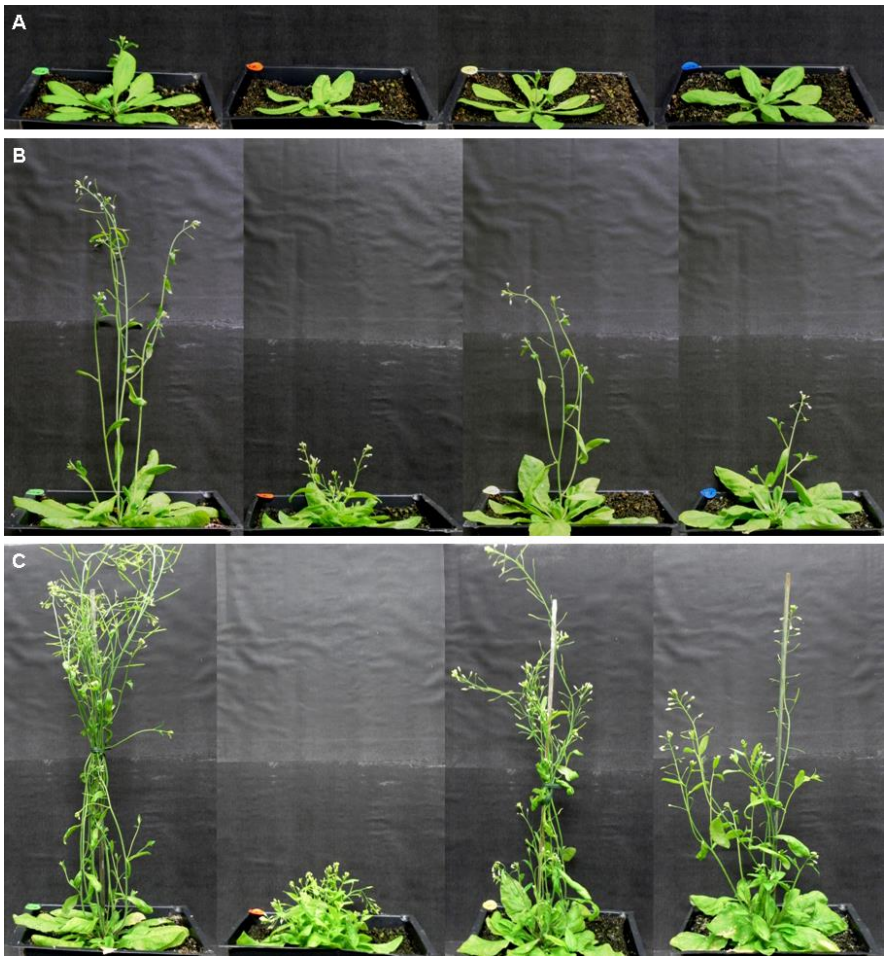

Figure 1.8. Morphology of suppressor mutants compared to Col-0 and atgsnor1-3 plants. From left to right: Col-0 (wild type), *atgsnor1-3*, *atgsnor1-3 spl7*, *atgsnor1-3 spl8*. (A) 5-week-old plants. (B) 6-week-old plants. (C) 7-week-old plants. (Brezezek, 2013).

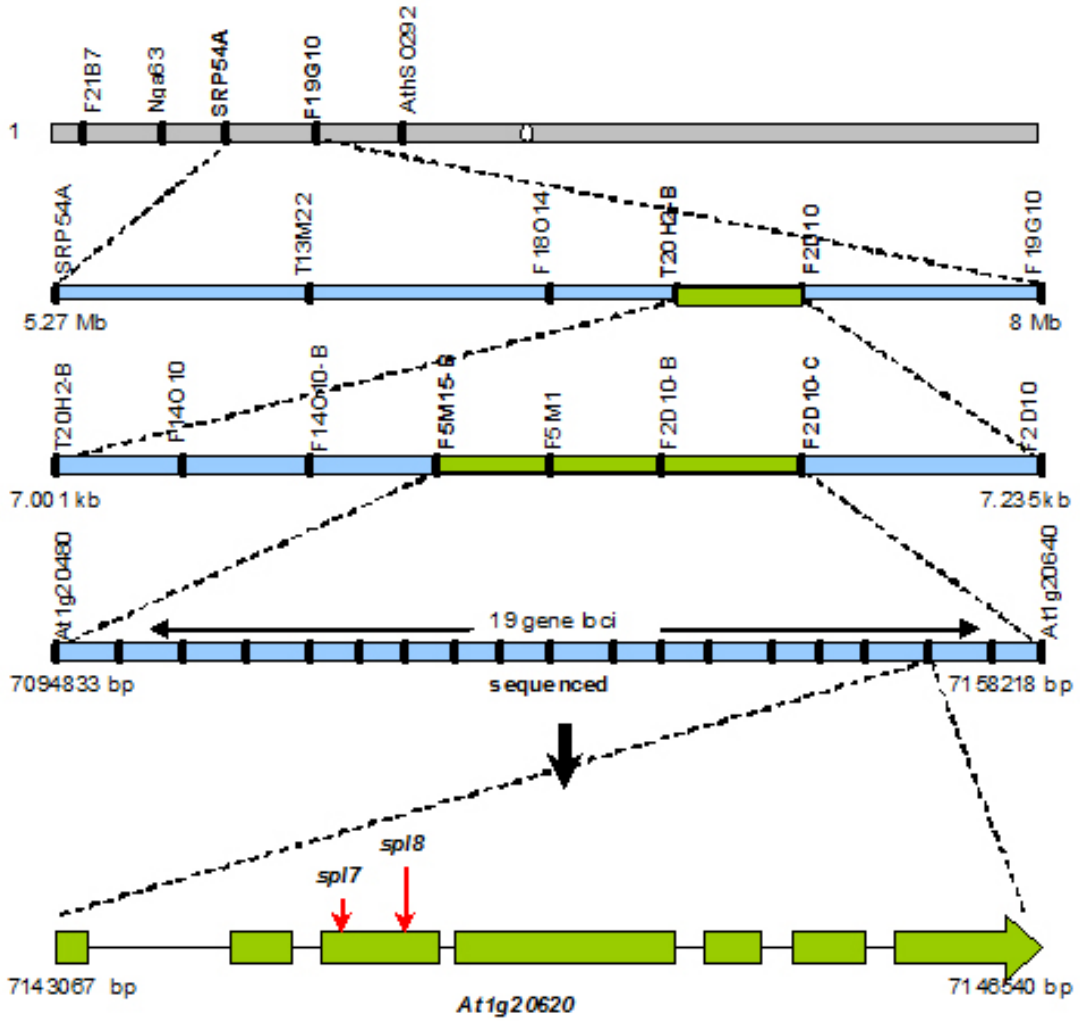

Figure 1.9. Schematic representation of the mapping procedure used to identify the spl7 and spl8 mutations. (graphic by Kirsti Sorhagen)

ATGGATCCTTACAAGTATCGTCCTTCAAGCGCGTACAACGCCCCATTCTACACCACAAACGGTGGTGCTCCAGTCTCCAACAACATCTCTTCCC
TCACCATCGGAGAAAGAGGTCCGGTTCTTCTTGAGGATTATCATTTGATCGAGAAGGTTGCTAATTTCACCA[G/A]AGAGAGGATCCCTGAGA
GAGTGGTTCATGCTAGAGGAATCAGTGCTAAGGGTTTCTTTGAAGTCACCCATGACATTTCAAACCTCACTTGTGCTGATTTTCTCAGAGCCCC
TGGTGTTCAAACTCCGGTTATTGTCCGTTTCTCCACCGTTGTCCACGAACGTGCCAGTCCTGAAACCATGAGGGATATT[C/T]GTGGTTTTGC
TGTCAAGTTTTACACCAGAGAGGGAAACTTGATCTTGTTGGGAACAACACTCCGGTGTTCTTCATCCGTGATGGGATTCAGTTCCCGGATGTT
GTCCACGCGTTGAAACCTAACCCGAAAACAAACATCCAAGAGTACTGGAGGATTCTGGACTACATGTCCCACTTGCCTGAGAGTTTGCTCACAT
GGTGCTGGATGTTTGATGATGTTGGTATTCCACAAGATTACAGGCACATGGAGGGTTTCGGTGTCCACACCTACACTCTTATTGCCAAATCTGG
AAAAGTTCTCTTTGTGAAGTTCCACTGGAAACCAACTTGTGGGATCAAGAATCTGACTGATGAAGAGGCCAAGGTTGTTGGAGGAGCCAATCAC
AGCCACGCCACTAAGGATCTCCACGATGCCATTGCATCTGGCAACTACCCCGAGTGGAAACTTTTCATCCAGACCATGGATCCTGCAGATGAGG
ATAAGTTTGACTTTGACCCACTTGATGTGACCAAGATCTGGCCTGAGGATATTTTGCCTCTGCAACCGGTTGGTCGCTTGGTTCTGAACAGGAC
CATTGACAATTTCTTCAATGAAACTGAGCAGCTTGCGTTCAACCCGGGTCTTGTGGTTCCTGGAATCTACTACTCAGACGACAAGCTGCTCCAG
TGTAGGATCTTTGCTTATGGTGACACTCAGAGACATCGCCTTGGACCGAATTATTTGCAGCTTCCAGTCAATGCTCCCAAATGTGCTCACCACA
ACAATCACCATGAAGGTTTTATGAACTTCATGCACAGAGATGAGGAGATCAATTACTACCCCTCAAAGTTTGATCCTGTCCGCTGCGCTGAGAA
AGTTCCCACCCCTACAAACTCCTACACTGGAATTCGAACAAAGTGCGTCATCAAGAAAGAGAACAACTTCAAACAGGCTGGAGACAGGTACAGA
TCATGGGCACCAGACAGGCAAGACAGGTTTGTTAAGAGATGGGTGGAGATTCTATCGGAGCCACGTCTCACCCACGAGATCCGCGGCATCTGGA
TCTCTTACTGGTCTCAGGCTGATCGATCCTTGGGACAGAAACTTGCAAGCCGTCTGAACGTGAGGCCAAGCATCTAG

Figure 1.10. The DNA sequence of At1g20620 (*CAT3*).
The bases that are mutated in *atgsnor1-3 spl7* and *atgsnor1-3 spl8* are underlined and highlighted in yellow and red, respectively (Brezezek, 2013).

MDPYKYRPSSAYNAPFYTTNGGAPVSNNISSLTIGERGPVLLEDYHLIEKVANFT[R/K]ERIPERVVHARGISAKGFFEVTHDISNLTCADFL
RAPGVQTPVIVRFSTVVHERASPETMRDI[R/C]GFAVKFYTREGNFDLVGNNTPVFFIRDGIQFPDVVHALKPNPKTNIQEYWRILDYMSHLP
ESLLTWCWMFDDVGIPQDYRHMEGFGVHTYTLIAKSGKVLFVKFHWKPTCGIKNLTDEEAKVVGGANHSHATKDLHDAIASGNYPEWKLFIQTM
DPADEDKFDFDPLDVTKIWPEDILPLQPVGRLVLNRTIDNFFNETEQLAFNPGLVVPGIYYSDDKLLQCRIFAYGDTQRHRLGPNYLQLPVNAP
KCAHHNNHHEGFMNFMHRDEEINYYPSKFDPVRCAEKVPTPTNSYTGIRTKCVIKKENNFKQAGDRYRSWAPDRQDRFVKRWVEILSEPRLTHE
IRGIWISYWSQADRSLGQKLASRLNVRPSI

Figure 1.11. The protein sequence of At1g20620 (CAT3).
The amino acids that are changed as a result of the mutations in *atgsnor1-3 spl7* and *atgsnor1-3 spl8* are underlined and highlighted in yellow and red, respectively. The *spl7* mutation leads to an arginine (R) to lysine (K) change, and *spl8* leads to an arginine (R) to cysteine (C) change (Brezezek, 2013).

1.6 Aims

S-nitrosylation is an important post-translational modification and plays a major role in various biological processes (Lamotte et al., 2015). Most importantly, *S*-nitrosylation regulates both plants and animals innate immune system (Casalongué, 2013; Foster et al., 2003). Therefore, a comprehensive understanding of *S*-nitrosylation regulation is needed. Additionally, previous unpublished result in our lab showed the lack of *CAT3* in *Arabidopsis* suppresses the *gsnor1-3* phenotype. The aim of this work is therefore to uncover the mechanisms of *S*-nitrosylation regulation in the *gsnor1-3 cat3*. Firstly, other redox-related genes and *CAT3* paralogs mutation in the *gsnor1-3* background were generated to investigate their plausible suppression effects as the *cat3* mutation. Secondly, the *gsnor1-3 cat3* plants were used as the standard model for uncovering the mechanisms on the absence of the *CAT3* suppresses *gsnor1-3*. Lastly, the *Drosophila gsnor*$^{-/-}$ *cat*$^{-/-}$ double mutant line was used to evaluate if our hypothesised *S*-nitrosylation regulation applies on animal system.

Chapter-2 Materials and Methods

2.1 Plant materials

All transgenic plant lines and wild-type origins are listed in Table 1.1. *Arabidopsis* seeds were spread evenly in the small pots. Each pot was covered with a transparent lid to maintain humidity. After 7 days, the seedlings were then transferred to large square pots. Plants were grown in compost contained peat moss, vermiculite and sand (4:1:1, w: w: w). All plants were grown under 21 ℃ with the long day photoperiod (16 hours light, 8 hours dark), 100 μmol m^2 s^{-1} light intensity and 65% humidity. Four-week-old plants were used to assess the disease-related phenotypes (pathogen growth, cell death and resistance gene expression) and total protein *S*-nitrosylation level. The developmental phenotypes (shoot length, shoot weight and shoot numbers) were analysed after 8 weeks.

For the experiment of the plant on growth media, *Arabidopsis* seeds were surface sterilised before growth. Seeds were immersed in 70% bleach (containing 4.5% sodium hydrochloride) for 5 min. After bleach incubation, the seeds were then serial washed with 70%, 50% and 20% ethanol. Following the ethanol wash, the seeds were washed with sterilised water and vernalized at 4℃. The seeds were placed on MS (4.4 g MS (Murashige and Skoog medium) salt, 1 % (w/v) sucrose and 0.8 % (w/v) agar) medium and incubated under 21℃ with a long day photoperiod (16 hours light, 8 hours dark) and 100 μmol m^2 s^{-1} light intensity. Within a week of growth, the seedlings were then used for hydroxyl radical analysis.

Table 2. 1. List of *Arabidopsis* wild-type and mutant lines.

Line	Gene	Mutation/function	Source	Reference
Col-0		Wild type	NASC	
gsnor1-3	At5g43940	*GSNOR1* T-DNA insert High levels of protein *S*-nitrosylation	Gary Loake Edinburgh, UK	(Feechan et al., 2005)
cat1	At1g20630	*CAT1* T-DNA insert Reduced catalase activity	Ye-Qin Hi Wuhan, China	(Hu et al., 2010)
cat2	At4g35090	*CAT2* T-DNA insert Reduced catalase activity	Ulrike Zentgraf Tuebingen, Germany	
cat3	At1g20620	*CAT3* T-DNA insert Reduced catalase activity	Ulrike Zentgraf Tuebingen, Germany	
pad2-1	At4g23100	Point mutation on y-glutamylcysteine synthetase gene Reduced glutathione levels	Gary Loake Edinburgh, UK	(Parisy et al., 2006)
vtc2-1	At4g26850	Point mutation on GDP-L-galactose phosphorylase 1 gene Reduced ascorbate levels	Nick Smirnoff Exeter, UK	(Conklin et al., 2000)
trx3 trx5	At5g42980 At1g45145	*TRX3* and *TRX5* T-DNA inserts Reduced thioredoxin levels	Steven Spoel Edinburgh, UK	(Tada et al., 2008)

2.2 Plant crossing and genotyping

Crossing candidates were grown in 21℃ under 16 hour photoperiods. After the plant flowering stage, the unfertilised *gsnor1-3* carpels were cross-pollinated by target mutants' stamens (listed in table 2.1). Seeds from the cross-pollinated siliques were transferred into selection MS medium. The selection MS medium contained 7.5 mg L^{-1} sulfadiazine (4-amino-

N-2-pyrimidinylbenzene sulphonamide) which is used to select the *gsnor1-3* mutation (Rosso et al., 2003). The selected-seedlings were transferred to the growth compost (same as ch. 2.1) for two weeks. The 2-week-old seedlings' leaves were collected for genomic DNA extraction and genotyping.

Plant genomic DNA extraction was using cetyltrimethylammonium bromide (CTAB) extraction method. Leaves for examining genotypes were separately collected in a 1.5 ml eppendorf or 500 µL strip tube and incubated in an -80℃ freezer for an hour. Frozen samples were added to 300 µL CTAB buffer (100mM Tris-HCl, pH 8; 1.4M NaCl (VWR, UK); 20mM EDTA (ethylenediaminetetraacetic acid) ;1% CTAB) then ground by micropestle or tissue lyser (Qiagen) with beads. The homogenised samples were incubated at 65℃ for an hour. After a 65℃ incubation, samples were mixed with 300 µL of chloroform and centrifuged at 12,000 ×g for 2 minutes. The supernatants of samples were transferred into a new Eppendorf and mixed with 200 µl isopropanol. The mixtures were centrifuged at 12,000 ×g for 5 minutes. After centrifugation, the precipitated pellets from mixtures were collected and washed by 500 µl 70% ethanol and centrifuged again at 12,000 ×g for 2 minutes. The remaining pellets were collected and air-dried in a laminar flow cabinet. Air-dried pellets were dissolved in 100 µl distilled water and subjected to polymerase chain reaction (PCR) for genotyping or stored in a 4℃ fridge. Primers for genotyping are listed in table 2.2.

All T-DNA insertion mutants (*gsnor1-3*, *cat1*, *cat2*, *cat3*, *trx3* and *trx5*) were carried out by using two gene-specific primers and a left boarder primer for the T-DNA in polymerase chain reaction (PCR). A large DNA fragment for wild-type genotype and a small DNA fragment for the T-DNA insertion were synthesised via PCR. For example, the genotyping *gsnor1-3* is shown in Fig. 2.1. Lane with only a small size fragment (asterisk) suggests the test sample as *gsnor* homozygous mutation. The genotyping of *trx5* had an exceptionally large fragment for the T-DNA insertion and small fragment for wild-type genotype. The PCR for T-

DNA insertion was performed in 25 µL volume of GoTaq® Flexi DNA Polymerase Kit (Promega, USA) that contained 5 µL 5X Flexi Green GoTaq® buffer, 0.5 µL 10mM dNTPs, 2.5 µL 25mM MgCl2, 1 µL 10 µM forward primer, 1 µL 10 µM reverse primer, 1 µL 10 µM left border primer, 0.1 µL GoTaq® DNA polymerase (5unit/µL) and 13.9 µL ddH_2O.

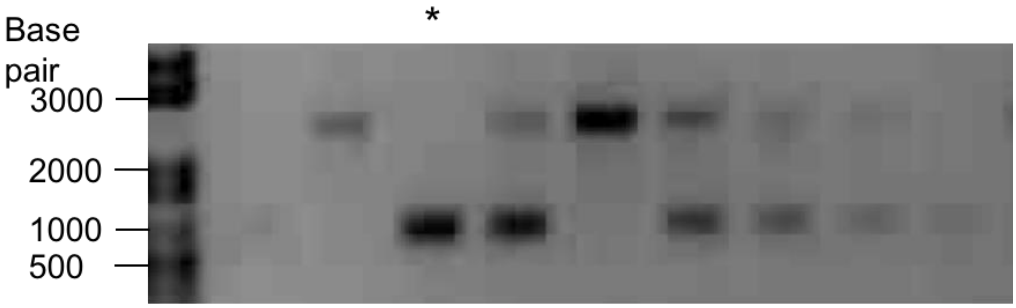

Figure 2.1. Genotyping of *gsnor1-3* mutations.
Two-week-age plants were collect a leaf and extract their genomic DNA. Genomic DNA from tested plants were subjected to polymerase chain reaction with *gsnor1-3* cycling conditions (94 ℃ for 1 min repeated 30 times of DNA assembling (94 ℃ for 30 sec, 55 ℃ for 30 sec and 72 ℃ for 1 min) and 72 ℃ for 7 min at the end of reaction). Lane with asterisk showed the examined-plant as homozygous of *gsnor1-3* mutation.

PCR conditions for genotyping *gsnor1-3* were 94 ℃ for 1 min, then repeated 30 times of DNA assembling (94 ℃ for 30 sec, 55 ℃ for 30 sec and 72 ℃ for 1 min) and 72 ℃ for 7 min at the end of reaction. PCR conditions for genotyping *cat2* were 94 ℃ for 1 min, then repeated 30 times of DNA assembling (94 ℃ for 30 sec, 70 ℃ for 30 sec and 72 ℃ for 1 min) and 72 ℃ for 7 min at the end of reaction. PCR conditions for genotyping other T-DNA insertion were 94 ℃ for 1 min, then repeated 30 times of DNA assembling (94 ℃ for 30 sec, 58 ℃ for 30 sec and 72 ℃ for 1 min) and 72 ℃ for 7 min at the end of reacation. The PCR products were run on 1% agarose TAE (40 mM tris acetate and 1 mM EDTA) gel (w/v) and stained with ethidium bromide.

The *vtc2-1* point mutation introduces a HindIII restriction digested site. After PCR amplification of *vtc2-1* genotype panel, a 767 bp DNA product following the HindIII enzyme digestion results in 588 and 179 bp fragments if the *vtc2-1* mutation exists (Fig. 2.2).

Genotyping for point mutation *pad2-1* were conducted using two pairs of primers (forward primer with single nucleotide difference) and PCR was performed separately. The PCR for point mutation were performed in 25 µL volume of GoTaq® Flexi DNA Polymerase Kit (Promega, USA) that contained 5 µL 5X Flexi Green GoTaq® buffer, 0.5 µL 10mM dNTPs, 2.5 µL 25mM MgCl2, 1 µL 10 µM forward primer, 1 µL 10 µM reverse primer, 0.1 µL GoTaq® DNA polymerase (5unit/µL) and 14.9 µL ddH_2O.

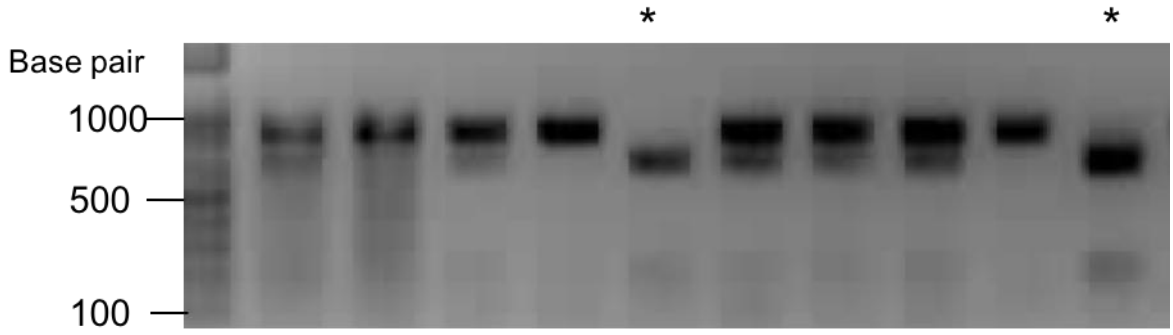

Figure 2.2. Genotyping of *vtc2-1* mutations.
Two-week-age plants were collect a leaf and extract their genomic DNA. Genomic DNA from tested plants were subjected to polymerase chain reaction with *vtc2-1* cycling conditions (94 ℃ for 1 min, repeated 30 times of DNA assembling (94 ℃ for 30 sec, 58 ℃ for 30 sec and 72 ℃ for 1 min) and 72 ℃ for 7 min at the end of reaction). The amplified-DNA were digested with HindIII restriction enzymes and running the samples in 1% agarose gel embedded with ethidium bromide. Lanes with asterisks showed the examined-plants as homozygous of *vtc2-1* mutation.

PCR conditions for genotyping *vtc2-1* were 94 ℃ for 1 min, then repeated 30 times of DNA assembling (94 ℃ for 30 sec, 58 ℃ for 30 sec and 72 ℃ for 1 min) and 72 ℃ for 7 min at the end of reaction. PCR conditions for genotyping *pad2-1* were 94 ℃ for 1 min, then repeated 30 times of DNA assembling (94 ℃ for 30 sec, 64 ℃ for 30 sec and 72 ℃ for 1 min) and 72 ℃ for 7 min at the end of reaction. The PCR products and digested products were run on 1% agarose TAE (40 mM tris acetate and 1 mM EDTA) gel (w/v) and stained with ethidium bromide.

Table 2. 2. The primers for genotyping of the mutant lines

Line	Gene	Primer name	Sequence
gsnor1-3	At5g43940	315 D11 Left border 315 D11 Forward 315 D11 Reverse	ATATTGAACATCATACTCATTG TATATAATGGTTCGACGATAT CCACCAACACTCTCAACAATC
pad2-1	At4g23100	PAD2-WT-FP PAD2-WT-RP PAD2-M-FP PAD2-M-RP	AAGGAAAGCCAAACGGATTTCTCCG GATCCAAAGCATCTTTCTATCTTGAACACAAACATA AAGGAAAGCCAAACGGATTTCCCAA GATCCAAAGCATCTTTCTATCTTGAACACAAACATA
vtc2-1	At4g26850	VTC2-FP VTC2-RP	TCAGCTTAACGAGGGTCGTCAC GGCAAACACAGCAGTCTGAAAC (*enzyme digestion: HindIII)
trx3	At5g42980	LBb1.3 TRX3-FP TRX3-RP	ATTTTGCCGATTTCGGAAC GCTGCGAGTAATCAAGTTTGC ACCGACACAGAGACGAAGAAG
trx5	At1g45145	LBb1.3 TRX5-FP TRX5-RP	ATTTTGCCGATTTCGGAAC GAAGCTACAAGACCACCATGC TTCTCTTGTTATGTCCAGGGC
cat1	At1g20630	LBb1 CAT1-LP2 CAT1-RP2	GCGTGGACCGCTTGCTGCAACT GTAAGAGATCCAAATGCTGCG ATTGAAACCGAATCCCAAGTC
cat2	At4g35090	LBb1 CAT2-LP2 CAT2-RP2	GCGTGGACCGCTTGCTGCAACT TCGCATGACTGTGGTTGGTTC ACCACCAACTCTGGTGCTCCT
cat3	At1g20620	LBb1 CAT3-LP2 CAT3-RP2	GCGTGGACCGCTTGCTGCAACT CACCTGAGTAATCAAATCTACACG TCAGGGATCCTCTCTCTGGTGAA

2.3 Pathogen preparation and inoculation

Pseudomonas syringae (*Pst* DC3000) and *Pst* DC3000(*avrB*) were taken from glycerol stocks. These pathogens were incubated in 5 mL LB (Luria-Bertani: tryptone 10 g/L, yeast

extract 5 g/L, NaCl 10 g/L) liquid medium with 50 ug/mL rifampicin (additional 50 ug/mL kanamycin for the *avr*B growth). After overnight 28 ℃ culture, the medium with bacteria growth were centrifuged at 10,000 ×g for 10 min in room temperature. The pellets of bacteria were then washed by 0.1M $MgCl_2$ for 2-3 times and centrifuged at 10,000 ×g for 10 min in room temperature. The pellets were suspended with 0.1M $MgCl_2$ and the pathogen concentration were adjusted by spectrophotometer (GeneQuant 1300, Cambridge, UK). Four-week-old plants were then infiltrated with *Pst* DC3000 suspension (OD_{600}= 0.002 for disease resistance assay and OD_{600}= 0.02 for defence gene expression assay) and *Pst* DC3000 (*avr*B) suspension (OD_{600}= 0.02 for cell death assay) on abaxial side of half leaf using 1 mL syringe (without needle) (Grant and Loake, 2000).

2.4 Disease resistance

Pst DC3000 was inoculated into different *Arabidopsis* mutants' leaves as outlined above. Fresh leaves were collected after zero and five days for the disease resistance assay. The inoculated leaf discs (around 0.5 cm^2) were homogenised in 200 uLof 0.1M $MgCl_2$. 200 uL of the homogenised solution was then serially diluted with 0.1 M $MgCl_2$. The diluted samples were then streaked on a LB medium agar (1% agar) plate with 50 μg/mL rifampicin. The bacterial colony forming units (CFU) in the leaf discs (CFU per cm^2) were calculated after 2 days' incubation under 28°C.

2.5 Cell death assay

The cell death assay was modified from Yun et al. (Yun et al., 2011). 4-week-old *Arabidopsis* were infiltrated, half a leaf, with *Pst* DC3000 (*avrB*) (same as ch 2.3). The inoculated leaves were then stained with Trypan Blue to observe cell death.

Trypan blue staining was used to quantify the intensity of cell death. After 24 hours inoculation, inoculated leaves were immersed in 5 mL trypan blue stain solution (0.01 g Trypan blue in 10 ml H_2O, 10 ml 80% (w/w) lactic acid, 10 ml phenol and 10 ml glycerol) and boiled for 5 minutes. The stained leaves were then immersed into destaining solution (2.5 % (w/v) chloral hydrate). Leaf destaining was undertaken for at least 2 days depending on the intensity of staining. Destained leaves were then mounted on slides for scanning and quantification the staining intensity. The staining intensity was analysed by the software Fiji which is a distribution version of ImageJ (Schindelin et al., 2012). The cell death intensity was measured by subtracting the mean grey value of the uninoculated area from the mean grey value of the inoculated area..

2.6 Gene expression assay

4-week-old *Arabidopsis* were inoculated with *Pst* DC3000 and gene expression of the pathogenesis-related protein 1 (*PR1*) was analysed by semi-quantified RT-PCR (reverse transcription polymerase chain reaction).

The plant leaves (around 10 mg) after inoculation were frozen in liquid nitrogen and homogenised with 200 uL Trizol (Invitrogen). The homogenised samples were left at room

temperature for 5 minutes followed by 12,000 ×g centrifugation at 4 ℃ for 10 miniutes. The 120 uL supernatants were transferred into a new 1.5 mL Eppendorfs and mixed vigorously with 40 μL of chloroform. After 3 min incubation at room temperature, the mixtures were centrifuged at 12,000 ×g for 15 min at 4 ℃. The upper layer (around 80 uL) of the mixture was transferred to a new Eppendorf and added to 100 uL of isopropanol to precipitate the RNA at room temperature for 5 minutes. After isopropanol precipitation, the mixtures were centrifuged at 12,000 ×g for 10 minutes at 4 ℃ and the supernatant removed. The pellets were washed by 70% ethanol two times and dried in the laminar flow cabinet. The RNA pellet was then dissolved in diethylpyrocarbonate (DEPC) treated water for the rest of procedure. Before cDNA synthesis, the RNA samples were quantified by a NanoDrop spectrophotometer (Thermo Scientific) and diluted as required (200 ng/mL). cDNA synthesis was following the manufacturer's instruction of Omniscript RT Kit (Qiagen).

Semi-quantitative RT-PCR was used to determine *PR1* gene expression of different mutants after inoculation with *Pst* DC3000. *PR1* primers (forward: ACGGGGAAAACTTAGCCTGG, reverse primer: TTGGCACATCCGAGTCTCAC) synthesise a 169 bp DNA fragment and were used to examine *PR1* expression levels in different samples. The ubiquitin-conjugating enzyme gene (UBC, housekeeping gene) primers (forward primer: TCCTTACGAAGGCGGTGTTT, reverse primer: AGACTGAAGCGT-CCAAGCAG) synthesise a 178 bp DNA fragment and were used as the control of basal level gene expression. The cycling conditions for RT-PCR were 94 ℃ for 1 min, then 25 times assembling (94 ℃ for 40 sec, 55 ℃ for 40 sec and 72 ℃ for 1 min) later with 72 ℃ for 7 min. The DNA products were run on 1% agarose TAE (40 mM tris acetate and 1 mM EDTA) gel (w/v) and stained with ethidium bromide.

2.7 LC-MS detection of GSH and GSSG

The LC-MS (liquid chromatography-mass spectrometry) quantification assay followed the workflow of Airaki et al. (2011). The standard sample of glutathione (reduced and oxidised form) and S-nitrosoglutathione were acquired from Sigma-Aldrich and self-synthesis (details in section 2.12.), respectively. The plant samples (0.3 g) were ground by pestle and mortar with liquid nitrogen in the presence of 1 ml 0.1M HCl. The crude plant samples were then centrifuged at 21,000 × g for 20 min at 4 ℃, and the supernatant was filtered through 0.45 μm nylon filter. The content of GSH, GSSG and GSNO in the extracts were then determined by LC-MS.

The LC-MS followed the same set-up as in the publication of Airaki et al. (2011). Sample separation was achieved by an Atlantis T3 column (3 × 150 mm, 3 μm, Waters). GSH, GSSG and GSNO were separated with through a mixture of acetonitrile : H2O (5 : 95) with 0.1% trifluoroacetic acid during 14 min at 0.6 mL min^{-1}. The effluents from HPLC (high performance liquid chromatography) were then introduced to MS by a orthogonal Z-spray electrospray interface. The ionization source temperature and desolvation gas temperature were 120 ℃ and 350 ℃, respectively. The cone gas flow rate was 600 h^{-1} and the desolvation gas flow rate was 1 h^{-1}. To optimize the MS parameter 10 ppm of GSH, GSSG and GSNO in 0.1 M HCl were continuously infused in MS. The compound detection was performed in positive ionization form.

2.8 Biotin-switch assay

The biotin-switch technique (BST) was applied to detect *S*-nitrosylated proteins (Jaffrey and Snyder, 2001). Different plant samples (0.5g) were extracted with 500 µL HEN buffer (250 mM HEPES (4-(2-hydroxyethyl)-1-piperazineethanesulfonic acid), 1 mM EDTA, 0.1 mM Neocuproine, protease inhibitor (cOmplete^{TM}, EDTA-free protease inhibitor (Roche)) and 0.5% (v/v) Triton, pH = 7.7) and stored in black Eppendorf tubes to avoid light exposure. The total protein concentration was analysed by the BCA method (bicinchoninic acid protein assay; BCA Protein Assay Kit II, BioVision^{TM}) using BSA (Bovine serum albumin) as the standard protein. Total protein (50 µg) was incubated with blocking solution (250 mM HEPES, 1 mM EDTA, 0.1 mM Neocuproine, 5% SDS (Sodium dodecyl sulfate polyacrylamide), 0.4 M NEM, pH = 7.7) in a 55 ℃ water bath for 20 min (with shaking every 5 min). After the blocking procedure, a two-fold volume of 100% ice-cold acetone was then added into the mixture of protein and blocking buffer. After acetone precipitation, the supernatants were discarded, and the pellets were washed with 75% acetone, then dryed out in a 37℃ incubator. The pellets were then dissolved in HEN buffer (1X HEN and 1% SDS). These protein samples were then separated into two Eppendorfs. In one Eppendorf, the mixing of 4mM biotin-HPDP (N-[6-(biotinamido)hexyl]-3'-(2'-pyridyldithio) propionamide) and 0.5mM sodium ascorbate was carried out and other Eppendorf mixing of biotin-HPDP and 0.5mM sodium chloride was undertaken as a negative control. The 500 µL biotinylated mixtures were then incubated under room temperature for one hour, then precipitated with same volume (500 µL) of pure ice-cold acetone. The precipitated proteins were then dried and resuspended in 10 µL 1% SDS and submitted to SDS-PAGE (sodium dodecyl sulfate polyacrylamide gel electrophoresis) and applied anti-biotin HRP-linked (horse radish peroxidase) antibody for Western blots (described in section 2.9).

2.9 SDS-PAGE and Western blots

A loading buffer was added to protein samples to a final concentration of 50 mM Tris-HCl (pH=6.8), 2% SDS, 0.02% bromophenol blue and 10% glycerol. The mixtures were then loaded onto a sel-cast SDS-PAGE gel. The self-cast SDS-PAGE gel was made of a 2.5 mL 4% stacking gel (0.625 mL 0.5M Tris-HCl (pH=6.8), 25 μL 10% SDS (w/v), 0.335 mL Acrylamide/Bis-acrylamide (30%/0.8%, w/v), 12.5 μL 10% ammonium persulfate (APS, w/v) and 2.5 μL 99% tetramethylethylenediamine (TEMED)) and a 7.5 mL 10% running gel (1.875 mL Tris-HCl (pH=8.8), 75 μL 10% SDS (w/v), 2.425 mL Acrylamide/Bis-acrylamide (30%/0.8%, w/v), 37.5 μL 10% APS (w/v) and 5 μL 99% TEMED). The protein samples were running in stacking gel with constant voltage (70V) until all samples stacked in line at the top of the running gel. Proteins samples were then separated in running gel with 140V. The SDS-PAGE gels were then subjected to the Coomassie Blue staining or western blot.

Coomassie Blue staining was used to compare the loading concentration of total protein. The gels were incubated in the staining solution (0.25% Brilliant Blue R, 40% methanol and 7% acetic acid) for 30 min and then destained overnight in the destaining solution (40% methanol and 10% acetic acid).

For Western blots, total proteins on the SDS-PAGE gels were transferred onto a nitrocellulose membrane overnight at a constant voltage (20V) in 4℃. The transferred membrane was washed with phosphate-buffered saline (PBS) with 0.1% TWEEN®20 (PBS-T) for two minutes. The washed membrane was then blocked with 2% BSA in PBS-T at room temperature for one hour. After blocking, the membrane was incubated with anti-Biotin HRP-

linked antibody in PBST at room temperature for one hour. The membrane was washed with PBST four times in an hour to remove the excess of antibody. After washing, the membrane was subjected to the chemiluminescent detection for the biotinylated proteins. The chemiluminescent signals were detected on X-ray film after adding SuperSignal West Pico/Dura Chemiluminescent Substrate (Thermo Scientific) on to the membrane.

2.10 Hydrogen peroxide quantification

Potassium iodide (KI) assay was used for hydrogen peroxide quantification in *Arabidopsis*. 4-week-old plants were weighed and extracted with 0.1% tricholoroacetic acid (TCA, Sigma). After homogenisation with TCA, the extracts were centrifuged at 10,000 ×g at 4 ℃ for 20 min and the supernatant retained.

The KI method was modified according to Loreto and Velikova (Loreto and Velikova, 2001). The 250 μL of plant extracts were diluted with 250 μL of 10 mM phosphate buffer (pH = 7.0) and mixed with 500 μL of 1M KI. The mixtures were then measured and the absorbance readings taken at 390 nm by spectrophotometer. H_2O_2 quantification was undertaken by a calibration curve using a known concentration of pure H_2O_2 (Sigma).

2.11 Hydroxyl radical detection and quantification

The spin trap electronic paramagnetic resonance (EPR) assay was used to detect the hydroxyl radical and was modified according to Renew et al (2005). *Arabidopsis* plants were sterilised and seeded on MS agar. The one-week-old seedlings were collected for EPR assay.

50 mg of seedlings were homogenised and incubated in 200 μL 20 mM phosphate buffer (pH = 7.0) with spin trap 50 mM 4-POBN (4-pyridyl l-oxide N-tert-butylnitrone) and 10% (v/v) ethanol which are used to stabilise hydroxyl radicals. The mixtures were sonicated for 10 minutes then left at room temperature for 50 minutes for the detection of hydroxyl radical production post-mortem.

EPR measurements were performed by the X-band EPR spectrometer (Magnettech MS-200, Berlin, Germany). The samples after incubation were centrifuged at 10,000 xg for 5 minutes to precipitate the debris. 50 μL of supernatant was drawn into a capillary tube (Braubrand, VWR UK) and sealed with soft sealant (Cristaseal, VWR International, UK). Spectra were recorded at room temperature with 9.717 GHz microwave frequency, 100 kHz modulation frequency, modulation amplitude 2G and 63 mW microwave power (Renew et al., 2005). The EPR intensity was expressed on an arbitrary scale based on the area under the spectrum curve and intensities of different samples were calculated by the programme Multiplot.

2.12 *In vitro* assay of chemical interactions

GSNO was generated by a simple chemical method. 50 mL of reduced glutathione (625mM, dissolved in 625mM HCl) was mixed thoroughly with equal molar amount of $NaNO_2$ (final concentration to 625mM) for 10 minutes at 4℃ temperature. After the reaction, a 2.5 volume (125mL) quantity of acetone was added to the mixture to crystallise the GSNO with constant stirring for more than 40 minutes at 4℃. The synthesised GSNO (fine pale pink powder) was filtered off. The remaining GSNO powder was washed with ice-cold water 5 times, followed by acetone for 3 times and finally, diethylether 3 times at 4℃. The GSNO powder was air-

dried in the dark in a laminar flow cabinet (Hart, 1985). GSNO has a characteristic *S*-glutathiol absorption peak in UV region at 335 nm in aqueous solutions and its molar extinction coefficient is 922 M^{-1} cm^{-1} (Broniowska et al., 2013). Therefore, purity of self-made GSNO can be examined with simple photometric techniques. The purity of GSNO obtained was around 70 % (w/w).

Determination of the degradation of GSNO by hydroxyl radicals was performed by mixing pure chemicals *in vitro*. Synthesised GSNO, H_2O_2 and $FeSO_4$ were used to examine these chemicals' interactions. The the photometer's photometric absorbance range (GeneQuant 1300, Cambridge, UK) is up to 2.5 A which equivalents to 2.75 mM GSNO. Therefore, the concentration of GSNO at start of chemical interaction was setting to around 2.65 mM. H_2O_2 provided a source for hydroxyl radicals and the $FeSO_4$ triggered the Fenton reaction to produce these molecules. The pure chemicals (H_2O_2, $FeSO_4$ and GSNO) were mixed with different combinations as listed in table 2.3. After mixing the three chemicals in different combinations, the GSNO concentrations were examined by the spectrophotometer (OD_{335}). The mixtures were incubated on ice and in the dark, and the GSNO concentrations were analysed by spectrophotometer (OD_{335}) hourly after incubation.

Table 2. 3. The chemical combinations the spectrophotometer assay for the GSNO contents.

Combination	1	2	3	4
GSNO	+	+	+	+
H_2O_2	−	+	−	+
$FeSO_4$	−	−	+	+

The final concentrations of three chemicals for the start of the reaction are 3mM for GSNO, 10mM for H_2O_2 and 10nM for FeSO4. + stands for add; − stands for missing.

To determine if GSNO could function as a scavenger of hydroxyl radicals, GSNO, H_2O_2 and $FeSO_4$ were mixed in various combination listed in table 2.4. After incubation at 4 ℃ for 1 hour, the mixtures were examined for the content of hydroxyl radicals by EPR method.

Table 2. 4. The chemical combinations of the EPR assay for the hydroxyl radical contents.

Combination	1	2	3	4	5	6	7
GSNO	+	−	−	+	+	−	+
H_2O_2	−	+	−	+	−	+	+
$FeSO_4$	−	−	+	−	+	+	+

The final concentrations of three chemicals for the start of the reaction are 10mM for GSNO, 10mM for H_2O_2 and 10nM for $FeSO_4$. + stands for add; − stands for missing.

2.13 Statistical analysis

All statistical analyses were undertaken using the statistical interface RStudio, which is based on the R language (RStudio). The statistical analysis results are presented in the results section.

Chapter-3 Investigating the other redox-related mutants on suppressing the developmental phenotype of *gsnor1-3* plant

3.1 Introduction

S-nitrosylation is thought to contribute to the control of plant growth and development. It has been **r**eported that loss- or gain-of-function of a key regulator of *S*-nitrosylation, nitrosoglutathione reductase (GSNOR), impacted the morphology of *Arabidopsis* (Kwon et al., 2012**;** Lee et al., 2008). Moreover, loss-of-function GSNOR mutant (*gsnor1-3*) plants had significant loss of apical dominance (Kwon et al., 2012). Also, the first order lateral shoots had greatly reduced fresh weight and increased numbers per plant. This remarkable phenotype makes *gsnor1-3* plants an effective tool for a suppressor screen to identify mutations that suppress excessive S-nitrosylation in *Arabidopsis*.

Based on the advantage of the *gsnor1-3* phenotype, a suppressor screening was performed with ethyl methane sulfonate (EMS) which identified two mutations, *snoplough*7 (*spl7*) and *spl8* that recover the loss of apical dominance in *gsnor1-3* plants (Sorhagen, 2011). The so-called *spl* suppressors identified mutation sites are both located on chromosome 1 within the *CAT3* gene (Brezezek, 2013). These findings suggest that disturbing the redox status controlled by CAT3 may trigger the suppression of increased cellular *S*-nitrosylation. Therefore, other proteins that control ROS levels are further candidates for potential suppression of *S*-nitrosylation.

Several redox-related enzymes are reported to be *S*-nitrosylated which might subsequently modulate their enzyme activity. To overview the potential relationship between redox regulation and *S*-nitrosylation, a graphic of redox regulation is presented in the Fig.3.1. The

figure illustrates redox-related enzymes that might be connected to *S*-nitrosylation. Peroxiredoxins (Prx) are a group of redox-regulated enzymes which detoxify peroxynitrite ($ONOO^-$) and hydrogen peroxide (H_2O_2). During the interaction of *Pseudomonas syringae* pv. *tomato* (*Pst*), PrxII E was shown to be *S*-nitrosylated (Romero-Puertas et al., 2007). *S*-nitrosylation of PrxII E impaired its activity against $ONOO^-$. Ascorbate peroxidase has also been found to be *S*-nitrosylated with the addition of *S*-nitrosoglutathione (GSNO) in *Arabidopsis* and its enzyme activity increased after *S*-nitrosylation (Yang et al., 2015).

In redox regulation, glutathione is a major redox couple controlling the redox environment. GSH exists in two different forms; a reduced form (GSH) and a thiol linked oxidised form (GSSG). Moreover, GSH can actively bind with NO to form GSNO. Recent reports suggest GSNO is the major NO donor during the process of *S*-nitrosylation (Liu et al., 2001). The phytoalexin-deficient mutant *pad2-1* is defective in a γ-glutamylcysteine synthetase which is required for the first step of GSH biosynthesis (Parisy et al., 2006). Besides the deficiency of GSH, *pad2-1* mutants are also impaired in the production of H_2O_2 and NO during pathogen challenge (Dubreuil-Maurizi et al., 2011).

Ascorbate, the most abundant low molecular weight antioxidant in plant cells, performs key functions in plant biology. As an antioxidant, ascorbate is able to reduce superoxide, singlet oxygen and hydroxyl radicals directly (Smirnoff, 2000). Besides its antioxidant character, ascorbate serves as a substrate for several enzymatic reactions such as ethylene production (McGarvey and Christoffersen, 1992). Four ascorbate-deficiency mutants, *vtc1*, *vtc2*, *vtc3* and *vtc4* have been identified (Conklin et al., 2000). These result in defects related to ascorbic acid synthesis which converts glucose to ascorbic acid (Wheeler et al., 1998). *vtc1* and *vtc2* decrease ascorbate by about 70% compared with wild-type (Colville and Smirnoff, 2008). The *vtc* mutants have been found to show elevated: H_2O_2, salicylic acid (SA) and *PR1* gene expression

(Mukherjee et al., 2010). Furthermore, the *vtc2* mutant was found to show signs of oxidative stress such as lipid peroxidation after high light treatment (Müller-Moulé et al., 2003).

Thioredoxins (TRX) are small proteins that serve as antioxidants and are involved in redox regulation in all organisms. In *Arabidopsis thaliana*, at least 20 TRX sequences have been reported (Gelhaye et al., 2005) and they are expressed in a variety of tissues (Meyer et al., 2005). TRX serves numerous roles during plant oxidative stress responses, such as being a modulator of enzyme activity in repair and detoxication of DNA damage, or as a supplier of reducing power for detoxification of lipid peroxidation (Santos and Rey, 2006). Interestingly, the TRX reduction system is reported to denitrosylate SNO proteins (Benhar et al., 2010); (Kneeshaw et al., 2014). Based on structural studies, thioredoxin *h* proteins are the largest group of thioredoxins in *A. thaliana* cytosol (Gelhaye et al., 2003). Among all *Trx-h* genes, *Trx-h3* is the most abundantly expressed at a basal level while *Trx-h5* is highly induced during pathogen challenge (Reichheld et al., 2002).

The identification of *cat3* as a suppressor of *gsnor1-3* suggests that perturbations of redox state might impact on *S*-nitrosylation regulation. Thus, we reasoned that loss of function for other redox-related proteins might also suppress elevated cellular *S*-nitrosylation.

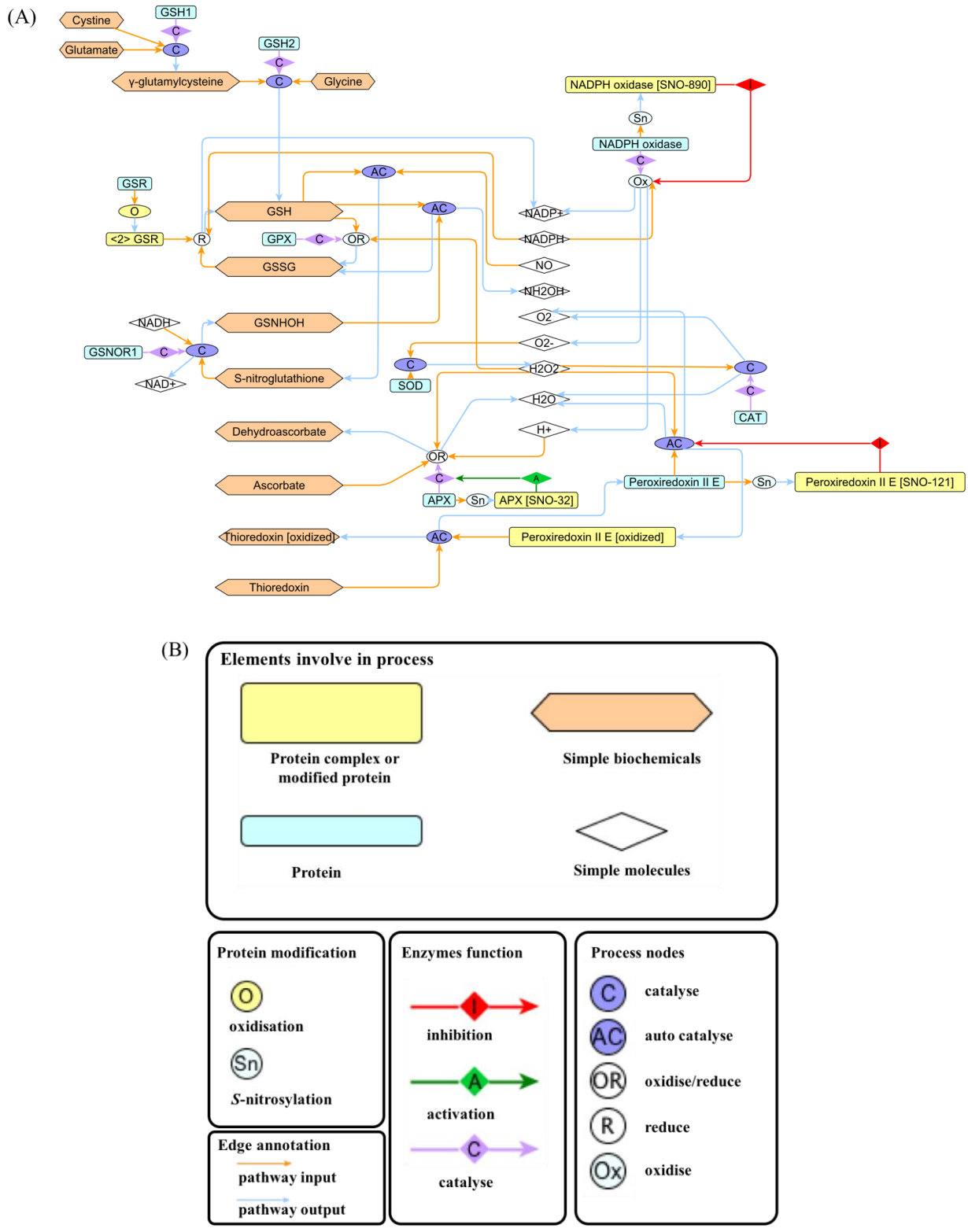

Figure 3.1. Redox regulation in *Arabidopsis*
(A) Modified Edinburgh Pathway Notation (mEPN) map illustrating redox couples and enzymes in relation to S-nitrosylation. (B) Symbols and their related terms used in the mEPN graphic. The map were generated by diagramming program yEd and followed the mEPN notation (Freeman et al., 2010).

3.2 Mutations within other redox-related genes do not suppress *atgsnor1-3*

To investigate if other redox-related mutations could suppress *atgsnor1-3*, the other redox-related mutants, *pad2-1, vtc2-1, trx3* and *trx 5*, were crossed with *gsnor1-3* plants to generate the corresponding double mutants. *pad2-1* impairs GSH synthesis, while *vtc2-1* has deceased ascorbate content. The *trx3* and *trx5* mutants contain T-DNA insertions within *TRX-h3* and *TRX-h5*, respectively. The *gsnor1-3 pad2-1*, *gsnor1-3 trx3* and *gsnor1-3 trx5* mutants were generated and confirmed the genotype by Kerstin Brezezek (2013). The production and confirmation of the *gsnor1-3 vtc2-1* was obtained in this thesis.

The developmental phenotype of these double mutants is shown (Fig.3.2). This figure shows all the redox-related double mutants: *gsnor1-3 pad2-1*, *gsnor1-3 vtc2-1*, *gsnor1-3 trx3* and *gsnor1-3 trx5*. Unlike the morphology of *gsnor1-3 cat3* (Fig.3.2), the other redox-related double mutants had no significant differences compared with the morphology of *gsnor1-3*.

To further explore the phenotypic details of these other redox-related double mutants, three developmental indexes, numbers of 1st order primary shoots, shoot weight and primary shoot length, were recorded from 8-week-old plants (Fig.3.3, 3.4 and 3.5). Most of the redox-related double mutants had no significant differences compared with *gsnor1-3* mutants. Interestingly, the double mutant *gsnor1-3 trx3* decreased the numbers of 1st order primary shoots to a level similar to that of wild type. Besides the morphology on the numbers of 1st order primary shoots, all other redox-related mutants showed no significant differences related to shoot weight or primary shoot length.

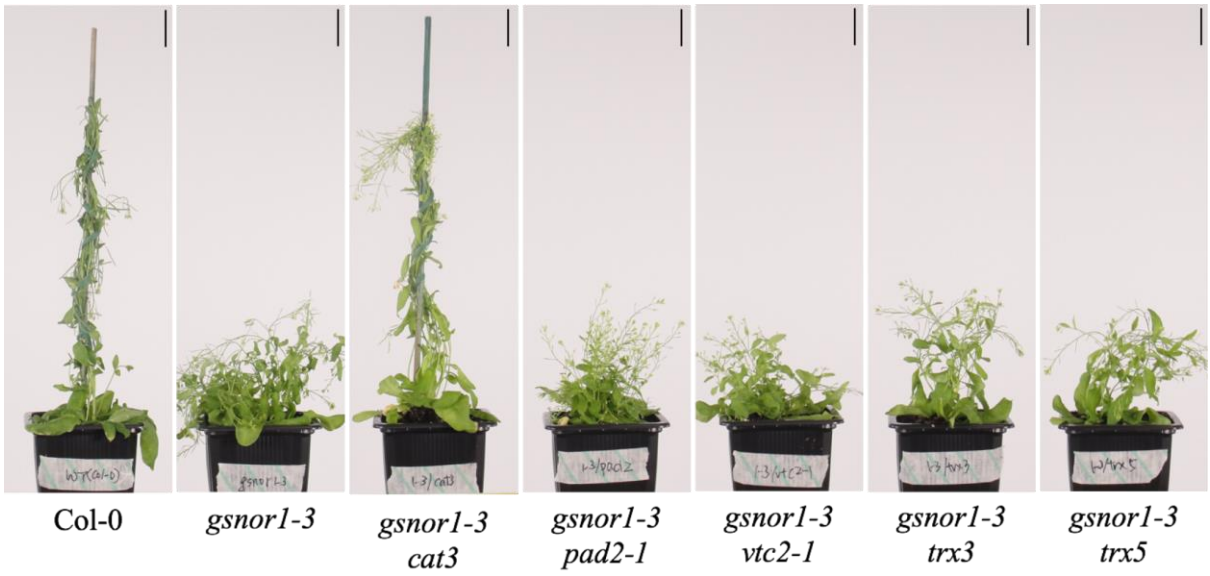

Figure 3.2. Morphology of redox-related double mutants in a gsnor1-3 background.
After 8 weeks of growth, the redox-related double mutants were photographed. The scale bars represent 1 cm.

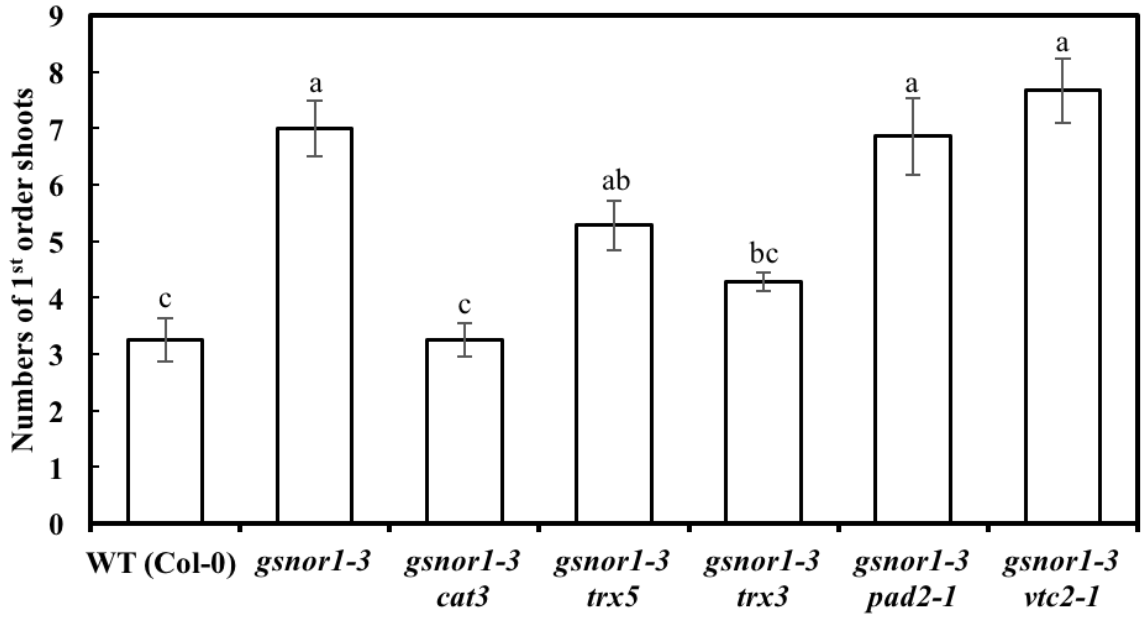

Figure 3.3. The numbers of 1st order shoots of redox-related double mutants.
The numbers of 1st order shoots were measured after 8 weeks of growth. Error bars represent standard error (n=8 or 7). Values with different letters are significantly different ($p < 0.01$, LSD (least significant difference) multiple test).

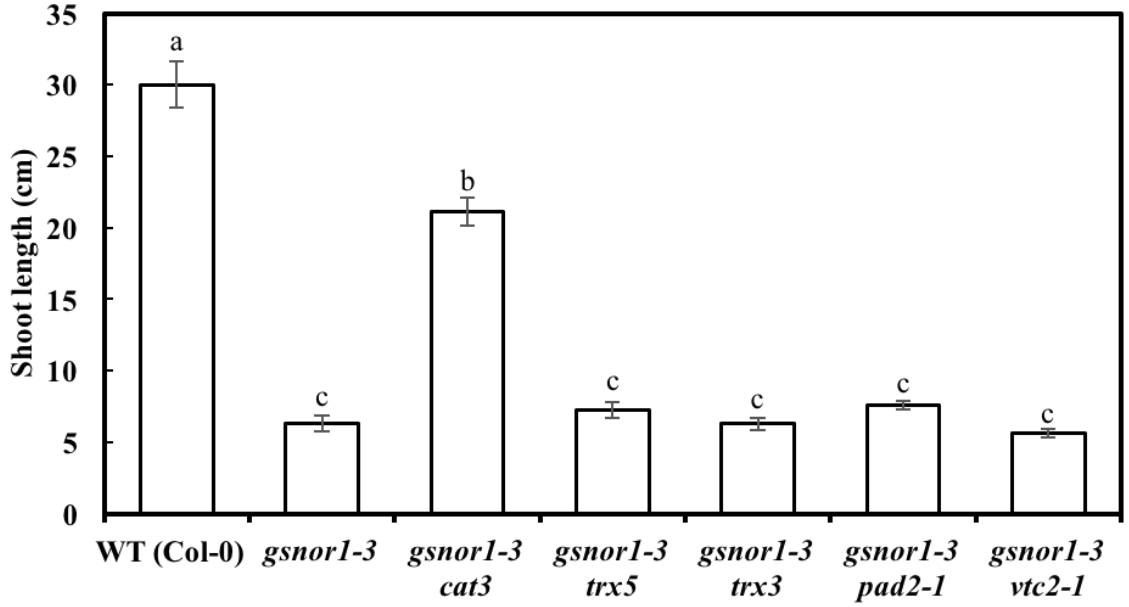

Figure 3.4. The shoot length of redox-related double mutants.
The shoots length was measured after 8 weeks of growth. Error bars represent standard error (n=8 or 7). Values with different letters are significantly different ($p < 0.01$, LSD multiple test).

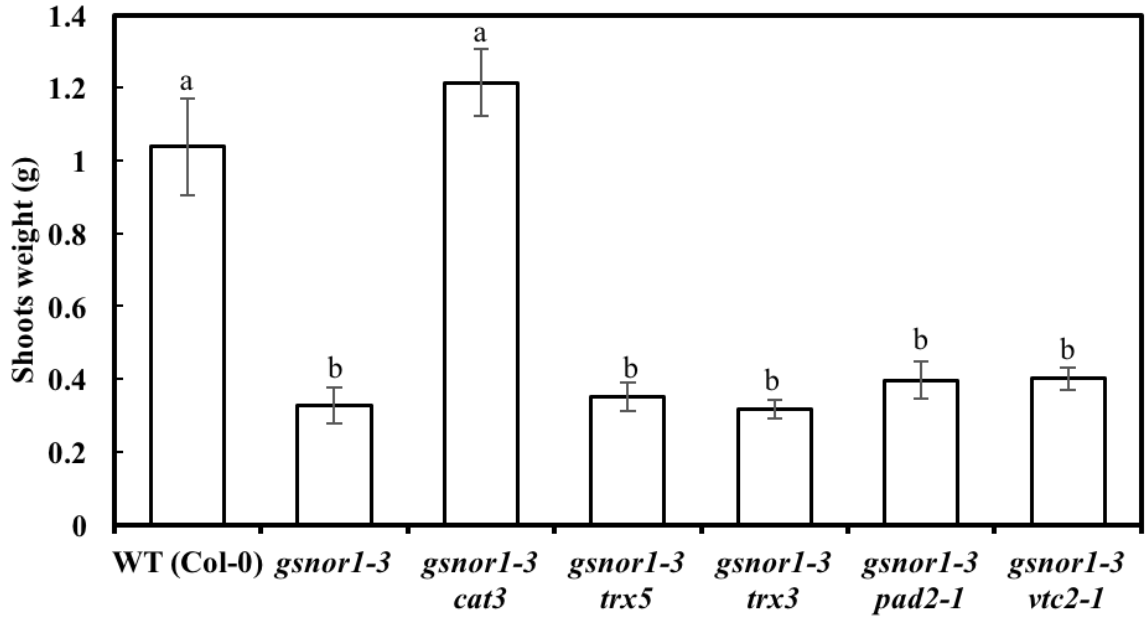

Figure 3.5. The shoot weight of redox-related double mutants.
The shoots weight was measured after 8 weeks of growth. Error bars represent standard error (n=8 or 7). Values with different letters are significantly different ($p < 0.01$, LSD multiple test).

3.3 Discussion

Mutations in other redox-related genes did not generally suppress *gsnor1-3*-dependent phenotypes. Ascorbate and glutathione are the heart of the redox hub and contribute to the homoeostasis of redox status (Foyer and Noctor, 2011). A deficiency of glutathione in *pad2* mutants and ascorbate in the *vtc2-1* mutant has been reported to change the redox state resulting from the accumulation of ROS in *A. thaliana* (Parisy et al., 2006; Conklin et al., 2000). Mutations which perturb GSH and ascorbate production result in redox disturbance, which might lead to redox changes similar to *cat3* mutants. However, a reduction in either of these two antioxidant molecules did not supress *gsnor1-3*. Thus, the double mutants *gsnor1-3 pad2-1* and *gsnor1-3 vtc2-1* have no significant morphological differences compared with *gsnor1-3* mutants which reveal these molecules may not be linked to the regulation of *S*-nitrosylation.

The double mutants *gsnor1-3 trx3* mediated recovery towards wild-type levels for the number of 1st order primary shoots. In the study of the *TRX h* gene family expression, transgenic *A. thaliana TRXh* gene promoters fusion with β-glucosidase (*GUS*) were used to demonstrate the expression pattern of these genes (Reichheld et al., 2002). The result showed four *TRXh* genes (*TRXh1, TRXh3, TRXh4* and *TRXh5*) are mostly expressed in the vascular tissues and *TRXh3* is the highest expressed among all *TRXh* genes. These observations suggest the *TRXh* gene family may play a role in redox regulation in vascular tissues. Interestingly, *CAT3* has been found to be specifically expressed in vascular tissues (Hu et al., 2010). The expression pattern of both *CAT3* and *TRXh* genes suggests redox regulation in the vascular tissues may relate to the regulation of *S*-nitrosylation.

Vascular tissues are essential for plant biology since they provide mechanical support and facilitate the transport of water, nutrients, hormones and signalling molecules. The apical dominance of *A. thaliana* is orchestrated by three hormones (auxin, cytokinin and strigolactone)

which are transported throughout the plant by the vascular tissues (Domagalska and Leyser, 2011). *S*-nitrosylation of TRANSPORT INHIBITOR RESPONSE1/AUXIN SIGNALLING F-BOX (TIR1/AFB) enhances the interaction of TIR1-auxin and results in degradation of auxin (Terrile et al., 2012). Moreover, auxin signalling and polar auxin transport are compromised by excessive *S*-nitrosylation and GSNO (Shi et al., 2015). The degradation of auxin will trigger the growth of secondary roots. Auxin controls the shoot apical dominance and inhibits the secondary shoot development (Dun et al., 2006). Likewise, the TRX redox regulation system has also been reported to influence auxin transport and metabolism (Bashandy et al., 2011). Their results demonstrated the *ntra ntrb* (NADPH thioredoxin reductase) plants increase auxin levels and auxin transport. The absence of *TRX3* genes may result to the accumulation of auxin and consequently mutualise the effect on auxin degradation in *gsnor1-3*. Therefore, the number of primary shoots in *gsnor1-3 trx3* was decreased compared to *gsnor1-3* plants.

On the other hand, the shoot length and shoot weight of *gsnor1-3 trx3* plants was not significantly different compared with *gsnor1-3* plants. Recently, TRX proteins have been shown to directly denitrosylate protein targets (Kneeshaw et al., 2014). This study demonstrated that *S*-nitrosylated bovine serum albumin (BSA) can be denitosylated with a combination of TRX and NADPH-dependent TRX reductase. It is possible that the absence of TRX might result in an increase in the level of *S*-nitrosylation and thus counter a possible increase in oxidative stress due to the loss of Trx function, which might suppress excessive *S*-nitrosylation in *gsnor1-3* plants. It might thus be informative to examine the *S*-nitrosylation level in both *trx3* and *gsnor1-3 trx3* plants. However, TRX proteins have been classified in 15 subgroups based on their sequences similarity (Meyer et al., 2006). Therefore, TRX proteins are likely functionally redundant, thus masking the possible impact of TRXh3. In this context, *gsnor1-3 trx3* only recovered the number of 1st primary shoots. This rather limited impact on

the shoots of *gsnor1-3* plants suggests that the absence of TRXh3 is not a key feature in suppressing *S*-nitrosylation.

Collectively the morphology results indicate that mutation in *CAT* plays an important role to suppress developmental phenotype in *gsnor1-3* plants. The double mutants *gsnor1-3 pad2-1* and *gsnor1-3 vtc2-1* showed no significant changes compared with *gsnor1-3* plants. These results suggest that GSH and ascorbate production are not relevant to the regulation of *S*-nitrosylation regarding plant development. The double mutant *gsnor1-3 trx3* partly reversed the developmental defects of *gsnor1-3* plants. *TRXh3* is predominantly expressed in vascular tissues which is similar to *CAT3*. The similar expression pattern of *TRXh3* and *CAT3* genes suggests vascular tissues might play an important role during the *S*-nitrosylation regulation. However, *trx3* conveys only a limited reversal of the shoot morphology of *gsnor1-3* plants back to wild-type. Thus, *TRXh3* may not be a key factor to regulate excessive *S*-nitrosylation. These results suggest *CAT3* is a major factor related to *S*-nitrosylation. The mutation of other *CAT* paralogs may also mediate similar suppression of excessive *S*-nitrosylation in *gsnor1-3* plants and will be investigated for the following chapter.

Chapter-4 Investigating the impacts of *cat3* and its paralogs *cat1* and *cat2* in *gsnor1-3* plants' morphology

4.1 Introduction

Catalases were the first antioxidant enzymes discovered to be conserved in all complex organisms. This enzyme was first discovered and named by Loew (1900) and found to turn over H_2O_2. Besides its presence in aerobic organisms, some anaerobes are also known to have catalase (Zamocky et al., 2008). Catalases are haem-dependent enzymes which consist of various 50-70 kDa polypeptides which form into tetramers (Regelsberger et al., 2002). Previous studies have demonstrated that catalases act by generating O_2 and H_2O from H_2O_2 in distinct steps (Kato et al., 2004). Binding with haem-iron is essential for catalase activity (Mhamdi et al., 2012). Phylogenetic classification of catalase sequences has been reported (Zamocky et al., 2008) and the genomic information suggests that most animals contain only one catalase gene. Unlike animals, plants including dicots and monocots all contain three catalase genes (Mhamdi et al., 2010a). According to expression patterns and physiological effects, plants' catalases have been categorised to three classes (Willekens et al., 1997). Class I catalases are strongly expressed in photosynthetic tissues such as leaves and are thought to scavenge H_2O_2 generated during photorespiration. Class II catalases are mainly expressed in vascular tissues and their function is related to lignification and stress responses (Orendi et al., 2001). Class III catalases are notably expressed in reproductive tissues such as pollen and seeds and help eliminate H_2O_2 during fatty acid degradation (Willekens et al., 1997).

In *Arabidopsis*, three catalase genes have been identified: class I catalase *CAT2*, class II catalase *CAT3* and class III catalase *CAT1*. Information from the *Arabidopsis* genome sequence

has demonstrated that *CAT1* and *CAT3* are located on chromosome 1, and *CAT2* is located on chromosome 2 (Frugoli et al., 1996). These three catalase genes all encode 492 amino acid and highly conserved proteins (Mhamdi et al., 2010a). CAT2 is the most abundant catalase and is expressed in leaves while CAT3 expresses specifically in vascular tissue (Hu et al., 2010). Interestingly, the day-night circadian expression pattern of *CAT2* and *CAT3* are distinct: while *CAT2* expresses with a morning-specific phase, *CAT3* is expressed with an evening-specific phase (Zhong and McClung, 1996). Moreover, the two *CAT* genes express differently depending on the age of plant with CAT2 activity declining during plant bolting, while CAT3 expression is increased with age and senescence (Zimmermann et al., 2006). *CAT1* is expressed in the reproduction tissues such as pollen and this protein is more abundant during the early stage of seedling growth and the late stages of senescence (Hu et al., 2010; Zimmermann et al., 2006). In T-DNA insertion CAT mutants, total catalase activities of *cat1*, *cat2*, *cat3* and *cat2 cat3* mutant lines decreased to 92%, 24%, 83% and 7% of wild-type activities, respectively (Hu et al., 2010).

As a major player in preventing excessive H_2O_2 accumulation, *cat2* mutation can result in severe impacts on *Arabidopsis* morphology dependent upon growth condition. Under normal irradiance (16 hours light / 8 hours night), *cat2* plants show SA-dependent lesion formation and related responses (Queval and Noctor, 2007). Curled leaves, reduced size and decreased fresh weight are common features of *cat2*. However, the irregular morphology of *cat2* mutants was not exhibited during short-day photoperiods (8 hours light / 16 hours dark) (Chaouch et al., 2010). Despite the clear evidence of oxidative stress in *cat2*, direct evidence of accumulation of H_2O_2 is unclear: while some studies showed no increase, others claimed a two-fold increase in of H_2O_2 in *cat2* leaves (Hu et al., 2010; Mhamdi et al., 2012). Although the level of H_2O_2 in *Arabidopsis* is hard to quantify, the glutathione status indicates the redox perturbation in *cat2* mutants (Queval and Noctor, 2007; Willekens et al., 1997). The loss of

CAT2 function increases the total glutathione level and especially the oxidised form of glutathione (GSSG) (Mhamdi et al., 2010b). Furthermore, transcriptomic analysis of *cat2* plants has revealed the modulation of ethylene and auxin homeostasis (Bueso et al., 2007) suggesting a significant impact of *cat2* on phytohormone signalling.

CAT3, like *CAT2* expression, increases in response to oxidative stress (Orendi et al., 2001). During sucrose starvation, *CAT3* expression and CAT3 activity also increase and the phenomenon is thought to compensate for the oxidative stress from the use of alternative catabolic substrates such as degradation of short-chain fatty acids (Contento and Bassham, 2010). CAT3 and CAT2 both interact with the Salt Overly Sensitive 2 (SOS2) protein in salt-stressed plants, revealing a relationship between H_2O_2 and salt stress (Verslues et al., 2007). However, the expression pattern of *CAT3* is distinct to *CAT2*. C*AT3* has been reported to be up-regulated during leaf senescence while *CAT2* is down-regulated (Zimmermann et al., 2006). CAT3 also modulates the H_2O_2 concentration in the vascular bundles in *Arabidopsis*. CAT3 function has also been linked to plant-pathogen interactions. *Cucumber mosaic virus* (CMV) protein 2b (CMV 2b), a known RNA-silencing suppressor, was reported to interact with CAT3 directly and consequently lead to host necrosis (Inaba et al., 2011). Calcium and calmodulin can bind to CAT3 which enhances CAT3 activity (Yang and Poovaiah, 2002). Recently, a calcium-dependent protein kinase (CPK8) has been identified that can phosphorylate CAT3 and regulate its activity (Zou et al., 2015).

4.2 *cat3* can suppress *gsnor1-3* developmental phenotype

In a screen for mutations that suppress the loss of apical dominance in *gsnor1-3 Arabidopsis* plants, *cat3* was identified (Brezezek, 2013). Thus, we generated the double mutants *gsnor1-3 cat3*, *gsnor1-3 cat2* and *gsnor1-3 cat1* and the triple mutant *gsnor1-3 cat2 cat3* to explore if mutations in other *CAT* genes could also suppress *gsnor1-3*-dependent phenotype.

The *gsnor1-3* line exhibits loss of apical dominance. We therefore determined if this phenotype is suppressed by *cat1*, *cat2*, *cat3* or *cat2 cat3*. The apical dominance of *gsnor1-3* plants was not suppressed by *cat1* or *cat2* (Fig 4.1). Only *gsnor1-3 cat3* and *gsnor1-3 cat2 cat3* reversed the morphology of a loss of apical dominance after 8-weeks-growth. The morphology of these two mutants was similar to the wild type. On the other hand, the double mutants *gsnor1-3 cat2* and *gsnor1-3 cat1* did not show an apical dominance phenotype.

Although the morphology of *gsnor1-3 cat3* and *gsnor1-3 cat2 cat3* had significant changes compared with *gsnor1-3*, the triple mutant *gsanor1-3 cat2 cat3* exhibited shorter shoot length compared with wild type. Thus, the details of shoot development morphology were then examined.

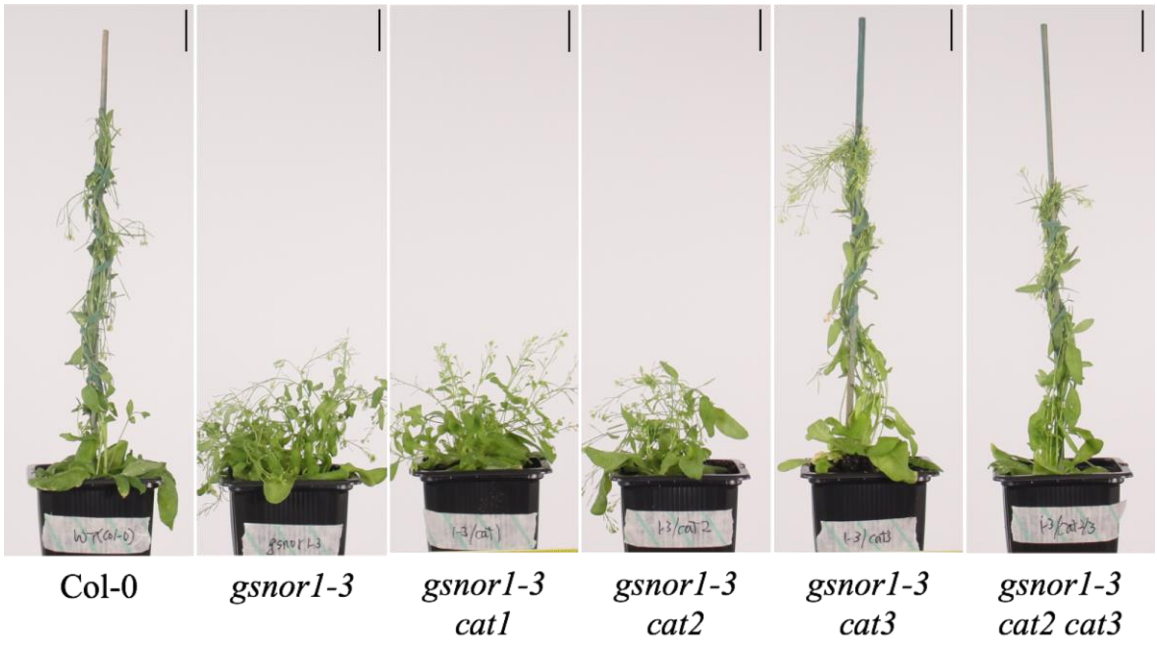

Figure 4.1. Morphology of *CAT* mutation within a gsnor1-3 background.
The stated plant genotypes are shown after 8 weeks of growth and photographed. The scale bars represent 1 cm.

To further investigate the details of the morphology of these double and triple mutants, the numbers of 1st order primary shoots, shoot weight and primary shoot length, were recorded after 8 weeks of growth (Fig.4.2, Fig.4.3 and Fig.4.4). Interestingly, the number of 1st order primary shoots of all the generated double mutants and triple mutants decreased compared with *gsnor1-3* mutants (Fig.4.2). The analysis of shoot weight of these mutants showed that only the weight of *gsnor1-3 cat3* plants increased compared with *gsnor1-3* plants (Fig.4.3). We also measured shoot length (Fig.4.4). The shoot length of *gsnor1-3 cat2* and *gsnor1-3 cat1* plants were not different compared with *gsnor1-3*. However, *gsnor1-3 cat3* and *gnsor1-3 cat2 cat3* plants exhibited a longer shoot length compared to *gsnor1-3* plants. Although the shoot lengths of *gsnor1-3 cat3* and *gsnor1-3 cat2 cat3* were significantly increased compared with *gsnor1-3* plants, they were still shorter than those of wild type plants.

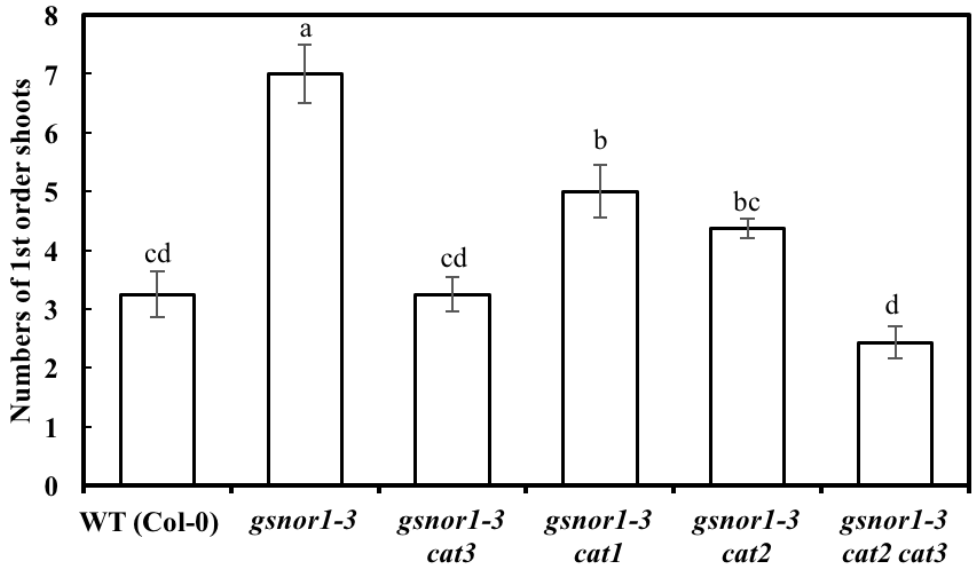

Figure 4.2. The number 1st order primary shoots of gsnor1-3 double and triple mutants. The number of 1st order primary shoots in the indicated plant lines were measured after 8 weeks of growth. Error bars represent standard error (n=8 or 7). Values with different letters are significantly different ($p < 0.01$, LSD multiple test).

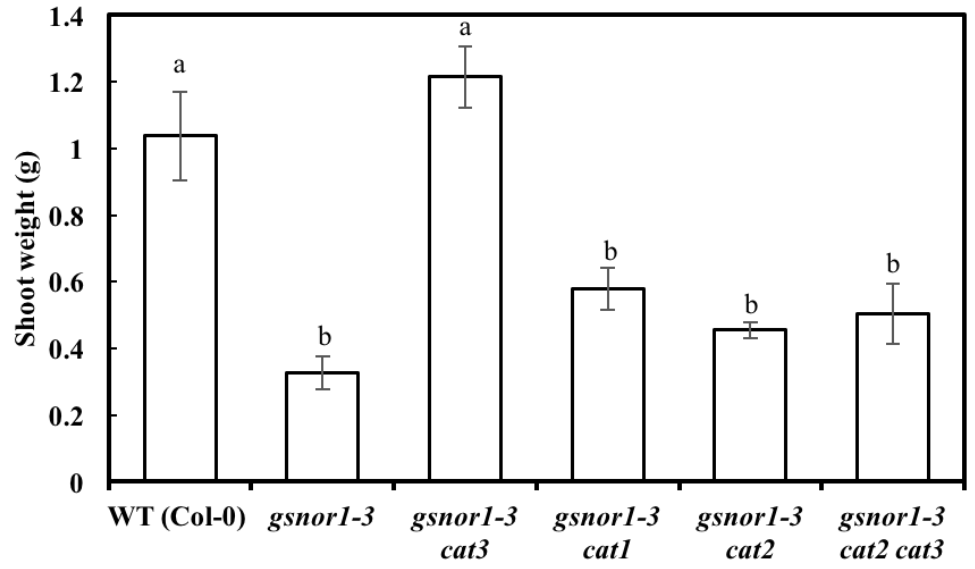

Figure 4.3. The shoot weight of gsnor1-3 double and triple mutants.
The shoots weight in the given in the indicated plant lines were measured after 8 weeks of growth. Error bars represent standard error (n=8 or 7). Values with different letters are significantly different ($p < 0.01$, LSD multiple test).

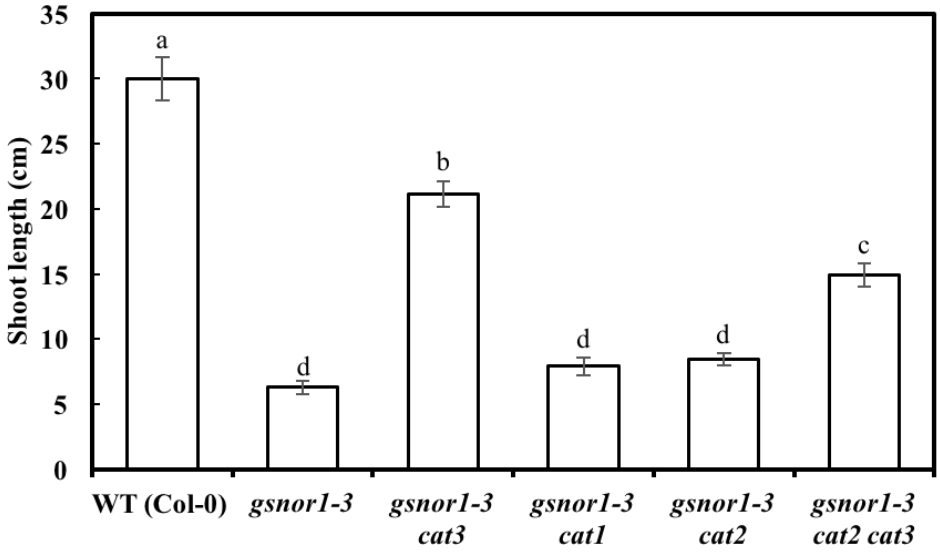

Figure 4.4. The shoot length of gsnor1-3 double and triple mutants.
The primary shoot length in the indicated plant lines were measured after 8 weeks of growth. Error bars represent standard error (n=8 or 7). Values with different letters are significantly different ($p < 0.01$, LSD multiple test).

4.3 Discussion

After crossing the *gsnor1-3* plant with different *CAT* gene mutants, the resulting plants show that *gsnor1-3 cat3* and *gsnor1-3 cat2 cat3* lines were similar to wild-type plants with respect to apical dominance. Although *gsnor1-3 cat2 cat3* had wild-type morphology, *gsnor1-3 cat2* were similar to *gsnor1-3* with respect to loss of apical dominance. In addition, *gsnor1-3 cat1* plants were also similar to *gsnor1-3* with respect to loss of apical dominance. This suggests that the *cat2* and *cat1* mutations may not able to suppress *gsnor1-3* dependent shoot developmental phenotypes. On the other hand, the image of *gsnor1-3 cat3* suggests that *cat3* can suppress *gsnor1-3* dependent shoot developmental phenotypes.

The number of 1st order primary shoots showed notable changes on *gsnor1-3 cat1, gsnor1-3 cat2, gsnor1-3 cat3* and *gsnor1-3 cat2 cat3* mutants relative to *gsnor1-3* plants. Previous

research suggested that *CAT* gene expression is triggered by the plant hormone auxin (Guan and Scandalios, 2002). All *gsnor1-3 cat* double mutants and the *gsnor1-3 cat2 cat3* triple mutant exhibited decreased 1st order primary shoots compared with *gsnor1-3* plants. In contrast, *gsnor1-3 cat1* plants had higher numbers of 1st order primary shoots compared with wild-type. CAT1 contributes to around 5% of total catalase activity (Hu et al., 2010). In addition, the expression of *CAT1* is restricted to reproductive tissues such as seeds and pollen (Willekens et al., 1997). Accordingly, the lack of *CAT1* did not significantly affect the morphology of *gsnor1-3* plant. However, the catalase activity of *gsnor1-3 cat1* is needed to provide further evidences.

In our results, the numbers of 1st order primary shoots of *gsnor1-3 cat3*, *gsnor1-3 cat2* and *gsnor1-3 cat2 cat3* were similar to wild type. However, in *gsnor1-3 cat1* plants, the number of 1st order primary shoots was higher than wild type and lower than *gsnor1-3* mutants. Moreover, *gsnor1-3 cat3* and *gsnor1-3 cat2 cat3* plants increased shoot length and shoot weight compared with *gsnor1-3* mutants while *gsnor1-3 cat2* and *gsnor1-3 cat1* plants are similar to *gsnor1-3* plants. CAT3 activity contributes around 17% of total catalase activity, while CAT2 is about 72% of activity (Hu et al., 2010). Additionally, previous work in *gsnor1-3 spl7* and *gsnor1-3 spl8* plant showed around 50% reduction of catalase activity compared with wild-type plant and *gsnor1-3* plant (Brezezek, 2013). This result suggests that changes of redox status from loss of CAT3 function, rather than a more substantial loss from the absence of CAT activity, could be a key element which suppresses the *gsnor1*-3 dependent phenotypes. Therefore, the catalase activities of *gsnor1-3 cat1*, *gsnor1-3 cat2* and *gsnor1-3 cat3* are needed to evaluate.

A key difference between *CAT3* and its paralogs is their transcriptional expression patterns. Firstly, *pCAT3*::*GUS* transgenic lines have demonstrated *CAT3* gene is highly expressed in the vascular tissues (Hu et al., 2010). Interestingly, the *gsnor1-3 spl7* developmental phenotype was complemented to *gsnor1-3* phenotype by the transgenic expression of *pCAT3::CAT2*

(Hussain, 2013). Vascular tissues (both xylem and pholem) are crucial in the plant to transport phytohormones and other small signal molecules such as reactive oxygen species (De Rybel et al., 2015). Further, the plant phloem network is an effective highway for transporting the signalling molecules including disease related signals like jasmonate and salicylic acid (Hedrich et al., 2016). For instance, the FLOWERING LOCUS T protein which is involved in flower induction is transported through phloem (Lucas et al., 2013). CAT3 is suspected to mediate the ROS signalling in vascular tissue. Therefore, the main feature of how *cat3* suppresses *gsnor1-3* may occur in the vascular tissue.

In sum, our results suggest that *CAT3* is a key factor involved in *S*-nitrosylation regulation. Although we cannot completely rule out the roles of the *CAT3*'s paralogs (*CAT2* and *CAT1*) in suppressing *S*-nitrosylation because they had suppressed the numbers of 1st order primary shoots compared to the *gsnor1-3* plants, it is worth focusing on the most significant suppression of at *gsnor1-3* plant phenotypes by *cat3.* In addition, several assumptions have been discussed while comparing differences between *cat3* and mutations of other *CAT* paralogs. First, *CAT3* is especially expressed in vascular tissues, and the lack of *CAT3* expression suppresses all the developmental phenotypes in *gsnor1-3 cat3* compared with *gsnor1-3* plants. These results suggest vascular tissues, where *CAT3* is expressed, might be an important location related to the suppression of developmental phenotype in *gsnor1-3* plants. Secondly, specific redox potential changes might help ameliorate the impact of the irregular developmental phenotype in *gsnor1-3* plants. The loss of CAT3 enzymes decreased 15% of total catalase activity which reduced the redox potential more mildly than the lack of CAT2 but stronger than the absence of CAT1. To prove our speculation, a comprehensive analysis of catalase activity is needed in future work.

Lastly, the results of *cat3* mutations reverse the developmental phenotypes of *gsnor1-3* plants back to wild type which suggest cross talk between the ROS and RNI. The *cat3* mutation

reverses the shoot developmental phenotype of *gsnor1-3* to wild type. The absence of CAT3 activity may result in accumulation of H_2O_2. In addition, the *gsnor1-3* plants had been reported to show increased cellular protein *S*-nitrosothiols (SNO) (Feechan et al., 2005). The ROS and RNI products in *cat3* and *gsnor1-3*, respectively, may interact and consequently reverse the developmental phenotypes to wild type. However, the cross talk of ROS and RNI have been reported to synergistically affect the plant defence responses, in particular in the development of hypersensitive responses (HR) (Delledonne et al., 2001). For example, NO and superoxide radicals ($O_2^{\cdot -}$) form peroxynitrite ($ONOO^-$) which could induce resistance gene expression and trigger the HR responses (Alamillo and García Olmedo, 2001).

Chapter-5 *cat3* suppresses the enhanced disease susceptibility phenotype of *gsnor1-3* plants

5.1 *S*-nitrosylation and plant immunity

The *Arabidopsis thaliana-Pseudomonas syringae* pathosystem is the most comprehensive model in studies of plant-pathogen interactions (Katagiri et al., 2002). *P. syringae* is the pathogen of a wide variety of plants and enters the host tissues through natural openings such as stomata or wounds (Katagiri et al., 2002). The host leaves which are susceptible to *P. syringae* show water-soaked patches leading to necrosis at later stages. The population size of *P. syringae* in host tissues determines the rate of disease progression (Hirano and Upper, 2000).

Programmed cell death (PCD) plays a key role in plant-pathogen interaction (Greenberg et al., 1994). Hypersensitive response (HR) is a form of PCD triggered by resistance (*R*) genes in response to pathogen avirulence factors (Heath, 2000). The accumulation of nitric oxide (NO) (Durner et al., 1998) and reactive oxygen species (ROS) (Grant and Loake, 2000) are a key feature during the early stage of the HR. Previous work has demonstrated that development of the HR is dependent upon the cooperation of NO and H_2O_2 (Delledonne et al., 2001). The HR is tightly related to plant-pathogen interactions and is thought to be a strategy for plants to constrain pathogen growth within a particular area, preventing further infection (Dickman and Fluhr, 2013).

The salicylic acid (SA)-dependent signalling pathway is a key feature of resistance against biotrophic and hemibiotrophic pathogens. SA triggers a complex signal transduction network upon pathogen challenge (Vlot et al., 2009). NPR1 plays a crucial role in the SA-dependent signalling pathway as a transcriptional coactivator of many defence-related genes (Moore et

al., 2011). Of these defence-related genes, *PR1* (*Pathogenesis-Related protein 1*) is known to be a marker of SA-dependent signalling (Luna et al., 2012). According to the gene-for-gene theory, plant *R* genes recognise pathogen *avr* genes and trigger an incompatible response between plant host and the pathogen (Flor, 1971). During the early process of the gene-for-gene interaction, signal molecules including SA will accumulate and trigger related gene expression (Katagiri et al., 2002). Studies of plants expressing the *NahG* gene (encoding salicylate hydroxylase that degrades SA) lead to a decrease in SA, reduced SA-dependent gene expression and consequently decreased resistance (Delaney et al., 1994; Gaffney et al., 1993).

S-nitrosylation is an important regulator of the plant immunity system. *S*-nitrosylation of nonexpresser of pathogenesis-related genes 1 (NPR1) results in NPR1 oligomer formation which decreases the translocation of NPR1 into the nucleus, where it is required for SA-dependent gene expression (Tada et al., 2008). Further, the *S*-nitrosylation of the NADPH oxidase RBOHD, which drives the oxidative burst, inhibits ROS synthesis and constrains pathogen-triggered cell death (Yun et al., 2011). Additionally, several ROS generation/detoxication enzymes including ascorbate peroxidase and peroxiredoxin II E have been show regulated by *S*-nitrosylation (Fares et al., 2011; Romero-Puertas et al., 2007).

As a key regulator of *S*-nitrosylation, GSNOR plays a central role in regulating the plant defence response. Mutations in *GSNOR1* have been found to disable *R* gene-mediated resistance, basal resistance and non-host resistance (Feechan et al., 2005). The loss of GSNOR activity in *Arabidopsis* compromised disease resistance against *Psedomans syringae* DC3000 (*Pst* DC3000) (Feechan et al., 2005). Also, *gsnor1-3* mutants were found to exhibit increased HR cell death when infiltrated with avirulent *Pst* DC3000 (*avr*B) (Yun et al., 2011). Further, *PR1* gene expression is reduced and delayed in *gsnor1-3* plants after *Pst* DC3000 challenge (Feechan et al., 2005). Furthermore, exogenous SA application did not increase *PR1* gene expression in *gsnor1-3* plants, suggesting SA signalling was impaired.

In our research, the deficiency of the *cat3* mutation plays a significant role in decreasing impact of morphology changes exhibited by *gsnor1-3* plants. To explore if *cat3* can suppress the disease related phenotypes of *gsnor1-3* plants we determined the response of this double mutant line to avirulent pathogen challenge.

5.2 Disease-related phenotype of *gsnor1-3 cat3* mutants

The *cat3* mutation in *gsnor1-3 cat3* plants suppressed the developmental morphology of *gsnor1-3* plants. Therefore, we determined if *cat3* can also suppress the immune related phenotypes of *gsnor1-3 cat3* plants. Thus, the plant lines *gsnor1-3, cat3* and *gsnor1-3 cat3* were inoculated with *Pst* DC3000 to score disease resistance. After inoculation, *gsnor1-3* plants exhibited significant disease susceptibility (Fig. 5.1). However, *Pst* DC3000 growth in *gsnor1-3 cat3* plants was reduced compared with *gsnor1-3* plants and was similar to that of wild type plants at 5 days after inoculation. Moreover, other redox-related genes and *CAT3* paralog mutations in *gsnor1-3* showed same disease resistance as *gsnor1-3* (Fig. 5.2). These results suggest that the loss of the *CAT3* suppresses disease susceptibility in *gsnor1-3* plants towards *Pst* DC3000.

The HR cell death response is regulated by *S*-nitrosylation and *gsnor1-3* plants show more rapid and widespread cell death relative to wild-type plants (Yun et al., 2011). We therefore also determined if *cat3* could suppress the cell death associated phenotype of *gsnor1-3* plants. Wild-type Col-0, *gsnor1-3, cat3* and *gsnor1-3 cat3* plants were inoculated with *Pst* DC3000 (*avrB*) to determine the cell death response (Fig. 5.3). Cell death was greatest in *gsnor1-3* plants. In contrast, HR cell death development in double *gsnor1-3 cat3* mutant plants was significantly decreased compared with the *gsnor1-3* line and was similar with that of wild type and *cat3*

plants. The *CAT3* paralog *CAT2* mutation in *gsnor1-3* demonstrated the same HR cell death as *gsnor1-3* (Fig. 5.4). These data imply that *cat3* also suppresses the cell death phenotype of *gsnor1-3* plants.

In addition to scoring the disease-related phenotype, the molecular expression of the SA marker gene, *PR1*, was also analysed in *gsnor1-3 cat3* plants after inoculation with *Pst* DC3000. *PR1* gene expression was determined by RT-PCR (Fig.5.5). Interestingly, *cat3* mutants exhibited constitutive *PR1* expression that was not further induced by virulent *Pst* DC3000 infiltration. *PR1* expression in *gsnor1-3* plants was delayed relative to that in wild-type, with maximal expression at 48 hours post *Pst* DC3000 infiltration, relative to 12 hours for wild-type plants. In contrast, in *gsnor1-3 cat3* plants *PR1* expression exhibited a low basal expression level, followed by maximal induction at 24 hours following *Pst* DC3000 challenge. Thus, *cat3* partially suppresses the delay in *PR1* expression exhibited in *gsnor1-3* plants. Therefore, suppression of disease susceptibility in *gsnor1-3* plants by *cat3* might be conveyed by the accelerated expression of SA-dependent genes.

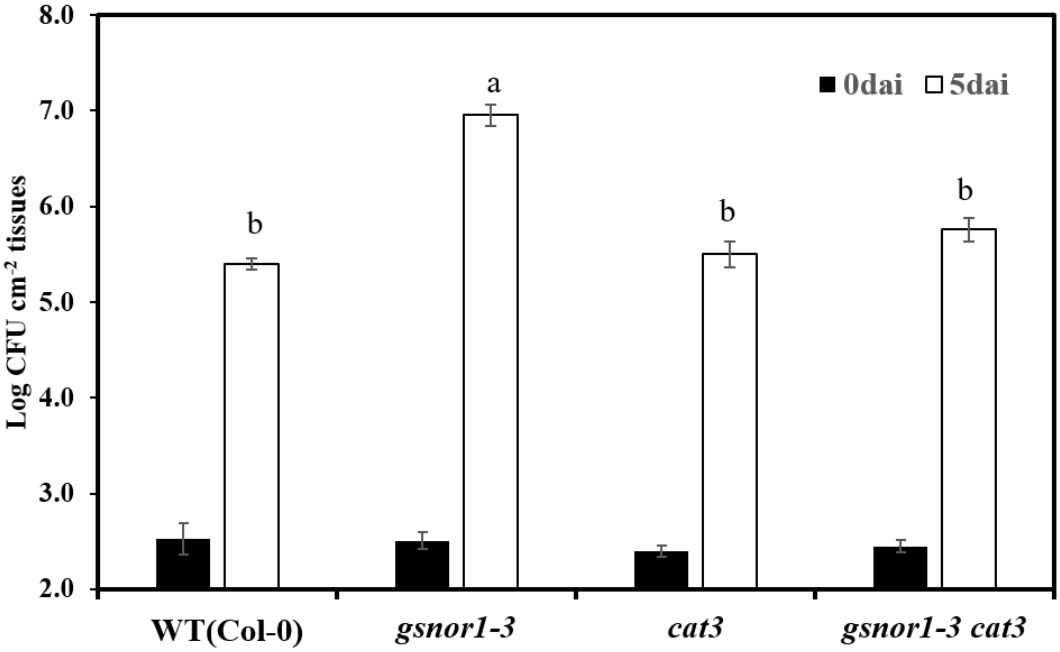

Figure 5.1. The disease resistance of wild-type and *gsnor1-3, cat3* and *gsnor1-3 cat3* *Arabidopsis* challenged with *Pseudomonas syringae* DC3000.
Colonies of *Pst* DC3000 in different plants were calculated after 0 and 5 days post-inoculation. Error bars show the standard error (n=6). Values with different letters are significantly different ($p < 0.05$, LSD multi-group test).

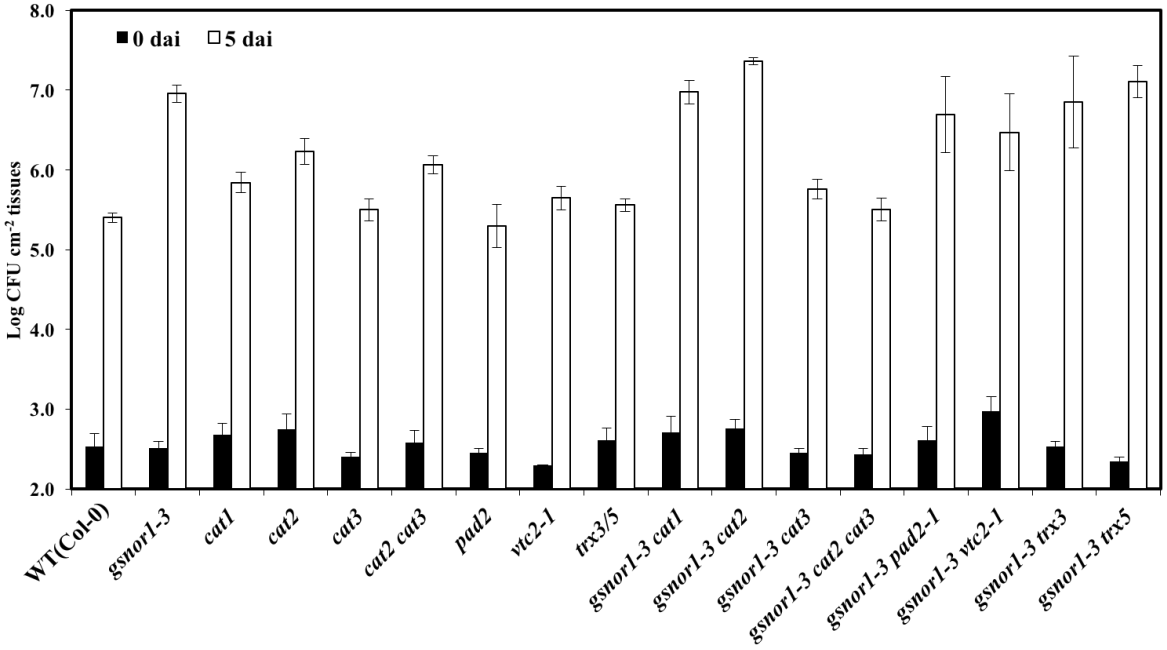

Figure 5.2. The disease resistance of the given mutant *Arabidopsis* challenged with *Pseudomonas syringae* pv. *tomato* DC3000.
Colonies of *Pst* DC3000 in the given mutants were calculated after 0 and 5 days post-inoculation. Error bars show the standard error (n=6).

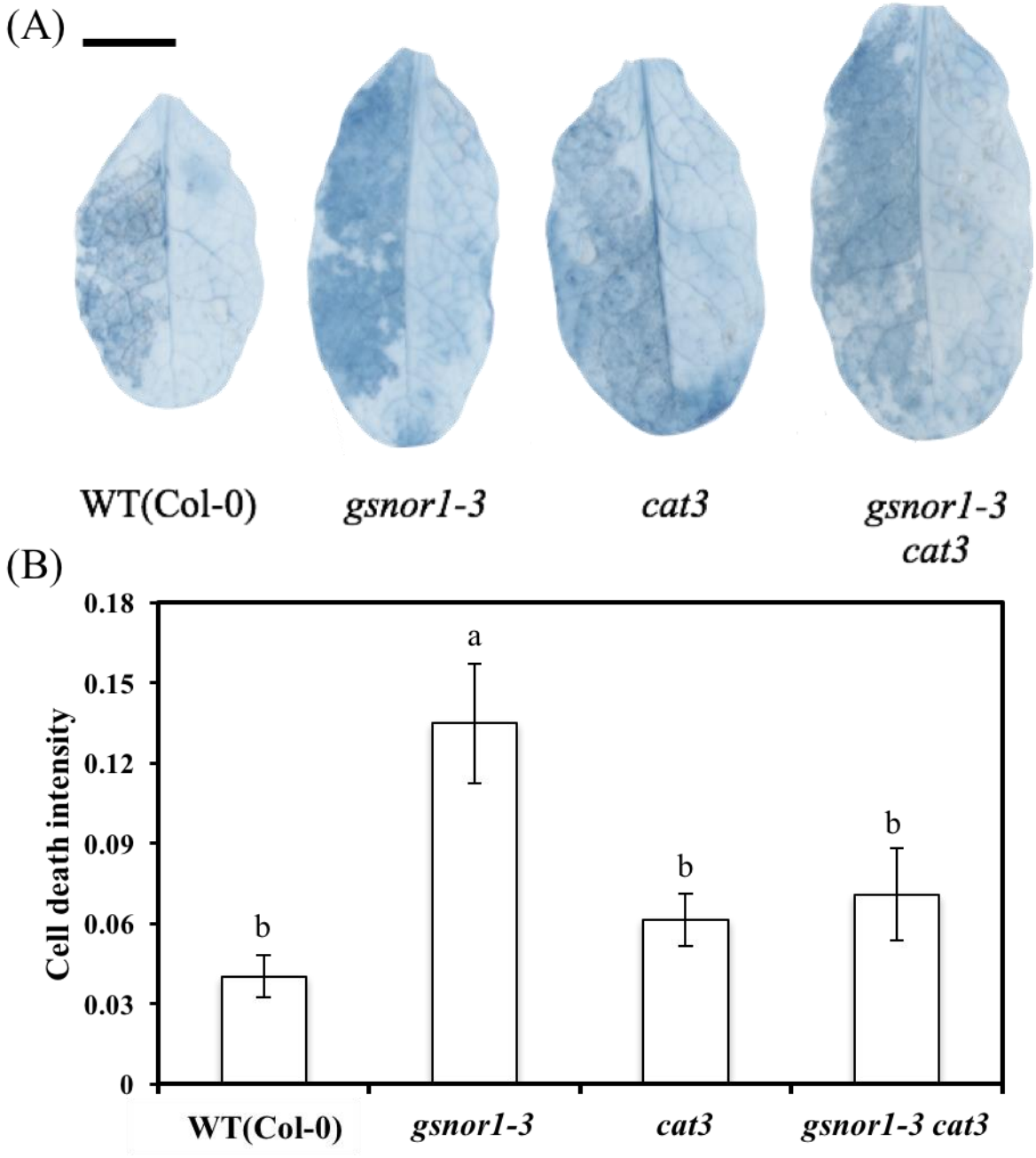

Figure 5.3. Cell death response of wild-type *Arabidopsis thaliana* (Col-0), *gsnor1-3*, *cat3* and *gsnor1-3 cat3* plants challenged with *Pseudomonas syringae* DC3000 (*avrB*).
(A) Trypan blue stained *Arabidopsis* leaves after 24 hours inoculation. Bar represents 1 cm. (B) Cell death intensities of *Arabidopsis* were quantified 24 hours after inoculation. The cell death intensity was measured by subtracting the mean grey value of the uninoculated area from the mean grey value of the inoculated area. Error bars represent standard error (n=4). Values with different letters are significantly different ($p < 0.5$, LSD multi-group test).

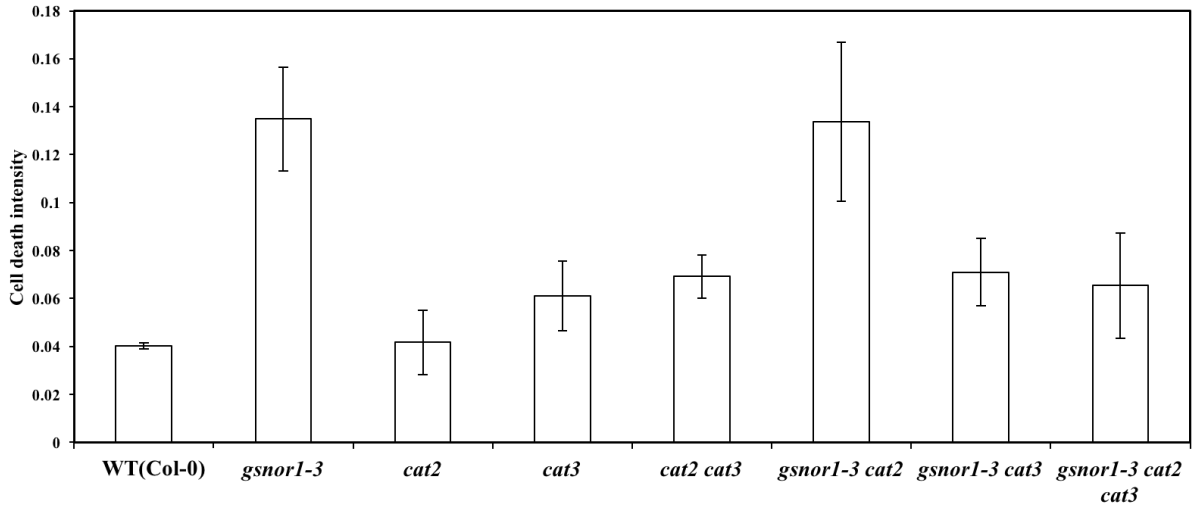

Figure 5.4. Cell death response of the given mutant plants challenged with *Pseudomonas syringae* pv. *tomato* DC3000 (*avrB*).
Trypan blue staining was applied for analysing cell death after challenge *Pseudomonas syringae* pv. *tomato* DC3000 (*avrB*) for 24 hours. The intensity was measured via ImageJ by analysing the mean grey value of inoculated area subtract the mean gray value of the uninoculated area. Error bars represent standard error (n=4).

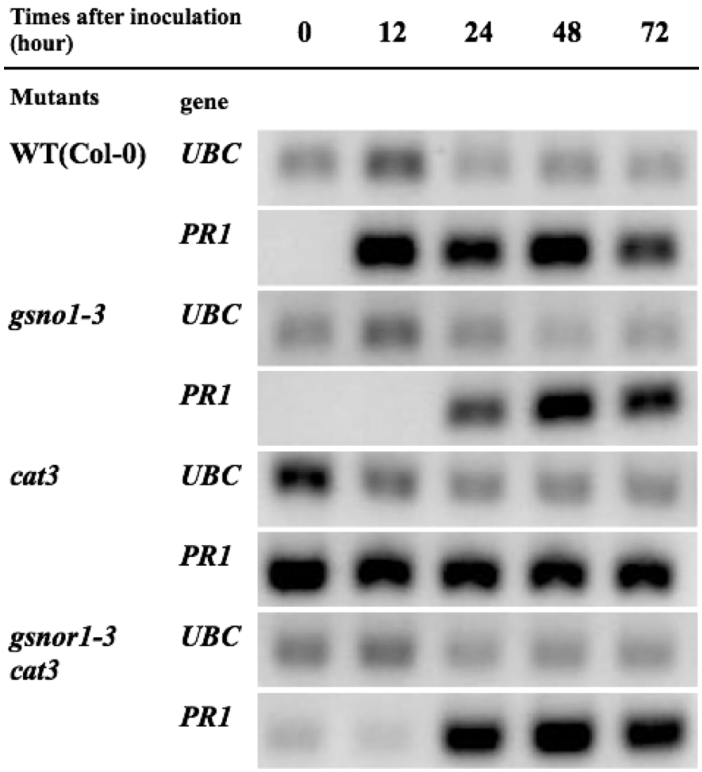

Figure 5.5. PR1 expression in wild-type (Col-0), *gsnor1-3*, *cat3* and *gsnor1-3 cat3* plants 0, 12, 24, 48 and 72 hours post-inoculation with Pst DC3000.
PR1 transcript accumulation was determined by RT-PCR. The gene encoding ubiquitin-conjugating enzyme (UBC, housekeeping gene) was utilised as a control due to its constitutive gene expression.

5.3 Discussion

The *gsnor1-3* mutants showed increased pathogen susceptibility and cell death intensity compared with wild type plants. Previous research has suggested that the enhanced disease susceptibility and programmed cell death phenotypes were related to the global *S*-nitrosylation level (Feechan et al., 2005; Yu et al., 2012). Interestingly, disease susceptibility in *gsnor1-3 cat3* plants was similar to wild-type levels. Bacterial growth levels are a direct indication of plant disease susceptibility (Hirano and Upper, 2000). Thus, the absence of *CAT3* function suppresses disease susceptibility in *gsnor1-3* plants. Therefore, *cat3* can suppress not only *gsnor1-3* dependent morphological perturbations but also disease susceptibility to *Pst* DC3000.

NO and ROS are a central feature in HR development. H_2O_2 is known to be a key signal molecule during the HR response (Grant and Loake, 2000). Previous research has suggested a model whereby the balance between H_2O_2, NO and O_2^- regulates the development of the HR response (Delledonne et al., 2001), with the HR cell death proposed to be driven by the accumulation of NO and H_2O_2 in combination. If the ratio of NO/O_2^- is in favour of O_2^-, NO is scavenged before it interacts with H_2O_2, forming $ONOO^-$, which is not thought to be an essential mediator of HR cell death (Delledonne et al., 2001). In *gsnor1-3* plants, the induction of cell death is due to the increasing of SNO level and the reduction of O_2^- with the *S*-nitrosylated NADPH oxidase (RBOHD) (Yun et al., 2011). However, the extent of cell death in *gsnor1-3 cat3* plants is decreased compared to the *gsnor1-3* mutant after inoculation with *Pst* DC3000 (*avr*B). Unlike CAT2, which is the major catalase in *Arabidopsis*, CAT3 contributes only approximately 20% of total catalase activity (Hu et al., 2010). Thus,

suppression of *gsnor1-3* by *cat3* but not *cat2*, might reflect the level of H_2O_2 accumulated. In this context, perhaps the lower level of H_2O_2 accumulation in *cat3* plants is sufficient for suppression of *gnsor1-3*, but the level of H_2O_2 accumulation in *cat2* plants is too high for suppression of *gnsor1-3*.

The SA-dependent signalling pathway is a central feature of plant immune responses (Pieterse et al., 2012). The SA-dependent signalling triggers redox changes that leads to the expression of SA-dependent gene expression (Vlot et al., 2009). CAT3 enzymes and GSNOR enzymes are responsible for the cell redox-environment adjustment and have a major impact on disease-related gene expression. The absence of the GSNOR enzyme is indirectly related to increased levels of *S*-nitrosylation (Feechan et al., 2005). Increasing global levels of *S*-nitrosylation impairs the SA-dependent signalling pathway through polymerisation of transcription factor NPR1 (Tada et al., 2008). CAT3, on the other hand, has showed increased gene expression and enzyme activity during oxidative stresses (Orendi et al., 2001). The CPK8 (Calcium-dependent Protein Kinase 8) phosphorylates CAT3 at Ser-261 and upregulate CAT3 activity in maintaining a low H_2O_2 content during drought stress (Zou et al., 2015). The relationship of *CAT3* and the SA-dependent signalling pathway remains unclear; however, the CAT3 enzyme might function in restraining the redox burst in SA-dependent signalling pathways.

The expression of *CAT3* is restricted to the vascular tissues (Mhamdi et al., 2010a). In chapter 4, the absence of *CAT3* was the only mutation that fully restored the loss-of-apical dominance phenotype (shoot weight, shoot length and numbers of 1st order shoot) in *gsnor1-3* while its paralogs *cat1* and *cat2* showed no significant changes. The three CAT enzymes have no physiological differences since expression of *CAT1* and *CAT3* sequences driven by the *CAT2* promoter complemented the phenotype of *cat2* (Hu et al., 2010). The differences distinguished between CAT1, CAT2 and CAT3 are their expression location and timing. *CAT3*

is specifically expressed in vascular bundles (Hu et al., 2010). The vascular tissues are a molecular super highway for intercellular signal transduction. The phloem network acts as the electrical wiring in plants (Hedrich et al., 2016). Expression of *CAT2* and *CAT3* with a *pCAT3* promoter both complement the suppression phenotype of *gsnor1-3 spl7* plants that had point mutation on *CAT3* (Hussain, 2013). Thus, CAT3 as a redox-related enzyme might play a pivotal role in redox signalling in the vasculature (Gilroy et al., 2014; Milthorpe and Moorby, 1969).

The role of catalase in vascular tissue may serve as a gatekeeper for the excessive ROS signals. Therefore, the defence signalling (like SA) transduction or related gene expression in *gsnor1-3 cat3* plant are considered earlier than in *gsnor1-3* plant. Our data suggest that the absence of *CAT3* accelerated *PR1* gene expression in *gsnor1-3 cat3* plants. *PR1* is a key marker for SA-dependent signalling responses. The acceleration of *PR1* gene expression in *gsnor1-3 cat3* mutants relative to *gsnor1-3* plants suggest that the loss of *CAT3* restores the kinetics of SA-dependent gene expression in *gnsor1*-3 plants. Presumably, the accelerated kinetics of *PR1* expression in *gsnor1-3 cat3* explains why this double mutant exhibits greater resistance to *Pst* (DC3000) than *gnsor1*-3 plants.

In summary, our findings suggest that *cat3* appears to suppress both developmental and immune-related defects in *gsnor1-3* plants, which exhibit increased global levels of protein S-nitrosylation. Increasing levels of H_2O_2 in the vasculature, resulting from the absence of CAT3 function, therefore appears to have a key role in reducing either S-nitrosylation or the consequences of this redox modification.

Chapter-6 Uncovering the mechanisms of *cat3* suppression of *gsnor1-3*

6.1 *S*-nitrosylation regulation

The mechanisms that control *S*-nitrosylation are notable since this post-translational modification underpins many cellular signallings across kingdoms. In plant immunity, *S*-nitrosylation is known to inhibit the defence gene expression by promoting oligomerisation of the transcriptional co-activator NPR1 (Tada et al., 2008) and the blunting of NADPH oxidase activity to curb pathogen-triggered PCD. It has also been reported that disease susceptibility of *Drosophila melanogaster* was affected by the absence of GSNOR function, an important *S*-nitrosylation regulating enzyme (Kanchanawatee, 2013). Dysregulation of *S*-nitrosylation is also known to be linked with human health and disease (Foster et al., 2009).

Three pathways for protein *S*-nitrosothiol synthesis have been proposed: direct *S*-nitrosylation, metal-mediated nitrosylation and trans-nitrosylation (Zaffagnini et al., 2016). Direct *S*-nitrosylation is mediated by NO and involves direct reaction with target protein thiols (Smith and Marletta, 2012). NO also reacts with transition metals of metalloproteins and forms metal-nitrosyl complexes. These metal-nitrosyl complexes can also transfer NO to target cysteine thiols. For example, the haeme centre of mammalian haemoglobin (Hb) can bind NO and auto-catalyse *S*-nitrosylation of Cys93, and consequently adjust its enzyme activity in response to oxygen tension (Jia et al., 1996). In addition, trans-nitrosylation of protein Cys thiols by low molecular weight nitrosothiols like GSNO or nitrosocysteine is another route for S-nitrosylation (Lamotte et al., 2014).

The level of total cellular *S*-nitrosylation is dependent on the balance between the rates of S-nitrosylation and denitrosylation. Denitrosylation can be accomplished by reduced glutathione *in vitro* and also *in vivo*, turning over a subset of S-nitrosothiols (Benhar et al., 2010). In addition, as described in previous chapters, there are two enzymes that can also turnover SNOs: GSNOR and TRX (Feechan et al., 2005; Benhar et al., 2010). However, there may be additional mechanisms that remain to be discovered.

6.2 *S*-nitrosolglutathione (GSNO)

Glutathione, a tripeptide antioxidant, is a major cellular redox hub (Foyer and Noctor, 2011), existing in two forms, oxidised glutathione (GSSG) and reduced glutathione (GSH). Glutathione can directly react with NO and produce GSNO (Malik et al., 2011). In cells, GSNO acts as an NO reservoir and is the main non-protein SNO (Liu et al., 2001). GSNO can directly transfer its NO group onto target protein cysteine thiols (Liu et al., 2001; 2004b).

GSNO is a highly light-sensitive chemical and is difficult to detect. New methods such as a liquid chromatography mass spectrometry (LC-MS) have been developed to detect GSNO (Airaki et al., 2011). However, the method has remained difficult to reproduce. Therefore, the biotin-switch technique (BST) which determines total protein *S*-nitrosylation levels is typically utilised as a marker for GSNO levels, as they are directly proportional (Foster and Stamler, 2004). The BST contains three major steps. First, *S*-thiol linked reagents such as *S*-methyl methanethiosulfonate (MMTS) or *N*-Ethylmaleimide (NEM) block the reduced protein thiols, leaving *S*-nitrosothiols (SNOs) unaltered. Second, ascorbate reduces SNOs and releases NO to form free cysteine thiols. Lastly, the newly formed thiols react with *N*-[6-(biotinamido)hexyl]-3′-(2′-pyridyldithio) propionamide (biotin–HPDP), a sulphydryl-specific biotinylation agent,

to tag the sites of SNO formation with biotin, which can be detected by western blot using an anti-biotin antibody. This method is the most common way to analyse the level of protein *S*-nitrosylation to date (Zaffagnini et al., 2016).

6.3 Hydrogen peroxide (H_2O_2)

Hydrogen peroxide (H_2O_2) is a key signalling molecule in plants (Neill et al., 2002). In response to various environmental stimuli, H_2O_2 generation is induced (Stone and Yang, 2006). H_2O_2 interacts with protein thiols and triggers cascades of signal transduction (Neill, 2002). In *Arabidopsis*, challenge with avirulent strains of *Pst* DC3000 triggers the rapid production of H_2O_2 by NADPH oxidases (Torres et al., 2005). Further, exogenously applied H_2O_2 has been reported to affect many biological processes such as programmed cell death and stomatal closure (Neill et al., 2002).

H_2O_2 can be dissociated by UV-light forming hydroxyl radicals (Halliwell and Gutteridge, 2015). Furthermore, H_2O_2 can release hydroxyl radicals by the Fenton's reaction with ferrous ions, which is a trace element in plant (Dunford, 1987). Hydroxyl radicals react with many biological molecules. For instance, hydroxyl radicals have been reported to attack cell wall polysaccharides resulting in the loosening of cell walls during germination and elongation growth (Müller et al., 2009).

Because the hydroxyl radical is short-lived and actively interacts with many biomolecules, the detection of hydroxyl radicals is more difficult than H_2O_2. Numerous methods to detect H_2O_2 have been established from simple spectrophotometric assays, such as the potassium iodide assay, and high-performance liquid chromatograpy based detection (Loreto and Velikova, 2001; Tarvin et al., 2011). Furthermore, key methods to detect hydroxyl radicals

have been developed (Buettner and Mason, 1990); an especially effective system is spin-trap electron paramagnetic resonance (EPR), which uses stable radical trap agents to acquire the radicals and detect the spin trap-radical adducts (Steffen-Heins and Steffens, 2015).

6.4 Proposed mechanism for *cat3* suppressesion of *gsnor1-3*

S-nitrosylated proteins are in dynamic equilibrium with de-nitrosylated proteins mainly due to the action of glutathione (Liu et al., 2001). The antioxidant tripeptide glutathione can denitrosylate protein SNOs to form GSNO. Also, GSNO can function as a natural NO donor, thus NO from GSNO can covalently attach to protein cysteine thiol groups to form SNOs (Corpas et al., 2013). The absence of a GSNO reductase function results in the accumulation of GSNO and a subsequent increase in the global levels of *S*-nitrosylation in both plants and animals (Kanchanawatee, 2013; Malik et al., 2011). However, this process is reversible as GSH can denitrosylate the *S*-nitrosothiol directly (Zaffagnini et al., 2013). Therefore, the concentrations of GSH and GSNO are key factors in the control of total cellular *S*-nitrosylation.

A previous report demonstrated that hydroxyl radicals degrade GSNO (Manoj and Aravindakumar, 2000). The hydroxyl radical is typically generated from H_2O_2 through the Fenton reaction (Hippeli and Elstner, 1997). Perhaps missing of *CAT3* results in induction of H_2O_2 level and consequently increased the level of hydroxyl radical. Therefore, we speculated the mechanism for *cat3* suppression of *gsnor1-3* might be the interaction of GSNO and hydroxyl radical. Accordingly, the interaction of GSNO and hydroxyl radicals should be explored *in vitro* and in the given *Arabidopsis* mutants to test our hypothesised-mechanism.

6.5 *cat3* mutants do not accumulate GSH

To further examine the proposed GSH accumulation in *cat* mutants, the content of GSH, GSSG and GSNO in *gsnor1-3*, *cat3* and *gsnor1-3 cat3* plants were analysed by liquid chromatogramphy-mass spectrometry (LC-MS). The calibration of three standard glutathione species are listed in table 6.1. The result shows that the concentration range from 50000-50 nmole of each glutathione species are linear, and the linear regression is shown in table 6.1. This result suggests GSH, GSSG and GSNO able to detect *in vitro* by LC-MS down to at least 50 nmole. The results of LC-MS analysis show the GSH concentration (Fig. 6.1.A) in *gsnor1-3* plants was similar to that of WT (Col-0). Furthermore, *gsnor1-3 cat3* plants had a lower GSH content. Also, the GSSG concentration (Fig. 6.1.B) in *gsnor1-3* plants was significantly higher than that of wild-type plants. GSNO could not be detected in any of these plant lines and was assumed to have degraded during the sample preparation. Therefore, 0.5 µmole of GSNO was spiked in both wild-type and *gsnor1-3* extracts. Result of LC-MS was unable to detect the GSNO in the spiked plant extracts.

Table 6.1. Parameters of the linear regression (y=b+mx) obtained for the calibration curves of the standards of GSH, GSSG and GSNO. b is the y intercept, m is the slope, r is the correlation coefficient and r^2 is the squared correlation coefficient.

Compound	r	r^2	b	m
GSH	0.99681	0.99362	158.5	12.1
GSSG	0.97352	0.94774	125.9	4.1
GSNO	0.99879	0.99757	232.9	4.3

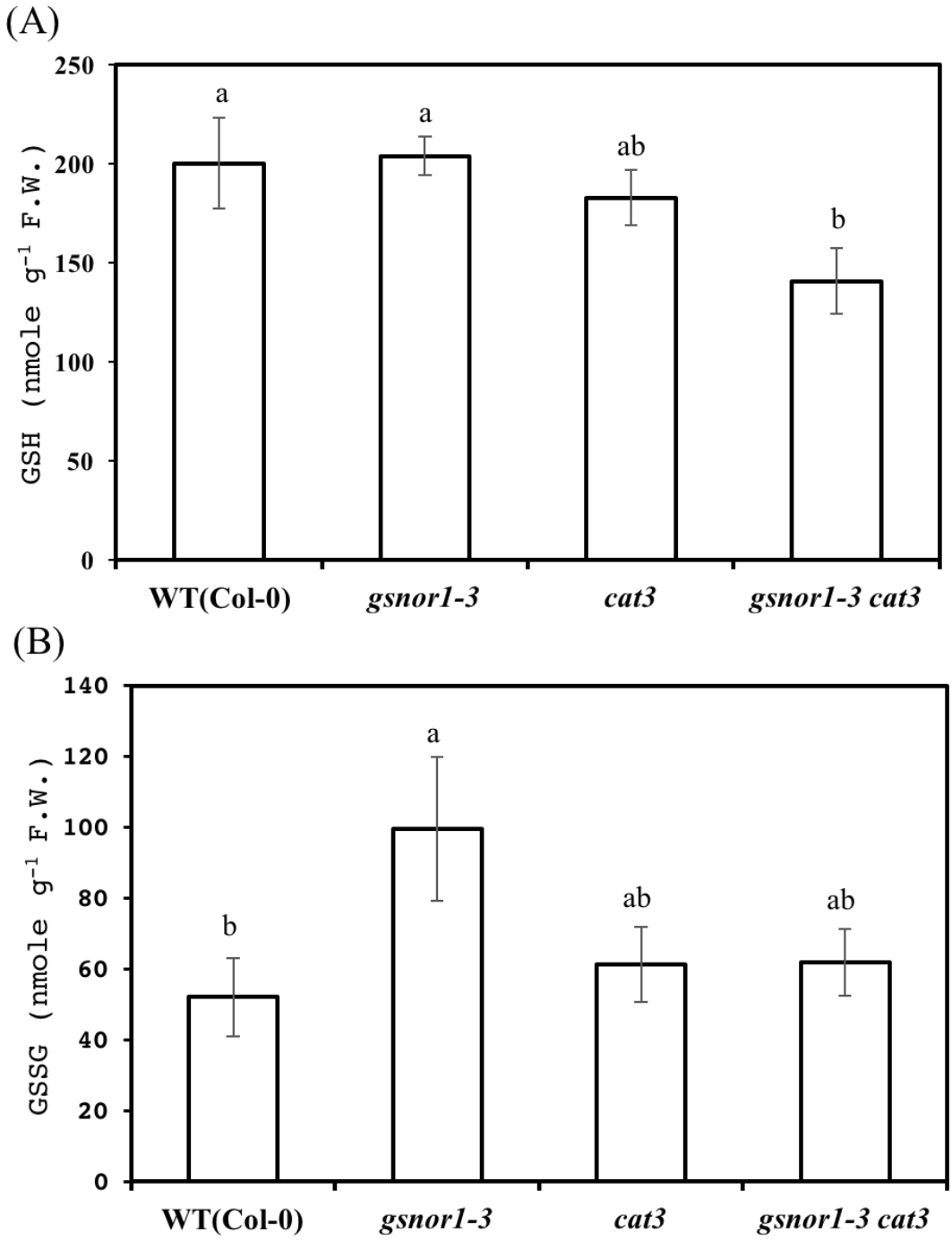

Figure 6.1. LC-MS analysis of GSH (A) and GSSG (B) concentrations in the stem of *Arabidopsis* wild-type (Col-0) and *gsnor1-3*, *cat3* and *gsnor1-3 cat3* lines.
4-week-old *Arabidopsis* stems were collected and extracted with 0.1M HCl and analysed with LC-MS. The bar chart shows the average concentration (n=4). Error bars represent standard error. Values with different letters are significantly different ($p < 0.05$, LSD test).

6.6 GSNO and hydroxyl radicals interact with each other

It has been proposed that GSNO and hydroxyl radicals react with each other (Manoj and Aravindakumar, 2000). To test this, a spectrophotometer based method was used to analyse the possible degradation of GSNO after incubating GSNO with H_2O_2 and $FeSO_4$. The ferrous ions from $FeSO_4$ drive the Fenton reaction and release hydroxyl radicals from H_2O_2. This resulted in GSNO degradation from 2.6 mM to 1.7 mM after an hour of incubation (Fig. 6.2). These results suggest that the release of hydroxyl radicals might contribute to the degradation of GSNO.

We also explored if the addition of GSNO could turnover hydroxyl radicals. The experimental design to test this was similar to the previous GSNO degradation experiment. According to the spectra (Fig. 6.3 A), hydroxyl radicals were significantly decreased when GSNO was added to H_2O_2 incubated with $FeSO_4$. The levels of hydroxyl radicals in the different chemical combinations were recorded. These data suggest that GSNO like any organic molecules can react with the hydroxyl radicals.

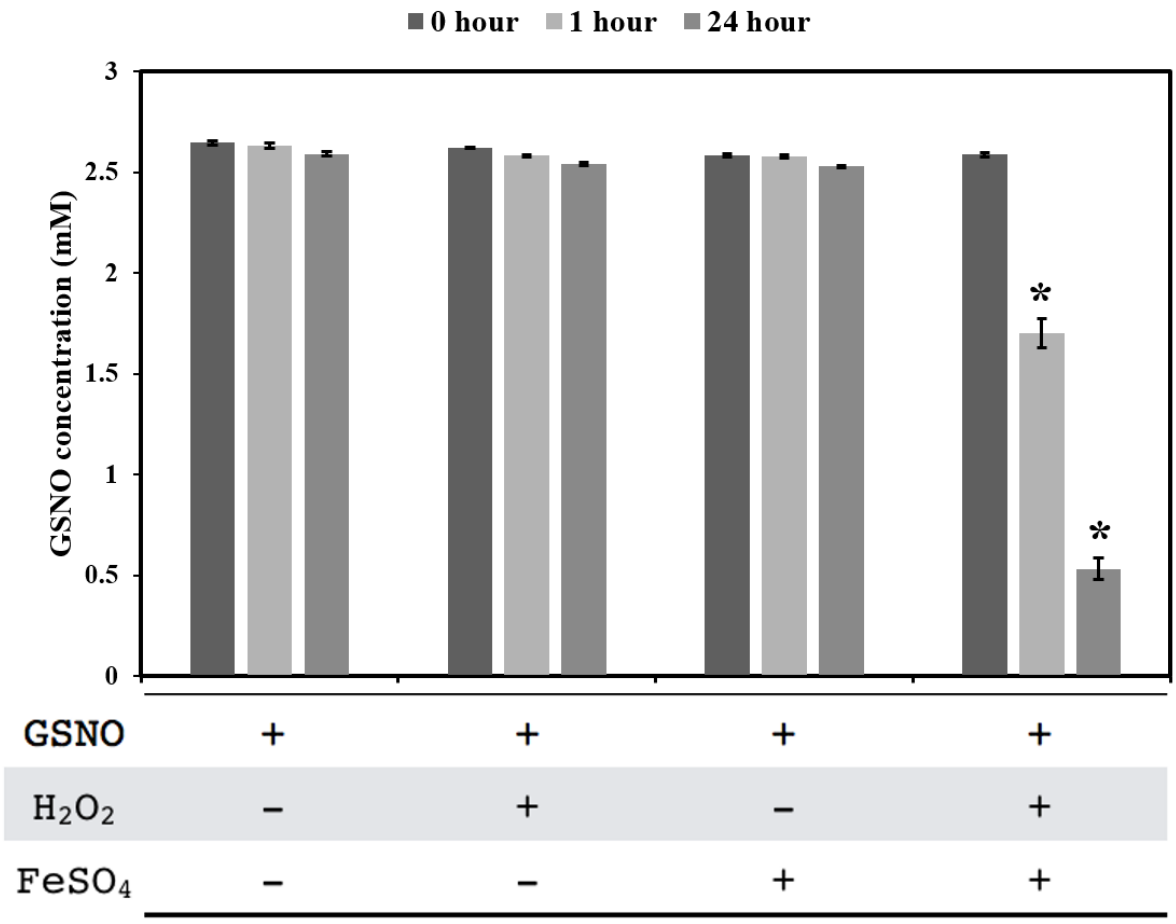

Figure 6.2. GSNO degradation *in vitro*.
The concentration of GSNO in combination with H_2O_2 and $FeSO_4$ were analysed by spectrophotometer. The photometer's (GeneQuant 1300) absorbance range is up to 2.5 A which equivalent to 2.7 mM GSNO. Therefore, the reaction was started with around 2.6 mM GSNO. GSNO (2.6 mM), H_2O_2 (10 mM) and $FeSO_4$ (10 nM) were mixed as listed and incubated for 24 hours. The bar chart shows the average concentration GSNO in the different treatments (n=10). Error bars represent standard error. Values with asterisk marks show significant differences compared with other treatments ($p < 0.01$, t-test).

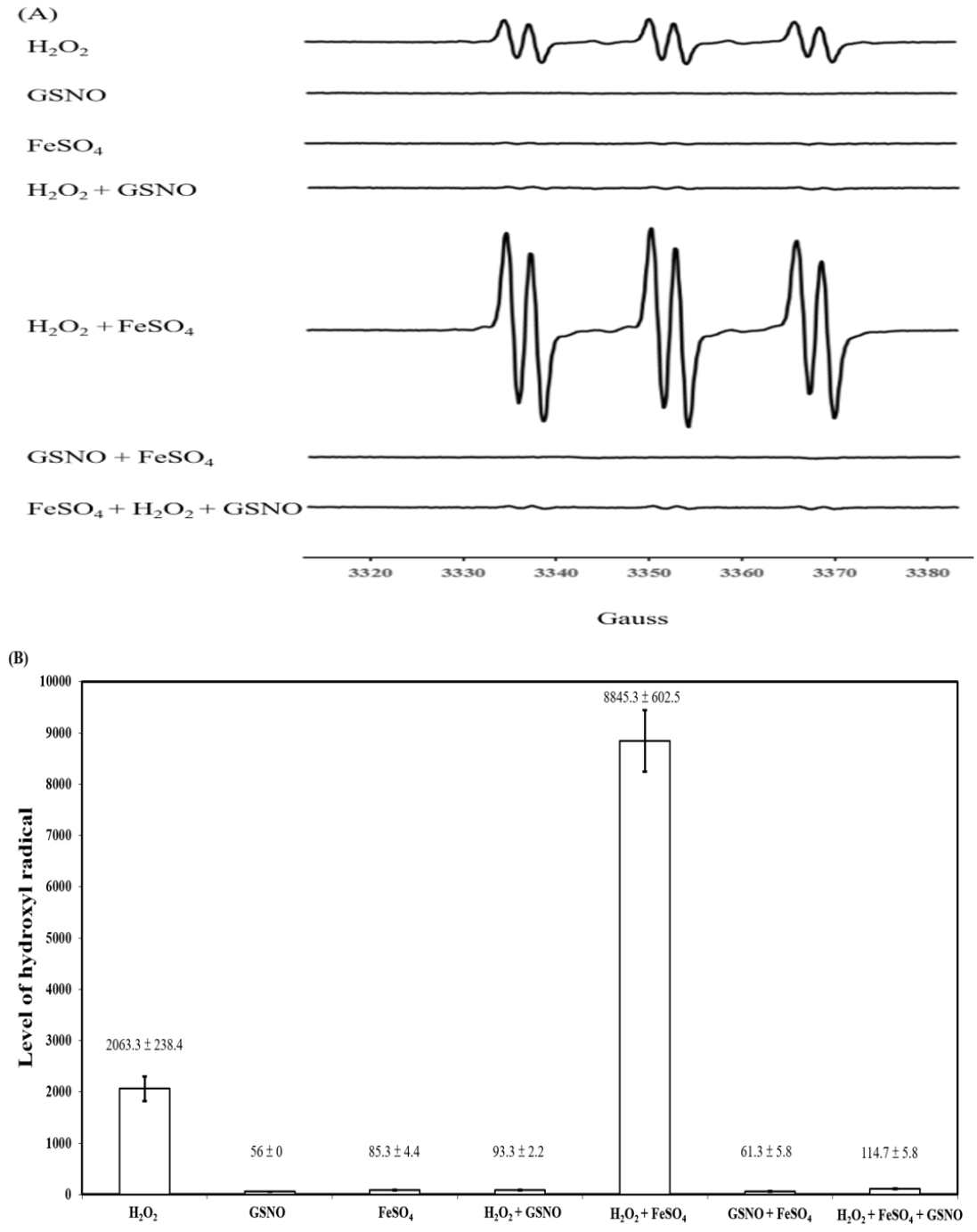

Figure 6.3. Hydroxyl radical decomposition by GSNO *in vitro*.
The level of hydroxyl radicals in different combinations of GSNO, H_2O_2 and $FeSO_4$ in distilled water were analysed by a spin-trap EPR method. GSNO (10 mM), H_2O_2 (10 mM) and $FeSO_4$ (10 nM) were mixed with different combinations and incubated for 1 hour. (A) Spectra of spin trap (4-POBN, α-(4-pyridyl-1-oxide)-N-tert-butylnitrone) analysis after incubation with the given chemical combinations. (B) Bar chart presenting the mean of level of hydroxyl radical from the stated chemical mixture (n=3). Error bars represent standard error. Values the top of bars represent the mean value of permutations and their standard error.

6.7 Global *S*-nitrosylation and hydroxyl radical levels are decreased in *gsnor1-3 cat3* plants

Our *in vitro* study supports previous data (Manoj and Aravindakumar, 2000), suggesting that GSNO and hydroxyl radicals generated from H_2O_2 can react with each other. Consequently, this might provide a mechanism for *cat3* suppression of *gsnor1-3* in *Arabidopsis*. To expore this hypothesis, the global *S*-nitrosylation level and hydroxyl radical content of *gsnor1-3, cat3* and *gsnor1-3 cat3* lines were analysed.

We employed a biotin-switch assay to quantify global levels of SNO formation in selected *Arabidopsis* mutant and double mutant lines. The resulting western blot analysis (Fig. 6.4) showed that *gsnor1-3* plants had significantly more global SNO formation compared to the wild type, *cat3* and *gsnor1*-3 *cat3* plants. The major band (close to 58KDa standard marker) in the blot result may be the RuBisCo (Ribulose-1,5-bisphosphate carboxylase/oxygenase). Rubisco is the most abundant enzyme in *Arabidopsis* and was reported to be *S*-nitrosylated (Fares et al., 2011). Interestingly, both *cat3* and *gsnor1-3 cat3* plants had a lower level of protein *S*-nitrosylation relative to wild-type. These results suggest that the absence of GSNOR function increases the level of S-nitrosylation in *Arabidopsis*. Also, the absence of *CAT3* activity reduced the global level of S-nitrosylation in *gsnor1-3 cat3* plants.

Next we determined the amount of H_2O_2 in these plant lines using the potassium iodide method (Loreto and Velikova, 2001). The results were shown in Fig. 6.5. H_2O_2 concentration in *cat3* plants was significantly higher compared with either *gsno1*-3 or *gsnor1*-3 *cat3* plants. The increase of H_2O_2 in *cat3* plants may result in elevated levels of hydroxyl radicals. Therefore, we determined the production of hydroxyl radicals in these lines post-mortem.

The amount of hydroxyl radicals in wild-type, *gsnor1*-3, *cat3* and *gsnor1*-3 *cat3* plants were analysed by a spin-trap EPR (Steffen-Heins and Steffens, 2015). As shown in Fig. 6.6.A,

the spectra of hydroxyl radical signal in *cat3* plants was higher than that of wild-type, *gsno1-3* and *gsnor1*-3 *cat3* plants. Thus, *cat3* plants had the highest level of hydroxyl radicals compared with the other plant lines tested (Fig. 6.6.B). Despite the absence of *cat3* ordinarily leading to increased levels of hydroxyl radicals, the *gsnor1-3 cat3* double mutant line did not exhibit an increase in these radicals relative to wild-type plants.

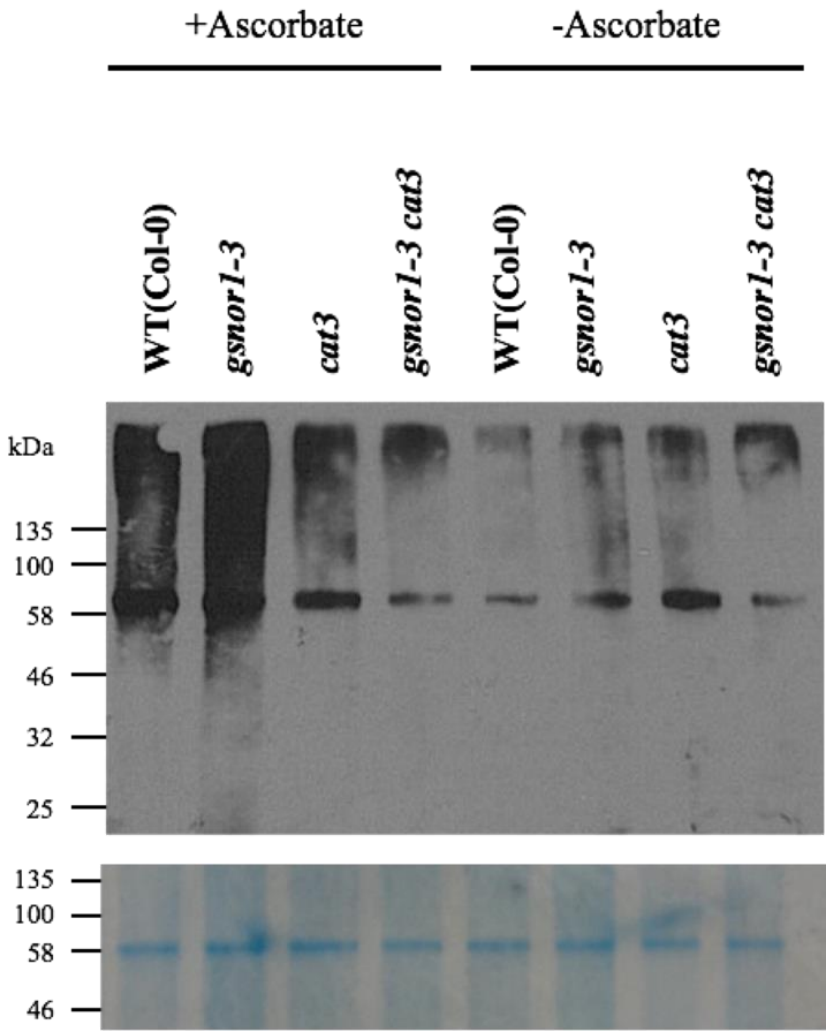

Figure 6.4. The biotin-switch method utilised to determine the global level of S-nitrosylation within the given *Arabidopsis* mutants and double mutants.
4-week-old *Arabidopsis* petioles were separated from laminae and used for the biotin-switch assay. The total protein concentration of each mutant was analysed by the BCA method and the same amount (50 µg) of the total protein was used for the biotin-switch technique (BST). The top panel shows a western blot utilising an antibiotin HRP (horseradish peroxidase)-linked antibody. Ascrobates were omitted as negative control for the last step (biotinylation of SNO-thiol) of BST. The bottom panel shows the corresponding loading control from a 7% SDS-PAGE gel after Coomassie blue staining.

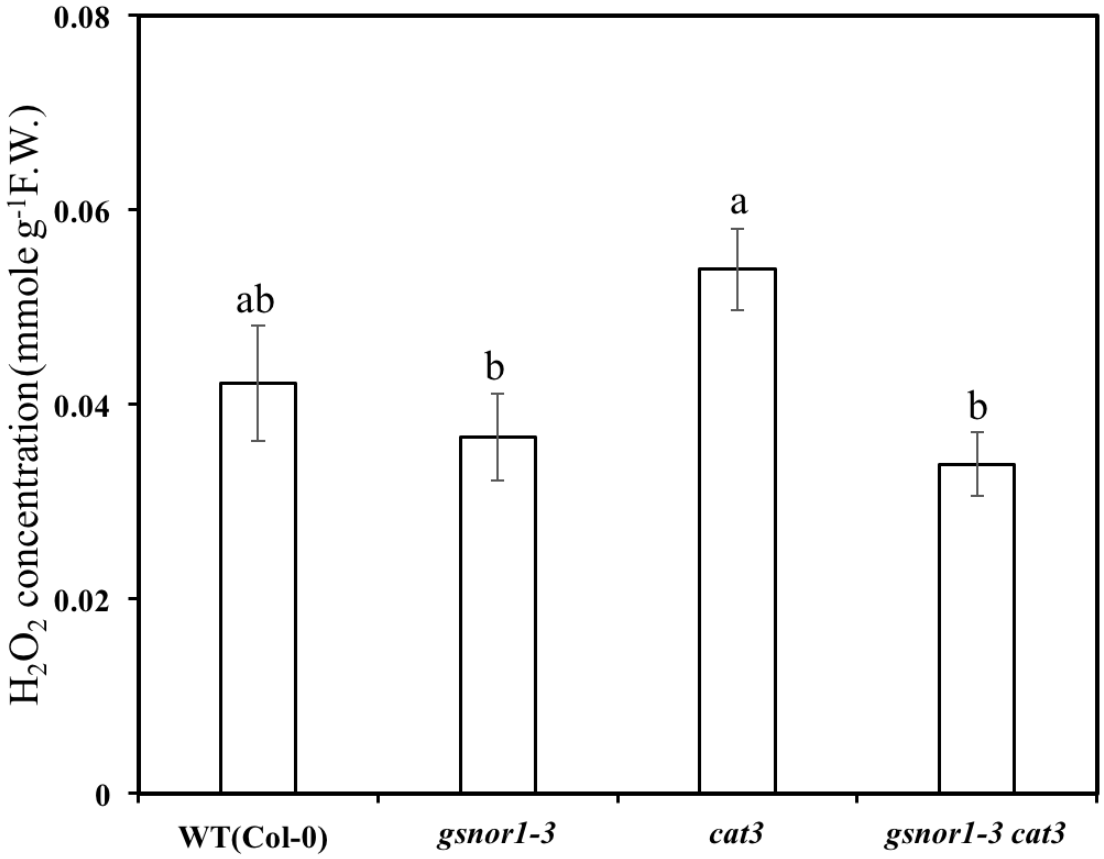

Figure 6.5. The H_2O_2 concentration of the *Arabidopsis* petioles and the related mutants. The concentration of H_2O_2 in the one-week age of *Arabidopsis* were analysed by potassium iodide (KI) methods. The bar chart presents the mean of concentration from different *Arabidopsis* mutants (n=4). Error bars represent standard error. Values with different letters are significantly different ($p < 0.05$, LSD test).

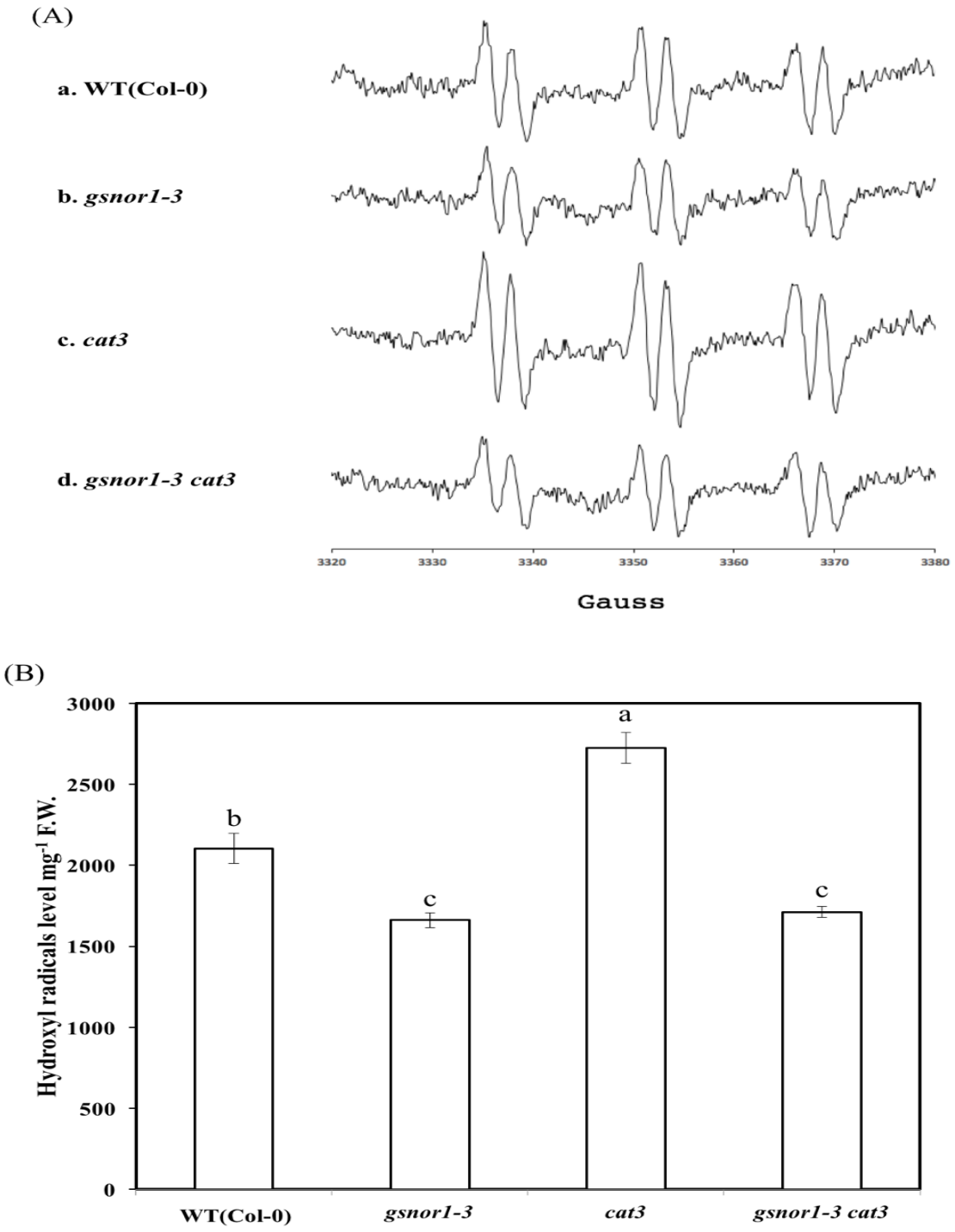

Figure 6.6. The level of hydroxyl radicals produced in wild-type (Col-0), *gsnor1-3, cat3* and *gsnor1-3 cat3 Arabidopsis* seedlings' extract.

The production of hydroxyl radicals in one-week-old *Arabidopsis* seedling extracts were analysed by spin-trap EPR. (A) Spectra of the spin trap (4-POBN, α-(4-pyridyl-1-oxide)-N-tert-butylnitrone) were analysed after incubating with the given homogenised *Arabidopsis* mutant extracts. (B) Bar chart presents the mean of signal intensity of hydroxyl radicals from different *Arabidopsis* mutants (n=12). Error bars represent standard error. Values with different letters are significantly different ($p < 0.05$, LSD test).

6.8 Exploring if H_2O_2 generated hydroxyl radicals can suppress increased S-nitrosylation in *Drosophila melanogaster gsnor* mutants

In view of the fact that *S*-nitrosylation is a pivotal biological process that functions across kingdoms, we attempted to explore if H_2O_2 generated hydroxyl radicals could suppress increased global *S*-nitrosylation in an animal model system, *Drosophila melanogaster* (Homem, 2016). Recent evidence from the Loake lab has suggested that loss of *gsnor* function in *Drosophila* results in increased global levels of SNO formation (Homem, 2016). In contrast to *Arabidopsis*, *Drosophila* possesses a single classical catalase enzyme, the absence of the CAT has been reported to suppress the malfunction of disease resistance in the *gsnor Drosophila* lines (Homem, 2016). We therefore generated *Drosophila gsnor*$^{-/-}$, *cat*$^{--/-}$ and *gsnor*$^{-/-}$ *cat*$^{-/-}$ mutants to explore if the absence of CAT function could suppress increased S-nitrosylation in *gsnor* flies. The homologous *Drosophila cat*$^{-/-}$ is lethal and unable to produce progeny, therefore, heterozygous *Drosophila cat*$^{-/+}$ was used instead. We attempted to determine global S-nitrosylation levels in *gsnor*$^{-/-}$, *cat*$^{-/+}$ and *gsnor*$^{-/-}$ *cat*$^{-/-}$ *Drosophila* lines using the BST as we employed in *Arabidopsis*. Unfortunately, establishing the BST for *Drosophila* proved difficult due to the small amounts of biological material available. Therefore, more time is required to fully the BST for this organism.

In parallel, we also attempted to determine the level of hydroxyl radicals in *gsnor*$^{-/-}$, *cat*$^{-/+}$ and *gsnor*$^{-/-}$ *cat*$^{-/-}$ *Drosophila* lines using spin-trap EPR. The application of this technology to *Drosophila* was successful. The amounts of hydroxyl radicals in the *cat*$^{-/+}$ and *cat*$^{-/-}$ mutants were significantly higher than wild-type (Fig. 6.7). Interestingly, the hydroxyl radical content of *gsnor*$^{-/-}$ *cat*$^{-/-}$ double mutants was lower than that of cat$^{-/+}$ mutants. This result paralleled that of *Arabidopsis cat3* and *gsnor1-3 cat3* mutants in which the former has a higher level of

hydroxyl radicals compared with the later. Collectively, these results suggest the ability of GSNO to suppress increased levels of hydroxyl radicals may be conserved across kingdoms.

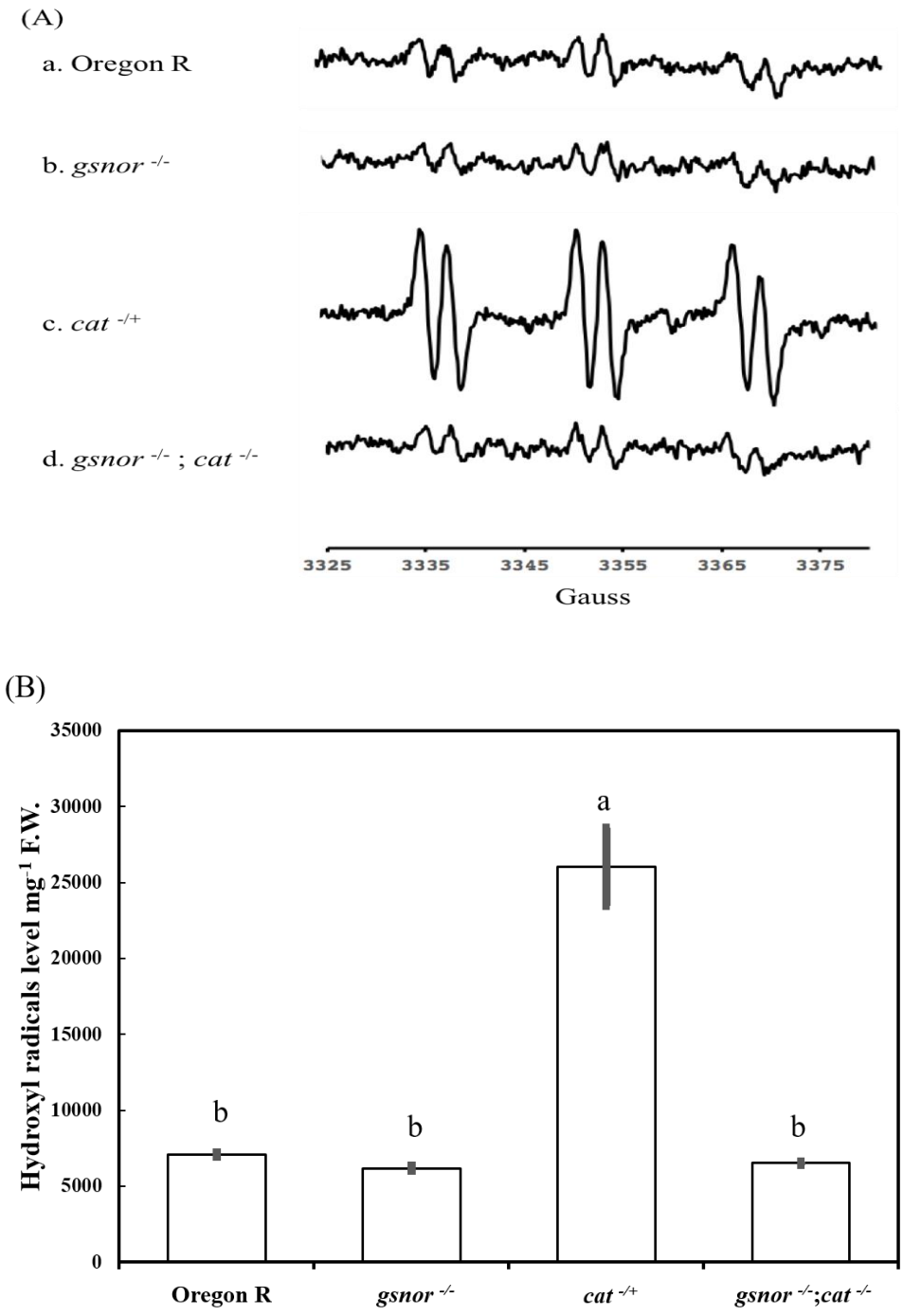

Figure 6.7. The level of hydroxyl radicals produced in the given *Drosophila* lines extracts. The hydroxyl radicals' production of tissue extracts from male adult *Drosophila* and related mutants *gsnor*$^{-/-}$, cat$^{-/+}$ and *gsnor*$^{-/-}$ *cat*$^{-/-}$ were analysed by spin-trap EPR. The *cat*$^{-/-}$ is lethal and was unable to acquire the samples for hydroxyl radical detection. (A) Spectra of the spin trap (4-POBN, α-(4-pyridyl-1-oxide)-N-tert-butylnitrone) after incubation with the given homogenised *Drosophila* line extracts. (B) Bar chart presents the mean of hydroxyl radical levels of different *Drosophila* mutants (n=9 or 6). Error bars represent standard error. Values with different letters are significantly different ($p < 0.01$, LSD test).

6.9 Discussion

The ratio of GSH and GSSG are used to indicate the redox potential of cells (Schafer and Buettner, 2001). Our data showing higher GSSG in *gsnor1-3* plants than in wild-type suggests *gsnor1-3* plants may be exhibiting oxidative stress. Several redox-related proteins in *Arabidopsis* have been reported to be *S*-nitrosylated. For example, an NADPH oxidase, AtRBOHD, can be *S*-nitrosylated resulting in a decrease of its enzyme activity (Yun et al., 2011).

A previous study suggests an LC-MS method might be able to detect GSH, GSSG and GSNO together (Airaki et al., 2011). However, we were unable to reproduce these findings. GSNO can be degraded through the metal ions, the lights and enzymes like GSNOR (Broniowska et al., 2013). The result of spiking GSNO in extract samples suggest that GSNO was degraded in the extracts. Other alternative methods of GSNO detection should be considered. Therefore, we employed the BST to demonstrate the total protein *S*-nitrosylation level which is in parallel with the GSNO level *in vivo*.

The details of reactive oxygen species (ROS) and reactive nitrogen intermediates (RNI) interactions remain largely unknown during the biotic and abiotic stresses. Previous research suggests NO and H_2O_2 might interact during the hypersensitive response (Delledonne et al., 2001). Further, in tomato roots, a novel framework suggested NO metabolism and redox state were specifically affected by salinity stress, which is conveyed by oxidative and nitrosative responses (Manai et al., 2014). These findings have suggested significant cross-talk between ROS and RNI.

The *in vitro* degradation of GSNO by hydroxyl radicals has already been proposed by Manoj and Aravindakumar (2000). Collectively, the *in vitro* chemical results of GSNO and hydroxyl radical degradation suggest that GSNO and hydroxyl radicals interact with each other.

These results support the notion that the reaction between hydroxyl radicals and GSNO may be a potential mechanism underpinning the ability of *cat3* to suppress excessive *S*-nitrosylation in *gsnor1*-3 plants.

The results from the BST and EPR methods collectively suggest that the mechanism of *cat3* suppression of *gsnor1-3* is as illustrated in Fig. 6.8. Previous research has suggested the absence of GSNOR function increases the content of GSNO and leads to a higher level of *S*-nitrosylation (Feechan et al., 2005). The BST also suggested the absence of GSNOR leads to higher protein *S*-nitrosylation in *Arabidopsis*. Additionally, the increase of hydroxyl radicals in *Arabidopsis cat3* mutants might react with GSNO and reverse the high level of S-nitrosylation in this line. Thus, the level of GSNO and H_2O_2 generated hydroxyl radicals may be interdependent and mutually balancing.

It appears the chemical reaction between GSNO and hydroxyl radical might be the mechanism which ameliorates dysregulation of *S*-nitrosylation. However, other mechanisms may also participate in the regulation of *S*-nitrosylation since CAT3 and GSNOR control cell redox and NO homoeostasis. *S*-nitrosylation of plant proteins is known to have several functional effects, such as negative regulation of NADPH oxidase or the transcription factor MYB2 (Astier et al., 2012). *CAT3* gene expression is also related to several environment stresses and biological processes (e.g. leaf senescence) (Hu et al., 2010). Furthermore, the hydroxyl radical is known to unspecifically attack and breakdown various biomolecules such as polysaccharides, proteins and nucleic acid *in vivo* (Hippeli and Elstner, 1997). Therefore, the accumulation of hydroxyl radicals in *cat3* plants suggests that many biomolecules may be modified. Since CAT3 and GSNOR function are linked to many biological processes, it will be a complex task to identify key elements related to their interaction. The employment of RNA sequence analysis to the suite of mutants and double mutants generated in this work may shed further light on these processes.

S-nitrosylation underpins many cellular signalling pathways across kingdoms. In plants, *S*-nitrosylation is already well established as a key player in the plant immune response (Feechan et al., 2005). Data from our lab suggests *Drosophila* immunity is also regulated by SNO formation and dysregulation of S-nitrosylation in this model system results in enhanced disease susceptibility (Kanchanawatee, 2013). Loss-of-function mutations in the single *Drosophila CAT* gene were able to ameliorate disease susceptibility of the *gsnor*$^{-/-}$ line (Homem, 2016). Thus, a similar mechanism is likely to underpin the ability of mutations in *CAT* to suppress *gsnor* related phenotypes in both *Arabidopsis* and *Drosophila*. In *Arabidopsis* hydroxyl radicals derived from H_2O_2 accumulation, in the absence of CAT functionality possibly generated by the Fenton reaction, appear to turnover GSNO and contribute to the suppression of *gsnor* related phenotypes. Our data also suggests that a similar mechanism enables *cat* mutations to suppress *gsnor* in *Drosophila* because increased hydroxyl radical formation in the absence of CAT activity appears to turnover GSNO. However, for confirmation, decreased global S-nitrosylation in *cat gsnor* lines relative to *gsnor* flies will need to be demonstrated.

In sum, this novel CAT-dependent mechanism to regulate *S*-nitrosylation may function across kingdoms. Thus, this regulatory machinery could present a potential target for the control of *S*-nitrosylation in the context of both agriculture and human medicine.

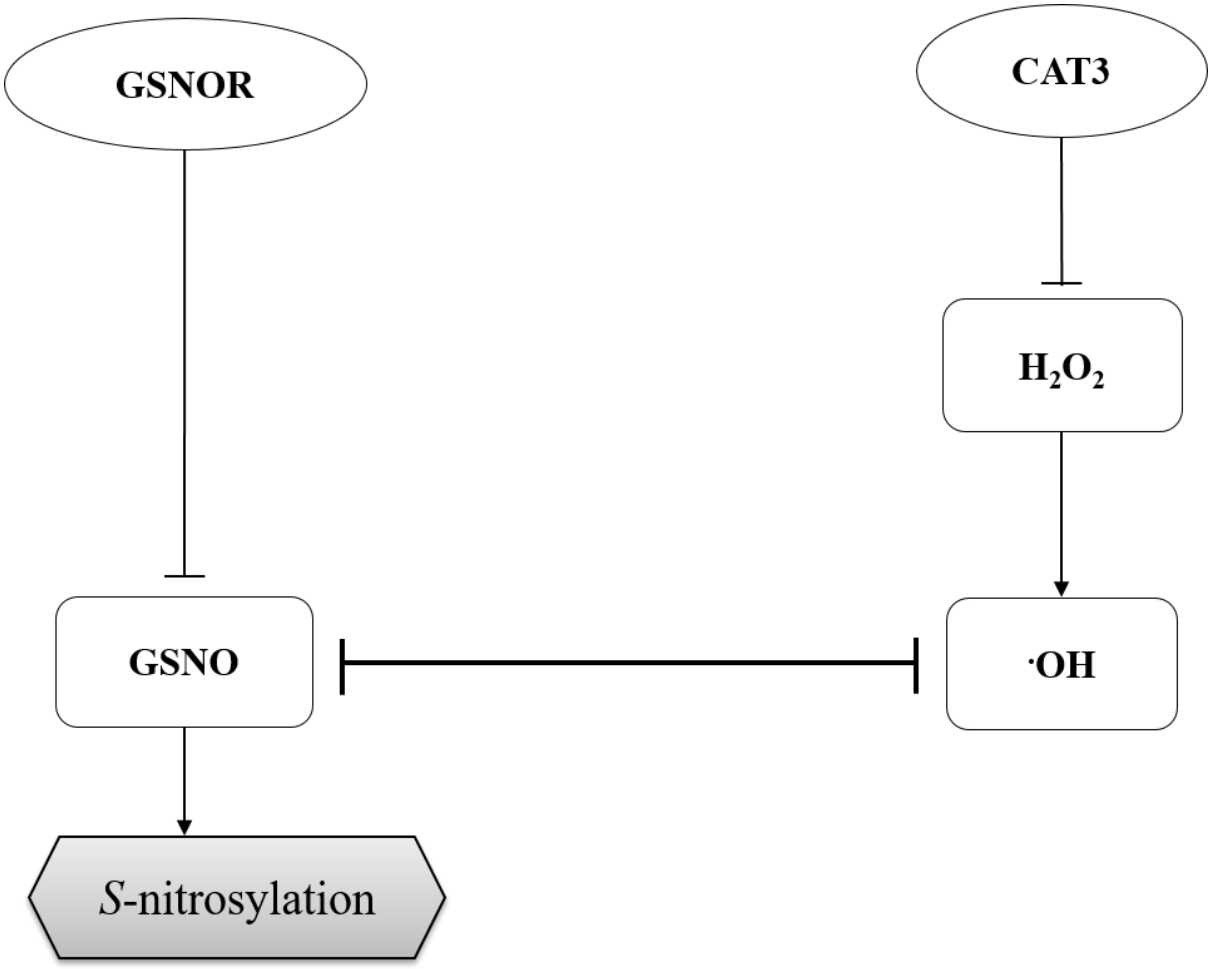

Figure 6.8. The proposed model of how *cat3* suppresses the *gsnor1-3*.
The *S*-nitrosylation process might be able to regulate by the interaction of the H_2O_2 and GSNO. The H_2O_2 and GSNO may interact with each other and result in decrease the level of protein *S*-nitrosylation. GSNOR: GSNO reductase. CAT3: class II catalase in *Arabidopsis.*

Chapter-7 General discussion

7.1 Mechanisms of *cat3* suppression of *gsnor1-3*

The absence of GSNOR function in *Arabidopsis* results in global accumulation of GSNO and enhanced cellular S-nitrosylation (Feechan et al., 2005). Interestingly, *gsnor1-3* plants are disabled in multiple modes of plant disease resistance and exhibit loss of apical dominance, in addition to other developmental perturbations (Kwon et al., 2012). Our findings imply that loss-of-function mutations in *CAT3* suppress multiple *gsnor1-3* phenotypes, including loss of apical dominance, enhanced pathogen-triggered HR cell death and increased disease susceptibility. CAT enzymes have a well-established role in the turnover of H_2O_2. Thus, loss of CAT3 function results in an increase of H_2O_2 accumulation in the vascular tissue of *Arabidopsis*. Our results imply that hydroxyl radicals generated as a direct result of H_2O_2 accumulation can deplete GSNO.

Hydroxyl radicals typically originate from H_2O_2 via the Fenton reaction which requires the involvement of metal ions (Aust et al., 1985; Fenton, 1894). Iron, common in biological systems, is the most frequently reported transition metal ion integral to the Fenton reaction and is also involved in the formation of metal-nitrosyl complexes (Pierre and Fontecave, 1999; Zaffagnini et al., 2016). Also, NO was reported to regulate plant root iron homoeostasis (Yu et al., 2014). NO is a key feature in controlling the iron nutrition and homoeostasis in roots, assisting the growth of the plant in an iron deficient environment (Graziano and Lamattina, 2007). The formation of iron-nitrosyl compounds under high NO conditions can increase the mobility and availability of iron facilitating plant growth under low iron conditions (Graziano and Lamattina, 2005).

The ferric-chelate reductase oxidase gene (*FRO2*) and the iron-regulated transporter gene (*IRT1*) are the dominant genes responsible for the absorption of ferrous ions across the root plasma membrane (Eide et al., 1996; Robinson et al., 1999). Among the eight members identified in *Arabidopsis*, *FRO2* is primarily expressed in roots and strongly induced in response to iron deficiency (Mukherjee et al., 2006). A FRO2 loss-of-function mutant *frd1* (ferric-chelate reductase deficiency) is unable to survive to maturity unless a high concentration of exogenous iron is supplied (Robinson et al., 1999; Yi and Guerinot, 1996). NO was suggested to activate the FER-LIKE IRON DEFICIENCY INDUCED TRANSCRIPTION FACTOR (FIT) and turnover the expression of *FRO2* and *IRT1* (Meiser et al., 2011). Thus, the absence of *GSNOR* indirectly increases the cell SNO level that may increase the iron uptake in the root of *gsnor1-3* plants.

An increase in ferrous ions caused by the increasing of NO content might accelerate the Fenton reaction, promoting the generation of hydroxyl radicals. The formation of these radicals would be increased further following the accumulation of H_2O_2 following loss of CAT3 function. This would be expected to lead to a reduction of total cellular *S*-nitrosylation since the hydroxyl radical can decompose GSNO *in vitro*. Furthermore, increasing NO levels in *gsnor1-3* may facilitate iron uptake. However, in the presence of *CAT3*, H_2O_2 is converted to H_2O and O_2, yielding less hydroxyl radicals. In *gsnor1-3* plants, endogenous GSNO and SNO levels are higher compared to wild-type plants leading to disease susceptibility and loss of apical dominance. In this context, determining the concentration of ferrous ions in *gsnor1-3 cat3* plants compared to wild-type, *gsnor1-3* and *cat3* plants might be informative. Total iron content can be quantified by the ferrozine spectrophotometric method (Stookey, 1970). For detecting iron in vascular tissues where *CAT3* expressed, a Prussian blue staining method could be used to detect the iron content *in situ* (Liu et al., 2007). Additionally, knocking out the iron uptake related genes such as *FRO2* (Robinson et al., 1999) or *IRT1* (Eide et al., 1996) in a

gsnor1-3 cat3 background could provide evidence for the role of iron in the suppression of *gsnor1-3* phenotype by mutations in *CAT3*. However, to achieve this exogenous iron would need to be provided to support growth and development in the absence of FRO2 function and then removed at given times before pathogen challenge. In this context, *frd1 gsnor1-3 cat3* plants might continue to display *gsnor1-3*-dependent phenotypes due to a reduction in hydroxyl radical content, resulting from ferrous ion deficiency, leading a reduction in hydroxyl radical production via the Fenton reaction.

Both NO and H_2O_2 can reprogram plant gene expression (Begara-Morales et al., 2014; Vanderauwera et al., 2005). Global analysis of gene expression in catalase deficient tobacco in the presence or absence of exogenous NO exposure showed that NO and H_2O_2 both have specific and overlapping target genes for transcriptional activation (Zago et al., 2006). Approximately 8,000 transcript fragments were evaluated in tobacco leaves after treating with either NO or H_2O_2 or both molecules combined. Large set of genes (152) related to signalling pathways and transcription factors are modulated by both NO and H_2O_2 independently while only 16 transcripts found to be regulated by both NO and H_2O_2. This result indicates that NO and H_2O_2 share components in signalling pathways or act on the same transcription factors. Thus, *cat3* mediated suppression of *gsnor1-3* may be the consequence of dual regulation of H_2O_2 and NO in signal transduction. Therefore, an investigation of global gene expression changes, utilising Next Generation Sequencing strategies (Nordborg and Weigel, 2008), in *gsnor1-3 cat3* plants compared with wild-type, *gsnor1-3* and *cat3* may provide additional insight into (S)NO and H_2O_2 cross-talk.

7.2 Absence of CAT function in suppression of *S*-nitrosylation across kingdoms

Due to frequently experienced endogenous and environmental changes which trigger accumulation of ROS, aerobic organisms have evolved a conserved redox regulation system, including enzymes such as SODs and CATs and various non-enzymatic antioxidants such as GSH, NADPH and NADH (Halliwell, 2006). Recently, a comparative analysis among different organisms including yeast, plant and human systems identified 1244 conserved protein families including SODs, CATs and Peroxiredoxins (Vandenbroucke et al., 2008). The same research identified that four families of eukaryotic proteins (DNAJ domain-containing heat shock proteins, small guanine triphosphate-binding proteins, Ca^{2+}-dependent protein kinases and ubiquitin-conjugating enzymes) are H_2O_2-responsive across all kingdoms (Vandenbroucke et al., 2008).

S-nitrosylation, in particular, has also been reported to be a key post-translational modification in plants, animals and microorganisms (Hess et al., 2005; Spadaro et al., 2010). GSNOR, an indirect regulator of *S*-nitrosylation, is highly conserved in plants, yeast, mice and bacteria (Feechan et al., 2005; Liu et al., 2001; 2004b). The higher susceptibility of plants, flies and mice to microbial pathogens in the absence of GSNOR (Feechan et al., 2005; Kanchanawatee, 2013; Tang et al., 2013), again suggests a highly-conserved role of GSNOR in the immune system across kingdoms. *S*-nitrosylation at Cys-890 of RBOHD, an NADPH oxidase, reduces ROS accumulation and curbs cell death in *Arabidopsis* during the HR response (Yun et al., 2011). This cysteine of NADPH oxidase is conserved and *S*-nitrosylated in both human and *Drosophila* at Cys-537 of NOX2 and Cys-1315 of NOX, respectively. Moreover, glyceraldehyde 3-phosphate dehydrogenase (GAPDH), a key enzyme in glycolysis, is *S*-nitrosylated in both plants and animals (Lindermayr et al., 2005; Stamler et al., 2001). *S*-

nitrosylation of GAPDH inhibits its enzyme activity which has been shown to be involved in cell death in animals (Hara et al., 2005).

It is interesting to note that the absence of *CAT* function also suppresses the disease susceptibility of a *gsnor*$^{-/-}$ *Drosophila* line (Homem, 2016). This result is similar *to Arabidopsis* where the absence of *CAT3* decreased disease susceptibility in *gsnor1-3 cat3* plants compared with *gsnor1-3* plants. Moreover, the *gsnor*$^{-/-}$ *cat*$^{-/-}$ *Drosophila* line also showed less hydroxyl radical accumulation compared to the *cat*$^{-/+}$ line. This finding is similar to *Arabidopsis*, since *gsnor1-3 cat3* plants have lower hydroxyl radical accumulation than *cat3* plants. Collectively, our data suggests that the suppression of *gsnor1-3* by loss-of-function mutations in *CAT* is conserved across kingdoms. Further, the associated mechanism responsible for these observations may also be conserved between plants and animals: the absence of *CAT* function reduces total cellular *S*-nitrosylation via the depletion of GSNO, mediated by the accumulation of hydroxyl radicals. However, to substantiate this posit, the level of total cellular S-nitrosylation in *Drosophila* wild-type, *gsnor*$^{-/-}$, *cat*$^{-/+}$ *and gsnor*$^{-/-}$ *cat*$^{-/-}$ lines should be determined. Unfortunately, due to time constraints it was impossible to complete this key experiment.

7.3 Future application of CAT inhibition in agriculture and medicine

The absence of GSNOR elevates the global level of *S*-nitrosylation disabling multiple modes of plant disease resistance (Feechan et al., 2005) and also impacts plant developmental processes (Kwon et al. 2012). We showed that a loss-of-function mutation in *Arabidopsis CAT3* (this study) and a reduction in *Drosophila CAT* expression recover disease resistance

that was initially lost due to excessive *S*-nitrosylation (Homem, 2016). These findings suggest potential agricultural applications of adjusting CAT function to ameliorate excessive *S*-nitrosylation. In this context, exogenous application of 3-amino-1, 2, 4-triazole (3-AT), a catalase inhibitor, has been reported to systemically protect rice from blast disease caused by the fungal pathogen *Magnaporthe oryzae* (Aver'yanov et al., 2015). The inhibition of catalase through 3-AT has also been found to prolong the vase-life of carnation (Altman and Solomos, 1993).

The dysregulation of S-nitrosylation has also been shown to underlie the development of a broad spectrum of human diseases, including Parkinson's, Alzheimer's, cancer and asthma, among others (Nakamura et al., 2013). Thus, drugs with a mode of action to reduce total cellular *S*-nitrosylation levels, might have important applications in biomedicine. Inhibiting the activity of catalase might be a potential method for suppressing diseases caused by aberrant *S*-nitrosylation. Acatalasemia is a human catalase deficiency disease (Ogata, 1991). In a recent report, surprisingly, acatalasemia is a relatively benign syndrome with similar life spans for those impacted (45 ± 19.3 years; n=62) compare to normacatalasemia individuals (42.9 ± 18.5 years; n=66) (Góth et al., 2004). Thus, catalase function is not essential for human life. Therefore, short-term inhibition of catalase may result in benign side effects but potentially ameliorate the dysregulation of *S*-nitrosylation.

Identifying small molecule inhibitors of catalase activity may therefore be an option for suppressing excessive levels of cellular *S*-nitrosylation levels. The most commonly used catalase inhibitor is 3-AT that decreases catalase activity by an irreversible modification (Margoliash et al., 1960). Catalase activity was shown to be decreased to 7% of original activity after 20 mM 3-AT incubation for 2 hours. 3-AT is a member of a class of triazoles with an amino group at position 3 and is widely used as a nonselective herbicide in controlling weeds in agriculture (E Margoliash, 1958). The herbicidal effect of 3-AT is mainly inhibited the

histidine synthesis in the weeds (Hilton et. al, 1965). 3-AT is also a competitive inhibitor and deactivates catalase by changing the structure of catalase and disrupting the binding site for peroxide (Havir, 1992; Putnam et al., 2000). Moreover, 3-AT treatment inhibiting brain catalase was reported to attenuate and block ethanol-triggered behaviour (Koechling and Amit, 1994). However, because of its carcinogenic property (Chao and Yang, 2001; Furukawa et al., 2010), the use of 3-AT within the EU will be banned after September 2017. To discover an alternative catalase inhibitor, the properties of 3-AT may be a reference chemical for computational drug discovery (Sliwoski et al., 2014). Screening of a library of computer-predicted candidates via a high-throughput procedure may facilitate future drug development (Hoelder et al., 2012; Taylor, 2005). Moreover, the model proposed in this thesis is cross-kingdom, thus the effect of novel catalase inhibitors can be evaluated in *Arabidopis* and *Drosophila* during early stages of the discovery process.

Another alternative for catalase inhibitor such as catechin, a green tea flavonoid, can also be considered. The benefits of green tea on human health are well established (Pal et al., 2014). Green tea has been reported to protect against cancer, cardiovascular and neurodegenerative diseases (Zaveri, 2006). The green tea flavonoids, catechins, have been used for cancer prevention (Trevisanato and Kim, 2000). Catechins are abundant in green tea, constituting up to 30 % of the dry weight of green tea leaves (Graham, 1992). Catechin extraction and formulation has been reported in detail (Gadkari and Balaraman, 2015). The anticancer property of catechins is mainly because of ROS accumulation, which is the result of catalase inhibition (Pal et al., 2014). In this report, an application of a catechin ((-)-epigallocatechin gallate, EGCG) demonstrated the catalase inhibition in cancer cell K562 accompanied with significant induction of ROS and suppression of cell viability (Pal et al.,2014). Based on this property, catechins may be potential chemicals that could be utilised for suppressing catalase activity in the absence of harmful side effects.

7.4 Conclusions and future work

The model of how the absence of *CAT3* suppresses *gsnor1-3* has been described in chapter 6. The interaction of GSNO and hydroxyl radicals appears to be an important factor in the regulation of *S*-nitrosylation (Fig. 7). Under basal conditions, GSNO and hydroxyl radicals are in a delicate balance that may contribute to the stabilisation of the redox environment within wild type plants (Fig. 7A). This redox balance becomes dysregulated in the absence of GSNOR elevating GSNO levels and increasing total cellular *S*-nitrosylation (Fig. 7B). In the absence of *CAT3* expression, H_2O_2 and subsequently hydroxyl radicals accumulate, leading to a reduction of total cellular *S*-nitrosylation (Fig. 7C). Since both GSNO and hydroxyl radicals are mutual scavengers, redox homoeostasis is re-established in a *gsnor1-3 cat3* double mutant (Fig. 7D). These observations on *cat3*, *gsnor1-3* and *gsnor1-3 cat3* mutants suggest the interaction of hydroxyl radicals and GSNO are a key feature in balancing the redox environment. However, the catalase activity in *gsnor1-3 cat3* is needed to further determine our mechanism.

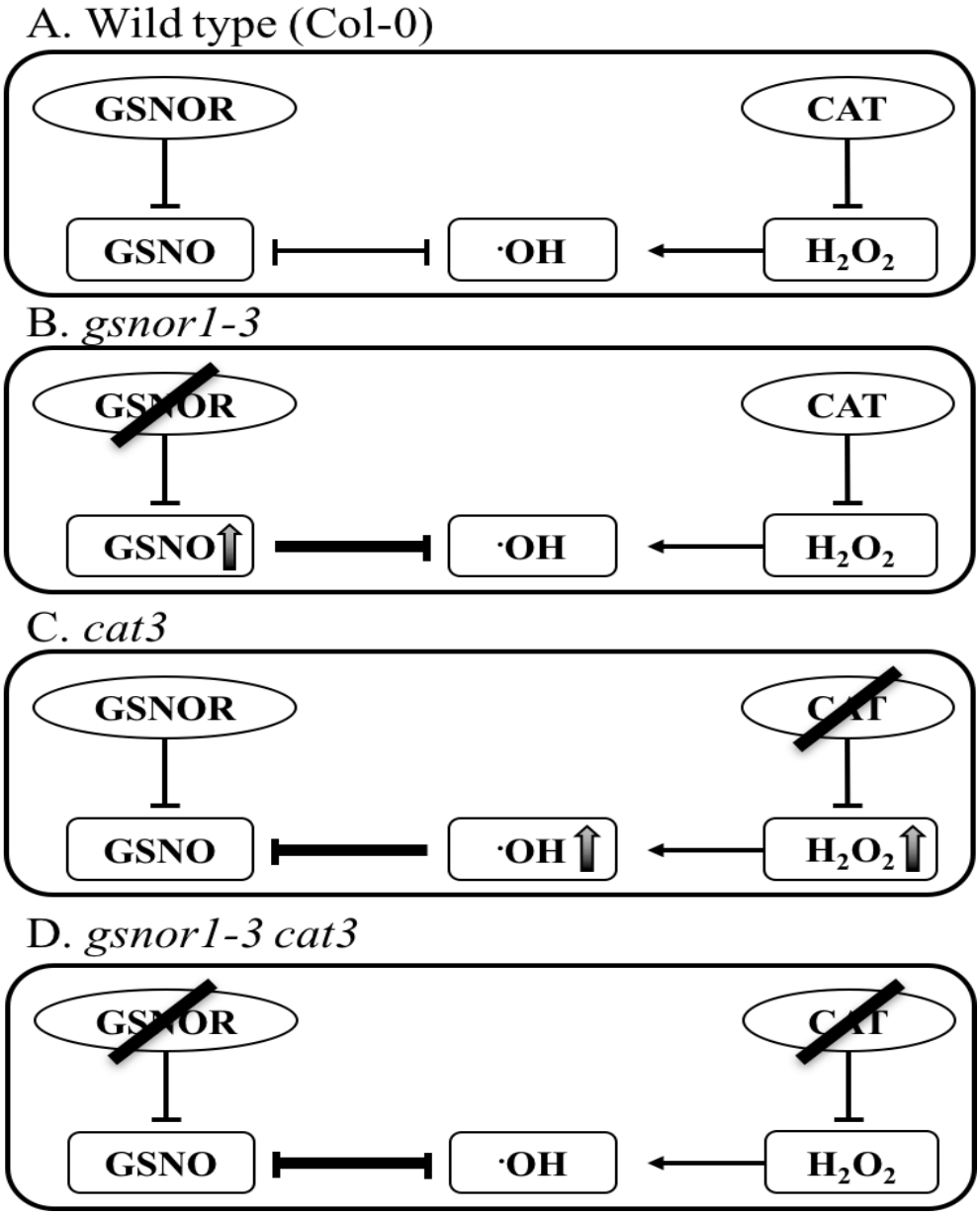

Figure 7.1 Model of GSNO and hydroxyl radical interaction in wild-type (Col-0, A), gsnor1-3 (B), cat3 (C) and gsnor1-3 cat3 plants (D). GSNOR: *S*-nitrosoglutathione reductase, CAT: catalase.

The ferrous ions which conduct the Fenton reaction may be an integral feature of this mechanism to regulate *S*-nitrosylation. An elevated SNO level might increase the uptake of ferrous ions and supporting an enhanced Fenton reaction in the presence of H_2O_2 (Fig. 7.2). The accumulation of H_2O_2 from the absence of CAT function may therefore result in elevated accumulation of hydroxyl radicals. These molecules may deplete total GSNO levels and by

extension suppress excessive cellular *S*-nitrosylation. Therefore, the concentration of ferrous ions in the *gsnor1-3 cat3* double mutant compared with wild-type, *gsnor1-3* and *cat3* plants should be investigated to test this hypothesis.

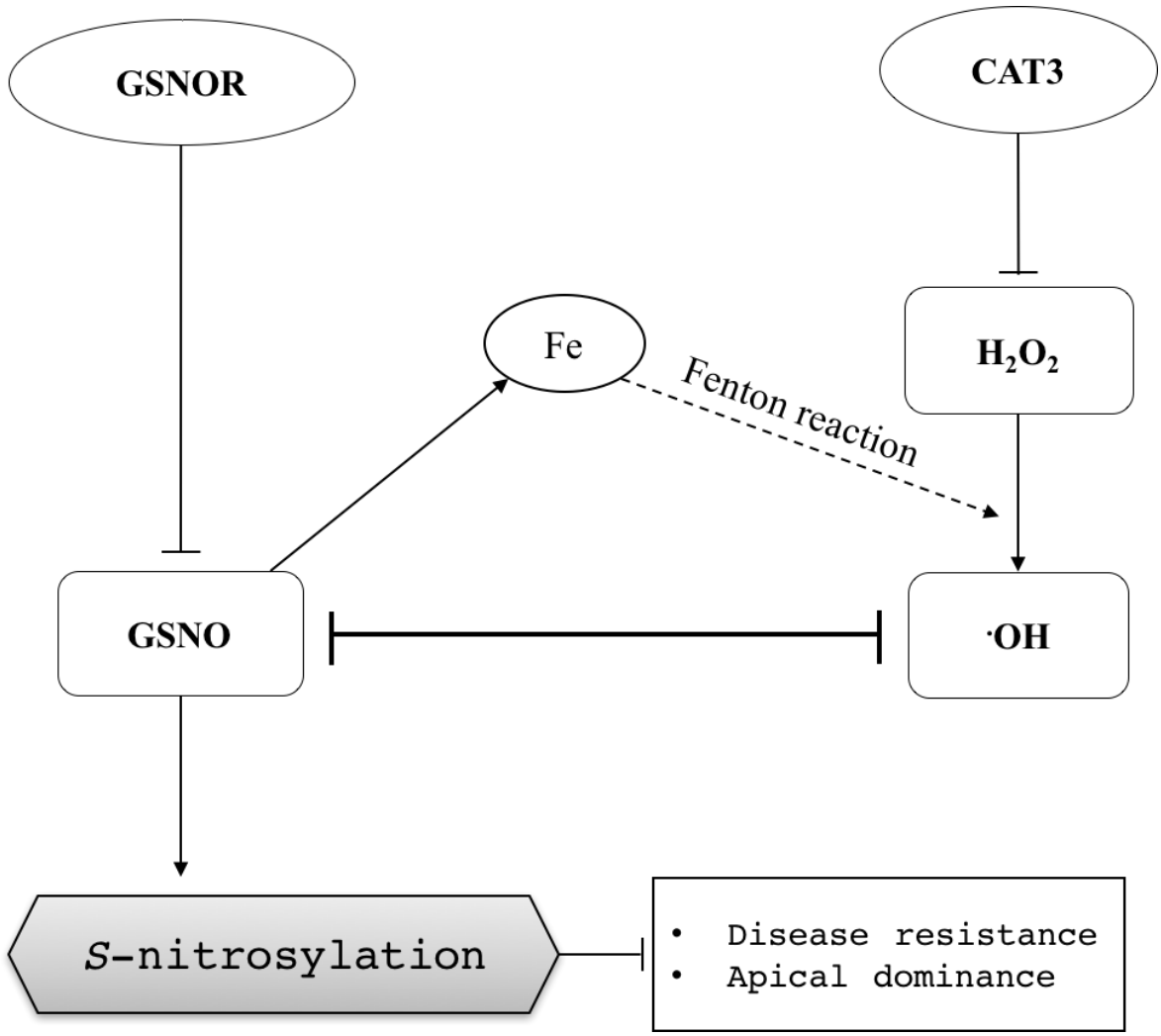

Figure 7.2. The proposed mechanism of CAT and GSNOR interaction during redox regulation in *Arabidopsis*. GSNOR: S-nitrosoglutathione reductase, CAT: catalase. Blunt arrows represent inhibition. Pointed arrows represent activation. The dashed line means unclear.

Significantly, in contrast to *Arabidopsis*, *Drosophila* possesses a single classical catalase enzyme. A decrease in catalase activity also suppresses the loss of disease resistance due to the absence of GSNOR function in *Drosophila* (Homem, 2016). The hydroxyl radical content in *Drosophila* wild-type, $gsnor^{-/-}$, $cat^{-/+}$ *and* $gsnor^{-/-}$ $cat^{-/-}$ lines showed a similar pattern relative to the corresponding *Arabidopsis* mutants. The $gsnor^{-/-}$ $cat^{-/-}$ line has a decreased hydroxyl

radical content compared to the *cat*$^{-/+}$ line. This result suggests that GSNO depletion by hydroxyl radicals may also occur in *Drosophila*. However, further investigation of the *S*-nitrosylation level in the *gsnor*$^{-/-}$ *cat*$^{-/-}$ line compared to wild-type, *gsnor*$^{-/-}$, *cat*$^{-/+}$ line is required to confirm this.

Work presented in this thesis therefore uncovers a possible mechanism underpinning *cat3* suppression of *gsnor1-3*, and demonstrates that GSNO and hydroxyl radicals can function as mutual scavengers across kingdoms.

.

References

Abramovitch, R.B., Anderson, J.C., and Martin, G.B. (2006). Bacterial elicitation and evasion of plant innate immunity. Nat Rev Mol Cell Biol *7*, 601–611.

Airaki, M., Sanchez-Moreno, L., Leterrier, M., Barroso, J.B., Palma, J.M., and Corpas, F.J. (2011). Detection and Quantification of S-Nitrosoglutathione (GSNO) in Pepper (Capsicum annuum L.) Plant Organs by LC-ES/MS. Plant and Cell Physiology *52*, 2006–2015.

Alamillo, J.M., and García Olmedo, F. (2001). Effects of urate, a natural inhibitor of peroxynitrite-mediated toxicity, in the response of *Arabidopsis thaliana* to the bacterial pathogen *Pseudomonas syringae*. The Plant Journal *25*, 529–540.

Altman, S.A., and Solomos, T. (1993). 3-Amino-1,2,4-triazole Prolongs Carnation Vase Life. HortScience *28*, 201–203.

Apel, K., and Hirt, H. (2004). REACTIVE OXYGEN SPECIES: Metabolism, Oxidative Stress, and Signal Transduction. Annu. Rev. Plant Biol. *55*, 373–399.

Apostol, I., Heinstein, P.F., and Low, P.S. (1989). Rapid Stimulation of an Oxidative Burst during Elicitation of Cultured Plant Cells: Role in Defense and Signal Transduction. Plant Physiology *90*, 109–116.

Asada, K. (2006). Production and scavenging of reactive oxygen species in chloroplasts and their functions. Plant Physiology *141*, 391–396.

Astier, J., Kulik, A., Koen, E., Besson-Bard, A., Bourque, S., Jeandroz, S., Lamotte, O., and Wendehenne, D. (2012). Protein S-nitrosylation What's going on in plants? Free Radical Biology and Medicine *53*, 1101–1110.

Aust, S.D., Morehouse, L.A., and Thomas, C.E. (1985). Role of metals in oxygen radical reactions. Journal of Free Radicals in Biology & Medicine *1*, 3–25.

Aver'yanov, A.A., Pasechnik, T.D., Lapikova, V.P., Romanova, T.S., and Baker, C.J. (2015). Systemic reduction of rice blast by inhibitors of antioxidant enzymes. Russ J Plant Physiol *62*, 586–594.

Aviv, D.H., Rustérucci, C., Iii, B.F.H., Dietrich, R.A., Parker, J.E., and Dangl, J.L. (2002). Runaway cell death, but not basal disease resistance, in lsd1is SA- and NIM1/NPR1-dependent. The Plant Journal *29*, 381–391.

Bardoel, B.W., van der Ent, S., Pel, M.J.C., Tommassen, J., Pieterse, C.M.J., van Kessel, K.P.M., and van Strijp, J.A.G. (2011). *Pseudomonas* evades immune recognition of flagellin in both mammals and plants. PLoS Pathog *7*, e1002206.

Barth, C., De Tullio, M., and Conklin, P.L. (2006). The role of ascorbic acid in the control of flowering time and the onset of senescence. Journal of Experimental Botany *57*, 1657–1665.

Bashandy, T., Meyer, Y., and Reichheld, J.P. (2011). Redox regulation of auxin signaling and

plant development in Arabidopsis. Plant Signal Behav *6*, 117–119.

Begara-Morales, J.C., Sánchez-Calvo, B., Luque, F., Leyva-Pérez, M.O., Leterrier, M., Corpas, F.J., and Barroso, J.B. (2014). Differential Transcriptomic Analysis by RNA-Seq of GSNO-Responsive Genes Between *Arabidopsis* Roots and Leaves. Plant and Cell Physiology *55* (6), 1080-1095.

Belenghi, B., Romero-Puertas, M.C., Vercammen, D., Brackenier, A., Inzé, D., Delledonne, M., and Van Breusegem, F. (2007). Metacaspase Activity of *Arabidopsis* thaliana Is Regulated by S-Nitrosylation of a Critical Cysteine Residue. J. Biol. Chem. *282*, 1352–1358.

Beligni, M.V., Fath, A., Bethke, P.C., Lamattina, L., and Jones, R.L. (2002). Nitric oxide acts as an antioxidant and delays programmed cell death in barley aleurone layers. Plant Physiology *129*, 1642–1650.

Benhar, M., Thompson, J.W., Moseley, M.A., and Stamler, J.S. (2010). Identification of S-Nitrosylated Targets of Thioredoxin Using a Quantitative Proteomic Approach. Biochemistry *49*, 6963-6969

Bent, A.F., and Mackey, D. (2007). Elicitors, Effectors, and R Genes: The New Paradigm and a Lifetime Supply of Questions. Annu Rev Phytopathol *45*, 399–436.

Berrocal-Lobo, M., and Molina, A. (2004). Ethylene response factor 1 mediates *Arabidopsis* resistance to the soilborne fungus Fusarium oxysporum. Mol Plant Microbe Interact *17*, 763–770.

Bethke, P.C., Badger, M.R., and Jones, R.L. (2004). Apoplastic synthesis of nitric oxide by plant tissues. The Plant Cell *16*, 332–341.

Birtić, S., Colville, L., Pritchard, H.W., Pearce, S.R., and Kranner, I. (2011). Mathematically combined half-cell reduction potentials of low-molecular-weight thiols as markers of seed ageing. Free Radical Research *45*, 1093–1102.

Brezezek, K. (2013). PhD thesis. S-nitrosothiols and reactive oxygen species in plant disease resistance and development. 1–207.

Broniowska, K.A., Diers, A.R., and Hogg, N. (2013). S-Nitrosoglutathione. Biochimica Et Biophysica Acta (BBA) - General Subjects *1830*, 3173–3181.

Buchanan Wollaston, V., Page, T., Harrison, E., Breeze, E., Lim, P.O., Nam, H.G., Lin, J.F., Wu, S.H., Swidzinski, J., Ishizaki, K., et al. (2005). Comparative transcriptome analysis reveals significant differences in gene expression and signalling pathways between developmental and dark/starvation-induced senescence in *Arabidopsis*. The Plant Journal *42*, 567–585.

Bueso, E., Alejandro, S., Carbonell, P., Perez Amador, M.A., Fayos, J., Bellés, J.M., Rodriguez, P.L., and Serrano, R. (2007). The lithium tolerance of the *Arabidopsis* cat2 mutant reveals a cross-talk between oxidative stress and ethylene. The Plant Journal *52*, 1052–1065.

Buettner, G.R., and Mason, R.P. (1990). Spin-trapping methods for detecting superoxide and hydroxyl free radicals *in vitro* and in vivo. Meth. Enzymol. *186*, 127–133.

Casalongué, C.A. (2013). Functions of S-nitrosylation in plant hormone networks. Front Plant Sci. *4*. 294. doi: 10.3389/fpls.2013.00294. eCollection.1–6.

Chao, J.I., and Yang, J.L. (2001). Alteration of cadmium-induced mutational spectrum by catalase depletion in Chinese hamster ovary-K1 cells. Mutat. Res. *498*, 7–18.

Chaouch, S., Queval, G., Vanderauwera, S., Mhamdi, A., Vandorpe, M., Langlois-Meurinne, M., Van Breusegem, F., Saindrenan, P., and Noctor, G. (2010). Peroxisomal hydrogen peroxide is coupled to biotic defense responses by ISOCHORISMATE SYNTHASE1 in a daylength-related manner. Plant Physiology *153*, 1692–1705.

Chen, R., Jiang, H., Li, L., Zhai, Q., Qi, L., Zhou, W., Liu, X., Li, H., Zheng, W., Sun, J., et al. (2012). The *Arabidopsis* mediator subunit MED25 differentially regulates jasmonate and abscisic acid signaling through interacting with the MYC2 and ABI5 transcription factors. The Plant Cell *24*, 2898–2916.

Chini, A., Fonseca, S., Chico, J.M., Fernández Calvo, P., and Solano, R. (2009). The ZIM domain mediates homo- and heteromeric interactions between *Arabidopsis* JAZ proteins. The Plant Journal *59*, 77–87.

Choi, J., Choi, D., Lee, S., Ryu, C.-M., and Hwang, I. (2011). Cytokinins and plant immunity: old foes or new friends? Trends in Plant Science *16*, 388–394.

Chung, K.K.K., Thomas, B., Li, X., Pletnikova, O., Troncoso, J.C., Marsh, L., Dawson, V.L., and Dawson, T.M. (2004). S-Nitrosylation of Parkin Regulates Ubiquitination and Compromises Parkin's Protective Function. Science *304*, 1328–1331.

Clark, D., Durner, J., Navarre, D.A., and Klessig, D.F. (2000). Nitric oxide inhibition of tobacco catalase and ascorbate peroxidase. Mol Plant Microbe Interact *13*, 1380–1384.

Clarke, A., Desikan, R., Hurst, R.D., Hancock, J.T., and Neill, S.J. (2000). NO way back: nitric oxide and programmed cell death in *Arabidopsis thaliana* suspension cultures. The Plant Journal *24*, 667–677.

Coll, N.S., Epple, P., and Dangl, J.L. (2011). Programmed cell death in the plant immune system. Cell Death Differ *18*, 1247–1256.

Coll, N.S., Vercammen, D., Smidler, A., Clover, C., Van Breusegem, F., Dangl, J.L., and Epple, P. (2010). *Arabidopsis* Type I Metacaspases Control Cell Death. Science *330*, 1393–1397.

Collmer, A., Lindeberg, M., Petnicki-Ocwieja, T., Schneider, D.J., and Alfano, J.R. (2002). Genomic mining type III secretion system effectors in *Pseudomonas syringae* yields new picks for all TTSS prospectors. Trends in Microbiology *10*, 462–469.

Colville, L., and Smirnoff, N. (2008). Antioxidant status, peroxidase activity, and PR protein transcript levels in ascorbate-deficient *Arabidopsis thaliana* vtc mutants. Journal of Experimental Botany *59*, 3857–3868.

Conklin, P.L., Saracco, S.A., Norris, S.R., and Last, R.L. (2000). Identification of Ascorbic Acid-Deficient *Arabidopsis thaliana* Mutants. Genetics *154*, 847–856.

Contento, A.L., and Bassham, D.C. (2010). Increase in catalase-3 activity as a response to use of alternative catabolic substrates during sucrose starvation. Plant Physiology Et Biochemistry *48*, 232–238.

Corpas, F. J., Alché, J. D., and Barroso, J. B. (2013). Current overview of *S*-nitrosoglutathione (GSNO) in higher plants. Front Plant Sci *4*, 126. http://doi.org/10.3389/fpls.2013.00126

Crawford, N.M., Galli, M., Tischner, R., Heimer, Y.M., Okamoto, M., and Mack, A. (2006). Response to Zemojtel et al: Plant nitric oxide synthase: back to square one. Trends in Plant Science *11*, 526–527.

Dat, J., Vandenabeele, S., Vranová, E., Van Montagu, M., Inzé, D., and Van Breusegem, F. (2000). Dual action of the active oxygen species during plant stress responses. Cell Mol Life Sci *57*, 779–795.

De Rybel, B., Mähönen, A.P., Helariutta, Y., and Weijers, D. (2015). Plant vascular development: from early specification to differentiation. Nat Rev Mol Cell Biol *17*, 30–40.

del Río, L.A., Sandalio, L.M., Corpas, F.J., Palma, J.M., and Barroso, J.B. (2006). Reactive oxygen species and reactive nitrogen species in peroxisomes. Production, scavenging, and role in cell signaling. Plant Physiology *141*, 330–335.

Delaney, T.P., Uknes, S., Vernooij, B., Friedrich, L., Weymann, K., Negrotto, D., Gaffney, T., Gut-Rella, M., Kessmann, H., Ward, E., et al. (1994). A central role of salicylic Acid in plant disease resistance. Science *266*, 1247–1250.

Delledonne, M., Zeier, J., Marocco, A., and Lamb, C. (2001). Signal interactions between nitric oxide and reactive oxygen intermediates in the plant hypersensitive disease resistance response. Proc. Natl. Acad. Sci. Usa. *98*, 13454–13459.

Denancé, N. (2013). Disease resistance or growth: the role of plant hormones in balancing immune responses and fitness costs. Front Plant Sci *4.* 155. doi: 10.3389/fpls.2013.00155. eCollection. 1–12.

Dickman, M.B., and Fluhr, R. (2013). Centrality of host cell death in plant-microbe interactions. Annual Review of Phytopathology *51*, 543–570.

Doke, N. (1985). NADPH-dependent O2− generation in membrane fractions isolated from wounded potato tubers inoculated with Phytophthora infestans. Physiological Plant Pathology *27*, 311–322.

Domagalska, M.A., and Leyser, O. (2011). Signal integration in the control of shoot branching. Nat Rev Mol Cell Biol *12*, 211–221.

Dong, X. (2004). NPR1, all things considered. Current Opinion in Plant Biology *7*, 547–552.

Du, L., Ali, G.S., Simons, K.A., Hou, J., Yang, T., Reddy, A.S.N., and Poovaiah, B.W. (2009). Ca2+/calmodulin regulates salicylic-acid-mediated plant immunity. Nature *457*, 1154–1158.

Dubreuil-Maurizi, C., Vitecek, J., Marty, L., Branciard, L., Frettinger, P., Wendehenne, D.,

Meyer, A.J., Mauch, F., and Poinssot, B. (2011). Glutathione Deficiency of the *Arabidopsis* Mutant pad2-1 Affects Oxidative Stress-Related Events, Defense Gene Expression, and the Hypersensitive Response. Plant Physiology *157*, 2000–2012.

Dun, E.A., Ferguson, B.J., and Beveridge, C.A. (2006). Apical dominance and shoot branching. Divergent opinions or divergent mechanisms? Plant Physiology *142*, 812–819.

Dunford, H.B. (1987). Free radicals in iron-containing systems. Free Radical Biology and Medicine *3*, 405–421.

Durner, J., Wendehenne, D., and Klessig, D.F. (1998). Defense gene induction in tobacco by nitric oxide, cyclic GMP, and cyclic ADP-ribose. Proc. Natl. Acad. Sci. Usa. *95*, 10328–10333.

E Margoliash, A.N. (1958). A study of the inhibition of catalase by 3-amino-1:2:4-triazole. Biochemical Journal *68*, 468.

Eide, D., Broderius, M., Fett, J., and Guerinot, M.L. (1996). A novel iron-regulated metal transporter from plants identified by functional expression in yeast. Proc. Natl. Acad. Sci. Usa. *93*, 5624–5628.

Fares, A., Rossignol, M., and Peltier, J.-B. (2011). Proteomics investigation of endogenous S-nitrosylation in *Arabidopsis*. Biochemical and Biophysical Research Communications *416*, 331–336.

Feechan, A., Kwon, E., Yun, B.-W., Wang, Y., Pallas, J.A., and Loake, G.J. (2005). A central role for S-nitrosothiols in plant disease resistance. Proc. Natl. Acad. Sci. Usa. *102*, 8054–8059.

Feng, J., Wang, C., Chen, Q., Chen, H., Ren, B., Li, X., and Zuo, J. (2013). S-nitrosylation of phosphotransfer proteins represses cytokinin signaling. Nature Communications *4*, 1529.

Fenton, H. J. H. (1894). LXXIII.—Oxidation of tartaric acid in presence of iron. Journal of the Chemical Society, Transactions, *65*, 899-910.

Filonova, L.H., Bozhkov, P.V., Brukhin, V.B., Daniel, G., Zhivotovsky, B., and Arnold, von, S. (2000). Two waves of programmed cell death occur during formation and development of somatic embryos in the gymnosperm, Norway spruce. J. Cell. Sci. *113 Pt 24*, 4399–4411.

Flor, H.H. (1971). Current Status of the Gene-For-Gene Concept. Annual Review of Phytopathology *9*, 275–296.

Fonseca, S., Chini, A., Hamberg, M., Adie, B., Porzel, A., Kramell, R., Miersch, O., Wasternack, C., and Solano, R. (2009). (+)-7-iso-Jasmonoyl-L-isoleucine is the endogenous bioactive jasmonate. Nature Chemical Biology *5*, 344–350.

Foster, M.W., Hess, D.T., and Stamler, J.S. (2009). Protein S-nitrosylation in health and disease: a current perspective. Trends in Molecular Medicine *15*, 391–404.

Foster, M.W., McMahon, T.J., and Stamler, J.S. (2003). S-nitrosylation in health and disease. Trends in Molecular Medicine *9*, 160–168.

Foster, M. W., & Stamler, J. S. (2004). New Insights into Protein S-Nitrosylation MITOCHONDRIA AS A MODEL SYSTEM. Journal of Biological Chemistry, *279(24)*, 25891-25897.

Foyer, C.H., and Noctor, G. (2011). Ascorbate and Glutathione: The Heart of the Redox Hub. Plant Physiology *155*, 2–18.

Freeman, T.C., Raza, S., Theocharidis, A., and Ghazal, P. (2010). The mEPN scheme: an intuitive and flexible graphical system for rendering biological pathways. BMC Syst Biol *4*, 65.

Frugoli, J.A., Zhong, H.H., Nuccio, M.L., McCourt, P., McPeek, M.A., Thomas, T.L., and McClung, C.R. (1996). Catalase Is Encoded by a Multigene Family in *Arabidopsis thaliana* (L.) Heynh. Plant Physiology *112*, 327–336.

Fu, Z.Q., Yan, S., Saleh, A., Wang, W., Ruble, J., Oka, N., Mohan, R., Spoel, S.H., Tada, Y., Zheng, N., and Dong, X. (2012). NPR3 and NPR4 are receptors for the immune signal salicylic acid in plants. Nature *486 (7402)*, 228–232.

Furukawa, A., Oikawa, S., Harada, K., Sugiyama, H., Hiraku, Y., Murata, M., Shimada, A., and Kawanishi, S. (2010). Oxidatively generated DNA damage induced by 3-amino-5-mercapto-1,2,4-triazole, a metabolite of carcinogenic amitrole. Mutation Research/Fundamental and Molecular Mechanisms of Mutagenesis *694*, 7–12.

Gadkari, P.V., and Balaraman, M. (2015). Catechins: Sources, extraction and encapsulation: A review. Food and Bioproducts Processing *93*, 122–138.

Gaffney, T., Friedrich, L., Vernooij, B., Negrotto, D., Nye, G., Uknes, S., Ward, E., Kessmann, H., and Ryals, J. (1993). Requirement of salicylic Acid for the induction of systemic acquired resistance. Science *261*, 754–756.

Gatz, C. (2013). From pioneers to team players: TGA transcription factors provide a molecular link between different stress pathways. Mol Plant Microbe Interact *26*, 151–159.

Gechev, T.S., Van Breusegem, F., Stone, J.M., Denev, I., and Laloi, C. (2006). Reactive oxygen species as signals that modulate plant stress responses and programmed cell death. Bioessays *28*, 1091–1101.

Gelhaye, E., Rouhier, N., Navrot, N., and Jacquot, J.P. (2005). The plant thioredoxin system. CMLS, Cell. Mol. Life Sci. *62*, 24–35.

Gelhaye, E., Rouhier, N., and Jacquot, J.-P. (2003). Evidence for a subgroup of thioredoxin hthat requires GSH/Grx for its reduction. FEBS Lett. *555*, 443–448.

Gilroy, S., Suzuki, N., Miller, G., Choi, W.-G., Toyota, M., Devireddy, A.R., and Mittler, R. (2014). A tidal wave of signals: calcium and ROS at the forefront of rapid systemic signaling. Trends in Plant Science *19*, 623–630.

Goretski, J., and Hollocher, T.C. (1988). Trapping of nitric oxide produced during denitrification by extracellular hemoglobin. J. Biol. Chem. *263*, 2316–2323.

Góth, L., Rass, P., and Páy, A. (2004). Catalase enzyme mutations and their association with

diseases. CNS Drugs *8*, 141–149.

Göhre, V., Spallek, T., Häweker, H., Mersmann, S., Mentzel, T., Boller, T., de Torres, M., Mansfield, J.W., and Robatzek, S. (2008). Plant pattern-recognition receptor FLS2 is directed for degradation by the bacterial ubiquitin ligase AvrPtoB. Curr. Biol. *18*, 1824–1832.

Graham, H.N. (1992). Green tea composition, consumption, and polyphenol chemistry. Prev Med *21*, 334–350.

Grant, J.J., and Loake, G.J. (2000). Role of reactive oxygen intermediates and cognate redox signaling in disease resistance. Plant Physiology *124*, 21–29.

Graziano, M., and Lamattina, L. (2005). Nitric oxide and iron in plants: an emerging and converging story. Trends in Plant Science *10*, 4–8.

Graziano, M., and Lamattina, L. (2007). Nitric oxide accumulation is required for molecular and physiological responses to iron deficiency in tomato roots. The Plant Journal *52*, 949–960.

Greenberg, J.T., Guo, A., Klessig, D.F., and Ausubel, F.M. (1994). Programmed cell death in plants: a pathogen-triggered response activated coordinately with multiple defense functions. Cell *77*, 551–563.

Grün, S., Lindermayr, C., Sell, S., and Durner, J. (2006). Nitric oxide and gene regulation in plants. Journal of Experimental Botany *57*, 507–516.

Guan, L.M., and Scandalios, J.G. (2002). Catalase gene expression in response to auxin-mediated developmental signals. Physiol Plant *114*, 288–295.

Guo, F.Q. (2003). Identification of a Plant Nitric Oxide Synthase Gene Involved in Hormonal Signaling. Science *302*, 100–103.

Guo, F.-Q., and Crawford, N.M. (2005). *Arabidopsis* nitric oxide synthase1 is targeted to mitochondria and protects against oxidative damage and dark-induced senescence. The Plant Cell *17*, 3436–3450.

Gupta, R., and Luan, S. (2003). Redox control of protein tyrosine phosphatases and mitogen-activated protein kinases in plants. Plant Physiology *132*, 1149–1152.

Halliwell, B. (2006). Reactive species and antioxidants. Redox biology is a fundamental theme of aerobic life. Plant Physiology *141*, 312–322.

Halliwell, B., and Gutteridge, J.M.C. (2015). Free Radicals in Biology and Medicine (Oxford University Press).

Hancock, J.T., Henson, D., Nyirenda, M., Desikan, R., Harrison, J., Lewis, M., Hughes, J., and Neill, S.J. (2005). Proteomic identification of glyceraldehyde 3-phosphate dehydrogenase as an inhibitory target of hydrogen peroxide in *Arabidopsis*. Plant Physiology and Biochemistry *43*, 828–835.

Hara, M.R., Agrawal, N., Kim, S.F., Cascio, M.B., Fujimuro, M., Ozeki, Y., Takahashi, M., Cheah, J.H., Tankou, S.K., Hester, L.D., et al. (2005). S-nitrosylated GAPDH initiates

apoptotic cell death by nuclear translocation following Siah1 binding. Nature Cell Biology *7*, 665–674.

Hara-Nishimura, I., Inoue, K., and Nishimura, M. (1991). A unique vacuolar processing enzyme responsible for conversion of several proprotein precursors into the mature forms. FEBS Lett. *294*, 89–93.

Hart, T.W. (1985). Some observations concerning the S-nitroso and S-phenylsulphonyl derivatives of L-cysteine and glutathione. Tetrahedron Letters *26*, 2013–2016.

Havir, E.A. (1992). The *in vivo* and *in vitro* Inhibition of Catalase from Leaves of Nicotiana sylvestris by 3-Amino-1,2,4-Triazole. Plant Physiology *99*, 533–537.

Heath, M.C. (2000). Hypersensitive response-related death. Plant Mol. Biol. *44*, 321–334.

Hedrich, R., Salvador-Recatalà, V., and Dreyer, I. (2016). Electrical Wiring and Long-Distance Plant Communication. Trends in Plant Science *21*, 376-387.

Hess, D.T., Matsumoto, A., Kim, S.-O., Marshall, H.E., and Stamler, J.S. (2005). Protein S-nitrosylation: purview and parameters. Nat Rev Mol Cell Biol *6*, 150–166.

Hilton, J.L., Kearney, P.C., and Ames, Bruce N. (1965). Mode of action of the herbicide, 3-amino-1,2,4-triazole(amitrole): Inhibition of an enzyme of histidine biosynthesis. Archives of Biochemistry and Biophysics *112*, 544-547 .

Hippeli, S., and Elstner, E.F. (1997). OH-Radical-Type Reactive Oxygen Species: A Short Review on the Mechanisms of OH-Radical-and Peroxynitrite Toxicity. Zeitschrift Für Naturforschung C *52*, 555–563.

Hirano, S.S., and Upper, C.D. (2000). Bacteria in the leaf ecosystem with emphasis on *Pseudomonas syringae*-a pathogen, ice nucleus, and epiphyte. Microbiol. Mol. Biol. Rev. *64*, 624–653.

Hoelder, S., Clarke, P.A., and Workman, P. (2012). Discovery of small molecule cancer drugs: Successes, challenges and opportunities. Molecular Oncology *6*, 155–176.

Homem, R.A. (2016). PhD thesis. Redox signalling and innate immunity: a role for protein S-nitrosylation in the immune response of *Drosophila melanogaster*. The University of Edinburgh. 1-166

Hong, J.K., Yun, B.W., Kang, J.G., Raja, M.U., Kwon, E., Sorhagen, K., Chu, C., Wang, Y., and Loake, G.J. (2008). Nitric oxide function and signalling in plant disease resistance. Journal of Experimental Botany *59*, 147–154.

Hu, X., Neill, S.J., Cai, W., and Tang, Z. (2003). NO-mediated hypersensitive responses of rice suspension cultures induced by incompatible elicitor. Chin. Sci. Bull. *48*, 358–363.

Hu, Y.-Q., Liu, S., Yuan, H.-M., Li, J., Yan, D.-W., Zhang, J.-F., and Lu, Y.-T. (2010). Functional comparison of catalase genes in the elimination of photorespiratory H2O2 using promoter- and 3′-untranslated region exchange experiments in the *Arabidopsis* cat2 photorespiratory mutant. Plant Cell Environ *33*, 1656–1670.

Hussain, A. (2013). PhD thesis. Role of tomato S-Nitrosoglutathione Reductase (GSNOR) in plant development and disease resistance. The University of Edinburgh. 1-192.

Hwang, I., Chen, H.-C., and Sheen, J. (2002). Two-component signal transduction pathways in *Arabidopsis*. Plant Physiology *129*, 500–515.

Inaba, J.I., Kim, B.M., Shimura, H., and Masuta, C. (2011). Virus-Induced Necrosis Is a Consequence of Direct Protein-Protein Interaction between a Viral RNA-Silencing Suppressor and a Host Catalase. Plant Physiology *156*, 2026–2036.

Jaffrey, S.R., and Snyder, S.H. (2001). The Biotin Switch Method for the Detection of S-Nitrosylated Proteins. Science STKE *86*, l1.

Jia, L., Bonaventura, C., Bonaventura, J., and Stamler, J.S. (1996). S-nitrosohaemoglobin: a dynamic activity of blood involved in vascular control. Nature *380*, 221–226.

Jones, J.D.G., and Dangl, J.L. (2006). The plant immune system. Nature *444*, 323–329.

Kaminaka, H., Näke, C., Epple, P., Dittgen, J., Schütze, K., Chaban, C., Ben F Holt, Merkle, T., Schäfer, E., Harter, K., et al. (2006). bZIP10-LSD1 antagonism modulates basal defense and cell death in *Arabidopsis* following infection. The EMBO Journal *25*, 4400–4411.

Kanchanawatee, K. (2013). PhD thesis. S-nitrosylation in immunity and fertility: a general mechanism conserved in plants and animals. The University of Edinburgh. 1-269.

Katagiri, F., Thilmony, R., and He, S.Y. (2002). The *Arabidopsis Thaliana-Pseudomonas Syringae* Interaction. The *Arabidopsis* Book *20*, 1, e0039

Kato, S., Ueno, T., Fukuzumi, S., and Watanabe, Y. (2004). Catalase Reaction by Myoglobin Mutants and Native Catalase MECHANISTIC INVESTIGATION BY KINETIC ISOTOPE EFFECT. J. Biol. Chem. *279*, 52376–52381.

Kidd, B.N., Kadoo, N.Y., Dombrecht, B., Tekeoglu, M., Gardiner, D.M., Thatcher, L.F., Aitken, E.A.B., Schenk, P.M., Manners, J.M., and Kazan, K. (2011). Auxin signaling and transport promote susceptibility to the root-infecting fungal pathogen Fusarium oxysporum in *Arabidopsis*. Mol Plant Microbe Interact *24*, 733–748.

Kliebenstein, D.J., Dietrich, R.A., Martin, A.C., Last, R.L., and Dangl, J.L. (2007). LSD1 Regulates Salicylic Acid Induction of Copper Zinc Superoxide Dismutase in *Arabidopsis* thaliana. Molecular plant-microbe interactions *12(11)*, 1022-1026

Klotz, L.O. (2002). Oxidant-Induced Signaling: Effects of Peroxynitrite and Singlet Oxygen. Biological Chemistry *383*, 443–456.

Kneeshaw, S., Gelineau, S., Tada, Y., Loake, G.J., and Spoel, S.H. (2014). Selective Protein Denitrosylation Activity of Thioredoxin-h5 Modulates Plant Immunity. Mol. Cell *56*, 153–162.

Kocsy, G., Tari, I., Vanková, R., ZECHMANN, B., Gulyás, Z., Poór, P., and Galiba, G. (2013). Redox control of plant growth and development. Plant Science *211*, 77–91.

Koechling, U.M., and Amit, Z. (1994). Effects of 3-amino-1,2,4-triazole on brain catalase in

the mediation of ethanol consumption in mice. Alcohol *11*, 235–239.

Kolbe, A., Oliver, S.N., Fernie, A.R., Stitt, M., van Dongen, J.T., and Geigenberger, P. (2006). Combined Transcript and Metabolite Profiling of *Arabidopsis* Leaves Reveals Fundamental Effects of the Thiol-Disulfide Status on Plant Metabolism. Plant Physiology *141*, 412–422.

Kombrink, E. (2012). Chemical and genetic exploration of jasmonate biosynthesis and signaling paths. Planta *236*, 1351–1366.

Koornneef, A., Leon-Reyes, A., Ritsema, T., Verhage, A., Otter, Den, F.C., Van Loon, L.C., and Pieterse, C.M.J. (2008). Kinetics of salicylate-mediated suppression of jasmonate signaling reveal a role for redox modulation. Plant Physiology *147*, 1358–1368.

Kovtun, Y., Chiu, W.L., Tena, G., and Sheen, J. (2000). Functional analysis of oxidative stress-activated mitogen-activated protein kinase cascade in plants. Proc. Natl. Acad. Sci. Usa. *97*, 2940–2945.

Kroemer, G., Galluzzi, L., Vandenabeele, P., Abrams, J., Alnemri, E.S., Baehrecke, E.H., Blagosklonny, M.V., El-Deiry, W.S., Golstein, P., Green, D.R., et al. (2008). Classification of cell death: recommendations of the Nomenclature Committee on Cell Death 2009. Cell Death Differ *16*, 3–11.

Kwon, E., Feechan, A., Yun, B.-W., Hwang, B.-H., Pallas, J.A., Kang, J.-G., and Loake, G.J. (2012). AtGSNOR1 function is required for multiple developmental programs in *Arabidopsis*. Planta *236*, 887–900.

Lamotte, O., Bertoldo, J.B., Besson-Bard, A., Rosnoblet, C., Aimé, S., Hichami, S., Terenzi, H., and Wendehenne, D. (2014). Protein S-nitrosylation: specificity and identification strategies in plants. Front Chem *2*, 114.

Lamotte, O., Bertoldo, J.B., Besson-Bard, A., Rosnoblet, C., Aimé, S., Hichami, S., Terenzi, H., and Wendehenne, D. (2015). Protein S-nitrosylation: specificity and identification strategies in plants. Front Chem *2*, 233.

Lee, U., Wie, C., Fernandez, B.O., Feelisch, M., and Vierling, E. (2008). Modulation of nitrosative stress by S-nitrosoglutathione reductase is critical for thermotolerance and plant growth in *Arabidopsis*. The Plant Cell *20*, 786–802.

Leon-Reyes, A., Spoel, S.H., De Lange, E.S., Abe, H., Kobayashi, M., Tsuda, S., Millenaar, F.F., Welschen, R.A.M., Ritsema, T., and Pieterse, C.M.J. (2009). Ethylene Modulates the Role of NONEXPRESSOR OF PATHOGENESIS-RELATED GENES1 in Cross Talk between Salicylate and Jasmonate Signaling. Plant Physiology *149*, 1797–1809.

Levine, A., Pennell, R.I., Alvarez, M.E., Palmer, R., and Lamb, C. (1996). Calcium-mediated apoptosis in a plant hypersensitive disease resistance response. Curr. Biol. *6*, 427–437.

Li, Y., Chen, L., Mu, J., and Zuo, J. (2013). LESION SIMULATING DISEASE1 interacts with catalases to regulate hypersensitive cell death in *Arabidopsis*. Plant Physiology *163*, 1059–1070.

Lindermayr, C. (2005). Proteomic Identification of S-Nitrosylated Proteins in *Arabidopsis*.

Plant Physiology *137*, 921–930.

Lindermayr, C., Saalbach, G., and Durner, J. (2005). Proteomic identification of S-nitrosylated proteins in *Arabidopsis*. Plant Physiology *137*, 921–930.

Liu, G., Greenshields, D.L., Sammynaiken, R., Hirji, R.N., Selvaraj, G., and Wei, Y. (2007). Targeted alterations in iron homeostasis underlie plant defense responses. J. Cell. Sci. *120*, 596–605.

Liu, H. (2005). Redox-Dependent Transcriptional Regulation. Circulation Research *97*, 967–974.

Liu, L., Hausladen, A., Zeng, M., Que, L., Heitman, J., and Stamler, J.S. (2001). A metabolic enzyme for S-nitrosothiol conserved from bacteria to humans. Nature *410*, 490–494.

Liu, L., Yan, Y., Zeng, M., Zhang, J., Hanes, M.A., Ahearn, G., McMahon, T.J., Dickfeld, T., Marshall, H.E., Que, L.G., et al. (2004a). Essential Roles of S-Nitrosothiols in Vascular Homeostasis and Endotoxic Shock. Cell *116*, 617–628.

Liu, L., Yan, Y., Zeng, M., Zhang, J., Hanes, M.A., Ahearn, G., McMahon, T.J., Dickfeld, T., Marshall, H.E., Que, L.G., et al. (2004b). Essential roles of S-nitrosothiols in vascular homeostasis and endotoxic shock. Cell *116*, 617–628.

Loew, O. (1900). A New Enzyme of General Occurrence in Organisms on JSTOR. Science.

Loreto, F., and Velikova, V. (2001). Isoprene Produced by Leaves Protects the Photosynthetic Apparatus against Ozone Damage, Quenches Ozone Products, and Reduces Lipid Peroxidation of Cellular Membranes. Plant Physiology *127*, 1781–1787.

Lucas, W.J., Groover, A., Lichtenberger, R., Furuta, K., Yadav, S.R., Helariutta, Y., He, X.Q., Fukuda, H., Kang, J., Brady, S.M., et al. (2013). The Plant Vascular System: Evolution, Development and Functions. Journal of Integrative Plant Biology *55*, 294–388.

Lukowitz, W., Gillmor, C.S., and Scheible, W.R. (2000). Positional cloning in *Arabidopsis*. Why it feels good to have a genome initiative working for you. Plant Physiology *123*, 795–805.

Luna, E., Bruce, T.J.A., Roberts, M.R., Flors, V., and Ton, J. (2012). Next-generation systemic acquired resistance. Plant Physiology *158*, 844–853.

Ma, Z., Marsolais, F., Bykova, N.V., and Igamberdiev, A.U. (2016). Nitric Oxide and Reactive Oxygen Species Mediate Metabolic Changes in Barley Seed Embryo during Germination. Front Plant Sci *7*, 138.

Mackey, D., Holt, B.F., Wiig, A., and Dangl, J.L. (2002). RIN4 interacts with *Pseudomonas syringae* type III effector molecules and is required for RPM1-mediated resistance in *Arabidopsis*. Cell *108*, 743–754.

Maffei, M., and Bossi, S. (2006). Electrophysiology and Plant Responses to Biotic Stress. In Plant Electrophysiology, (Berlin, Heidelberg: Springer Berlin Heidelberg), pp. 461–481.

Maffei, M.E., Mithöfer, A., and Boland, W. (2007). Insects feeding on plants: Rapid signals

and responses preceding the induction of phytochemical release. Phytochemistry *68*, 2946–2959.

Maldonado-Alconada, A.M., Echevarría-Zomeño, S., Lindermayr, C., Redondo-López, I., Durner, J., and Jorrín-Novo, J.V. (2011). Proteomic analysis of *Arabidopsis* protein S-nitrosylation in response to inoculation with *Pseudomonas syringae*. Acta Physiologiae Plantarum *33*, 1493–1514.

Malik, S.I., Hussain, A., Yun, B.-W., Spoel, S.H., and Loake, G.J. (2011). GSNOR-mediated de-nitrosylation in the plant defence response. Plant Sci. *181*, 540–544.

Manai, J., Gouia, H., and Corpas, F.J. (2014). Journal of Plant Physiology. Journal of Plant Physiology *171*, 1028–1035.

Manoj, V.M., and Aravindakumar, C.T. (2000). Hydroxyl radical induced decomposition of S-nitrosoglutathione. Chem. Commun. *23*. 2361–2362.

Margoliash, E., Novogrodsky, A., and Schejter, A. (1960). Irreversible reaction of 3-amino-1:2:4-triazole and related inhibitors with the protein of catalase. Biochemical Journal *74*, 339.

McGarvey, D.J., and Christoffersen, R.E. (1992). Characterization and kinetic parameters of ethylene-forming enzyme from avocado fruit. J. Biol. Chem. *267*, 5964–5967.

Meiser, J., Lingam, S., and Bauer, P. (2011). Posttranslational regulation of the iron deficiency basic helix-loop-helix transcription factor FIT is affected by iron and nitric oxide. Plant Physiology *157*, 2154–2166.

Meyer, Y., Reichheld, J.P., and Vignols, F. (2005). Thioredoxins in*Arabidopsis* and other plants. Photosynth Res *86*, 419–433.

Meyer, Y., Riondet, C., Constans, L., Abdelgawwad, M.R., Reichheld, J.P., and Vignols, F. (2006). Evolution of redoxin genes in the green lineage. Photosynth Res *89*, 179–192.

Mhamdi, A., Queval, G., Chaouch, S., Vanderauwera, S., Van Breusegem, F., and Noctor, G. (2010a). Catalase function in plants: a focus on *Arabidopsis* mutants as stress-mimic models. Journal of Experimental Botany *61*, 4197–4220.

Mhamdi, A., Mauve, C., Gouia, H., Saindrenan, P., Hodges, M., and Noctor, G. (2010b). Cytosolic NADP-dependent isocitrate dehydrogenase contributes to redox homeostasis and the regulation of pathogen responses in *Arabidopsis* leaves. Plant Cell Environ *33*, 1112–1123.

Mhamdi, A., Noctor, G., and Baker, A. (2012). Plant catalases: Peroxisomal redox guardians. Archives of Biochemistry and Biophysics *525*, 181–194.

Miller, E.W., Dickinson, B.C., and Chang, C.J. (2010). Aquaporin-3 mediates hydrogen peroxide uptake to regulate downstream intracellular signaling. Proc. Natl. Acad. Sci. Usa. *107*, 15681–15686.

Miller, G., Schlauch, K., Tam, R., Cortes, D., Torres, M.A., Shulaev, V., Dangl, J.L., and Mittler, R. (2009). The Plant NADPH Oxidase RBOHD Mediates Rapid Systemic Signaling in Response to Diverse Stimuli. Sci. Signal. *2(84)*, ra45–ra45.

Milthorpe, F.L., and Moorby, J. (1969). Vascular transport and its significance in plant growth. Annual Review of Plant Physiology *20*, 117-138..

Mittler, R., Vanderauwera, S., Suzuki, N., Miller, G., Tognetti, V.B., Vandepoele, K., Gollery, M., Shulaev, V., and Van Breusegem, F. (2011). ROS signaling: the new wave? Trends in Plant Science *16*, 300–309.

Modolo, L. V., Augusto, O., Almeida, I. M. G., Magalhaes, J. R. and Salgado, I. (2005). Nitrite as the major source of nitric oxide production by Arabidopsis thaliana in response to Pseudomonas syringae. FEBS Lett *579*, 3814–3820.

Monshausen, G.B., Bibikova, T.N., Messerli, M.A., Shi, C., and Gilroy, S. (2007). Oscillations in extracellular pH and reactive oxygen species modulate tip growth of *Arabidopsis* root hairs. Proc. Natl. Acad. Sci. Usa. *104*, 20996–21001.

Moon, H., Lee, B., Choi, G., Shin, D., Prasad, D.T., Lee, O., Kwak, S.-S., Kim, D.H., Nam, J., Bahk, J., et al. (2003). NDP kinase 2 interacts with two oxidative stress-activated MAPKs to regulate cellular redox state and enhances multiple stress tolerance in transgenic plants. Proc. Natl. Acad. Sci. Usa. *100*, 358–363.

Moore, J.W., Loake, G.J., and Spoel, S.H. (2011). Transcription Dynamics in Plant Immunity. The Plant Cell Online *23*, 2809–2820.

Mou, Z., Fan, W., and Dong, X. (2003). Inducers of Plant Systemic Acquired Resistance Regulate NPR1 Function through Redox Changes. Cell *113*, 935–944.

Mukherjee, I., Campbell, N.H., Ash, J.S., and Connolly, E.L. (2006). Expression profiling of the *Arabidopsis* ferric chelate reductase (FRO) gene family reveals differential regulation by iron and copper. Planta *223*, 1178–1190.

Mukherjee, M., Larrimore, K.E., Ahmed, N.J., Bedick, T.S., Barghouthi, N.T., Traw, M.B., and Barth, C. (2010). Ascorbic acid deficiency in *Arabidopsis* induces constitutive priming that is dependent on hydrogen peroxide, salicylic acid, and the NPR1 gene. Mol Plant Microbe Interact *23*, 340–351.

Mur, L.A.J., Carver, T.L.W., and Prats, E. (2006a). NO way to live; the various roles of nitric oxide in plant-pathogen interactions. Journal of Experimental Botany *57*, 489–505.

Mur, L.A.J., Kenton, P., Atzorn, R., Miersch, O., and Wasternack, C. (2006b). The outcomes of concentration-specific interactions between salicylate and jasmonate signaling include synergy, antagonism, and oxidative stress leading to cell death. Plant Physiology *140*, 249–262.

Mur, L.A.J., Kenton, P., Lloyd, A.J., Ougham, H., and Prats, E. (2008). The hypersensitive response; the centenary is upon us but how much do we know? Journal of Experimental Botany *59*, 501–520.

Müller, K., Linkies, A., Vreeburg, R.A.M., Fry, S.C., Krieger-Liszkay, A., and Leubner-Metzger, G. (2009). In vivo cell wall loosening by hydroxyl radicals during cress seed germination and elongation growth. Plant Physiology *150*, 1855–1865.

Müller-Moulé, P., Havaux, M., and Niyogi, K.K. (2003). Zeaxanthin Deficiency Enhances

the High Light Sensitivity of an Ascorbate-Deficient Mutant of *Arabidopsis*. Plant Physiology *133*, 748–760.

Nakamura, T., Tu, S., Akhtar, M.W., Sunico, C.R., Okamoto, S.-I., and Lipton, S.A. (2013). Aberrant Protein S-Nitrosylation in Neurodegenerative Diseases. Neuron *78*, 596–614.

Nathan, C., and Xie, Q. (1994). Nitric oxide synthases: roles, tolls, and controls. Cell *78(6)*, 915-918.

Neill, S. (2002). Hydrogen peroxide signalling. Current Opinion in Plant Biology *5*, 388–395.

Neill, S.J., Desikan, R., Clarke, A., Hurst, R.D., and Hancock, J.T. (2002). Hydrogen peroxide and nitric oxide as signalling molecules in plants. Journal of Experimental Botany *53*, 1237–1247.

Ninnemann, H., and Maier, J. (1996). Indications for the Occurrence of Nitric Oxide Synthases in Fungi and Plants and the Involvement in Photoconidiation of Neurospora crassa. Photochemistry and Photobiology *64*, 393–398.

Noctor, G., and Foyer, C.H. (1998). ASCORBATE AND GLUTATHIONE: Keeping Active Oxygen Under Control. Annu. Rev. Plant Physiol. Plant Mol. Biol. *49*, 249–279.

Nomura, K., Debroy, S., Lee, Y.H., Pumplin, N., Jones, J., and He, S.Y. (2006). A bacterial virulence protein suppresses host innate immunity to cause plant disease. Science *313*, 220–223.

Nordborg, M., and Weigel, D. (2008). Next-generation genetics in plants. Nature *456*, 720–723.

Ogata, M. (1991). Acatalasemia. Human genetics *86(4)*, 331-340.

Ogawa, K., Tasaka, Y., Mino, M., Tanaka, Y., and Iwabuchi, M. (2001). Association of glutathione with flowering in *Arabidopsis* thaliana. Plant and Cell Physiology *42*, 524–530.

Orendi, G., Zimmermann, P., Baar, C., and Zentgraf, U. (2001). Loss of stress-induced expression of catalase3 during leaf senescence in *Arabidopsis* thaliana is restricted to oxidative stress. Plant Sci. *161*, 301–314.

Ortega-Galisteo, A.P., Rodriguez-Serrano, M., Pazmino, D.M., Gupta, D.K., Sandalio, L.M., and Romero-Puertas, M.C. (2012). S-Nitrosylated proteins in pea (Pisum sativum L.) leaf peroxisomes: changes under abiotic stress. Journal of Experimental Botany *63*, 2089–2103.

Pal, S., Dey, S.K., and Saha, C. (2014). Inhibition of catalase by tea catechins in free and cellular state: a biophysical approach. PLoS ONE *9*, e102460.

Palmer, R.M.J., Hickery, M.S., Charles, I.G., Moncada, S., and Bayliss, M.T. (1993). Induction of Nitric Oxide Synthase in Human Chondrocytes. Biochemical and Biophysical Research Communications *193*, 398–405.

Panstruga, R., Parker, J.E., and Schulze-Lefert, P. (2009). SnapShot: Plant Immune Response Pathways. Cell *136*, 978.e1–978.e3.

Parisy, V., Poinssot, B., Owsianowski, L., Buchala, A., Glazebrook, J., and Mauch, F. (2006). Identification of PAD2 as a γ-glutamylcysteine synthetase highlights the importance of glutathione in disease resistance of *Arabidopsis*. The Plant Journal *49*, 159–172.

Pauwels, L., Barbero, G.F., Geerinck, J., Tilleman, S., Grunewald, W., Pérez, A.C., Chico, J.M., Bossche, R.V., Sewell, J., Gil, E., et al. (2010). NINJA connects the co-repressor TOPLESS to jasmonate signalling. Nature *464*, 788–791.

Petersen, M., Brodersen, P., Naested, H., Andreasson, E., Lindhart, U., Johansen, B., Nielsen, H.B., Lacy, M., Austin, M.J., Parker, J.E., et al. (2000). *Arabidopsis* MAP Kinase 4 Negatively Regulates Systemic Acquired Resistance. Cell *103*, 1111–1120.

Pierre, J.L., and Fontecave, M. (1999). Iron and activated oxygen species in biology: The basic chemistry. Biometals *12*, 195–199.

Pieterse, C.M.J., Van der Does, D., Zamioudis, C., Leon-Reyes, A., and Van Wees, S.C.M. (2012). Hormonal Modulation of Plant Immunity. Http://Dx.Doi.org/10.1146/Annurev-Cellbio-092910-154055 *28*, 489–521.

Pieterse, C.M., and Van Loon, L.C. (2004). NPR1: the spider in the web of induced resistance signaling pathways. Current Opinion in Plant Biology *7*, 456–464.

Planchet, E., Jagadis Gupta, K., Sonoda, M., and Kaiser, W.M. (2005). Nitric oxide emission from tobacco leaves and cell suspensions: rate limiting factors and evidence for the involvement of mitochondrial electron transport. The Plant Journal *41*, 732–743.

Putnam, C.D., Arvai, A.S., Bourne, Y., and Tainer, J.A. (2000). Active and inhibited human catalase structures: ligand and NADPH binding and catalytic mechanism. Journal of Molecular Biology *296*, 295–309.

Queval, G., and Noctor, G. (2007). A plate reader method for the measurement of NAD, NADP, glutathione, and ascorbate in tissue extracts: Application to redox profiling during *Arabidopsis* rosette development. Analytical Biochemistry *363*, 58–69.

Regelsberger, G., Jakopitsch, C., Plasser, L., Schwaiger, H., Furtmüller, P.G., Peschek, G.A., Zamocky, M., and Obinger, C. (2002). Occurrence and biochemistry of hydroperoxidases in oxygenic phototrophic prokaryotes (cyanobacteria). Plant Physiology and Biochemistry *40*, 479–490.

Regulski, M., and Tully, T. (1995). Molecular and biochemical characterization of dNOS: a *Drosophila* Ca2+/calmodulin-dependent nitric oxide synthase. Proc. Natl. Acad. Sci. Usa. *92*, 9072–9076.

Reichheld, J.P., Mestres-Ortega, D., Laloi, C., and Meyer, Y. (2002). The multigenic family of thioredoxin h in *Arabidopsis thaliana*: specific expression and stress response. Plant Physiology and Biochemistry *40*, 685–690.

Renew, S., Heyno, E., Schopfer, P., and Liszkay, A. (2005). Sensitive detection and localization of hydroxyl radical production in cucumber roots and *Arabidopsis* seedlings by spin trapping electron paramagnetic resonance spectroscopy. The Plant Journal *44*, 342–347.

Robinson, N.J., Procter, C.M., Connolly, E.L., and Lou Guerinot, M. (1999). A ferric-chelate

reductase for iron uptake from soils. Nature *397*, 694–697.

Robson, C.A., and Vanlerberghe, G.C. (2002). Transgenic Plant Cells Lacking Mitochondrial Alternative Oxidase Have Increased Susceptibility to Mitochondria-Dependent and -Independent Pathways of Programmed Cell Death. Plant Physiology *129*, 1908–1920.

Rojo, E., Martín, R., Carter, C., Zouhar, J., Pan, S., Plotnikova, J., Jin, H., Paneque, M., Sánchez-Serrano, J.J., Baker, B., et al. (2004). VPEγ Exhibits a Caspase-like Activity that Contributes to Defense against Pathogens. Current Biology *14*, 1897–1906.

Romero-Puertas, M.C., Laxa, M., Mattè, A., Zaninotto, F., Finkemeier, I., Jones, A.M.E., Perazzolli, M., Vandelle, E., Dietz, K.-J., and Delledonne, M. (2007). S-nitrosylation of peroxiredoxin II E promotes peroxynitrite-mediated tyrosine nitration. The Plant Cell *19*, 4120–4130.

Rosso, M.G., Li, Y., Strizhov, N., Reiss, B., Dekker, K., and Weisshaar, B. (2003). An *Arabidopsis thaliana* T-DNA mutagenized population (GABI-Kat) for flanking sequence tag-based reverse genetics. Plant Mol. Biol. *53*, 247–259.

RStudio: Integrated Development Environment for R (Boston, MA).

Santner, A., and Estelle, M. (2010). The ubiquitin-proteasome system regulates plant hormone signaling. The Plant Journal *61*, 1029–1040.

Santos, Dos, C.V., and Rey, P. (2006). Plant thioredoxins are key actors in the oxidative stress response. Trends in plant science *11(7)*, 329-334.

Schafer, F.Q., and Buettner, G.R. (2001). Redox environment of the cell as viewed through the redox state of the glutathione disulfide/glutathione couple. Free Radical Biology and Medicine *30*, 1191–1212.

Schindelin, J., Arganda-Carreras, I., Frise, E., Kaynig, V., Longair, M., Pietzsch, T., Preibisch, S., Rueden, C., Saalfeld, S., Schmid, B., et al. (2012). Fiji: an open-source platform for biological-image analysis. Nat Meth *9*, 676–682.

Seo, H.S., Song, J.T., Cheong, J.J., Lee, Y.H., Lee, Y.W., Hwang, I., Lee, J.S., and Choi, Y.D. (2001). Jasmonic acid carboxyl methyltransferase: a key enzyme for jasmonate-regulated plant responses. Proc. Natl. Acad. Sci. Usa. *98*, 4788–4793.

Seyfferth, C., and Tsuda, K. (2014). Salicylic acid signal transduction: the initiation of biosynthesis, perception and transcriptional reprogramming. Front Plant Sci *5*, 697.

Shi, Y.-F., Wang, D.-L., Wang, C., Culler, A.H., Kreiser, M.A., Suresh, J., Cohen, J.D., Pan, J., Baker, B., and Liu, J.-Z. (2015). Loss of GSNOR1 Function Leads to Compromised Auxin Signaling and Polar Auxin Transport. Molecular Plant *8*, 1350–1365.

Shi, Z.-Q., Sunico, C.R., McKercher, S.R., Cui, J., Feng, G.-S., Nakamura, T., and Lipton, S.A. (2013). S-nitrosylated SHP-2 contributes to NMDA receptor-mediated excitotoxicity in acute ischemic stroke. Proc. Natl. Acad. Sci. Usa. *110*, 3137–3142.

Sliwoski, G., Kothiwale, S., Meiler, J., and Lowe, E.W. (2014). Computational methods in drug discovery Pharmacological reviews *66(1)*, 334-395.

Smirnoff, N. (2000). Ascorbic acid: metabolism and functions of a multi-facetted molecule. Current Opinion in Plant Biology *3*, 229–235.

Smith, B.C., and Marletta, M.A. (2012). Mechanisms of S-nitrosothiol formation and selectivity in nitric oxide signaling. Current Opinion in Chemical Biology *16*, 498–506.

Sorhagen, K. (2011). PhD thesis. Unravelling the roles of S-nitrosothiols in plant biology. The University of Edinburgh.

Spadaro, D., Yun, B.-W., Spoel, S.H., Chu, C., Wang, Y.-Q., and Loake, G.J. (2010). The redox switch: dynamic regulation of protein function by cysteine modifications. Physiol Plant *138*, 360–371.

Spoel, S.H., and van OoijenGerben (2014). Circadian Redox Signaling in Plant Immunity and Abiotic Stress. Antioxidants & Redox Signaling *20*, 3024–3039.

Spoel, S.H., and Loake, G.J. (2011). Redox-based protein modifications: the missing link in plant immune signalling. Current Opinion in Plant Biology *14*, 358–364.

Stamler, J.S., Lamas, S., and Fang, F.C. (2001). Nitrosylation. the prototypic redox-based signaling mechanism. Cell *106*, 675–683.

Stamler, J.S., Singel, D.J., and Loscalzo, J. (1992). Biochemistry of nitric oxide and its redox-activated forms. Science *258*, 1898–1902.

Steffen-Heins, A., and Steffens, B. (2015). EPR spectroscopy and its use in planta—a promising technique to disentangle the origin of specific ROS. Front. Environ. Sci. *3*, 5139.

Stone, J.R., and Yang, S. (2006). Hydrogen peroxide: a signaling messenger. Antioxidants & Redox Signaling *8*, 243–270.

Stookey, L.L. (1970). Ferrozine---a new spectrophotometric reagent for iron. Anal. Chem. *42*, 779–781.

Suzuki, N., KOUSSEVITZKY, S., Mittler, R., and Miller, G. (2012). ROS and redox signalling in the response of plants to abiotic stress. Plant Cell Environ *35*, 259–270.

Tada, Y., Spoel, S.H., Pajerowska-Mukhtar, K., Mou, Z., Song, J., Wang, C., Zuo, J., and Dong, X. (2008). Plant immunity requires conformational changes [corrected] of NPR1 via S-nitrosylation and thioredoxins. Science *321*, 952–956.

Takeda, S., Gapper, C., Kaya, H., Bell, E., Kuchitsu, K., and Dolan, L. (2008). Local positive feedback regulation determines cell shape in root hair cells. Science *319*, 1241–1244.

Tang, C.-H., Seeley, E.J., Huang, X., Wolters, P.J., and Liu, L. (2013). Increased susceptibility to Klebsiella pneumonia and mortality in GSNOR-deficient mice. Biochemical and Biophysical Research Communications *442*, 122–126.

Tarvin, M., McCord, B., Mount, K., and Miller, M.L. (2011). Analysis of hydrogen peroxide field samples by HPLC/FD and HPLC/ED in DC mode. Forensic Sci. Int. *209*, 166–172.

Taylor, A.T.S. (2005). Screening a library of household substances for inhibitors of

phosphatases: An introduction to high-throughput screening. Biochem Mol Biol Educ *33*, 16–21.

Terrile, M.C., París, R., Calderón-Villalobos, L.I.A., Iglesias, M.J., Lamattina, L., Estelle, M., and Casalongué, C.A. (2012). Nitric oxide influences auxin signaling through S-nitrosylation of the *Arabidopsis* TRANSPORT INHIBITOR RESPONSE 1 auxin receptor. The Plant Journal *70*, 492–500.

Ton, J., Flors, V., and Mauch-Mani, B. (2009). The multifaceted role of ABA in disease resistance. Trends in Plant Science *14*, 310–317.

Torres, M.A., and Dangl, J.L. (2005). Functions of the respiratory burst oxidase in biotic interactions, abiotic stress and development. Current Opinion in Plant Biology *8*, 397–403.

Torres, M.A., Dangl, J.L., and Jones, J.D. (2002). *Arabidopsis* gp91phox homologues AtrbohD and AtrbohF are required for accumulation of reactive oxygen intermediates in the plant defense response. Proc. Natl. Acad. Sci. Usa. *99*, 517–522.

Torres, M.A., Jones, J.D.G., and Dangl, J.L. (2005). Pathogen-induced, NADPH oxidase–derived reactive oxygen intermediates suppress spread of cell death in *Arabidopsis* thaliana. Nat Genet *37*, 1130–1134.

Trevisanato, S.I., and Kim, Y.I. (2000). Tea and Health. Nutrition Reviews *58*, 1–10.

Truman, W., Zabala, M.T., and Grant, M. (2006). Type III effectors orchestrate a complex interplay between transcriptional networks to modify basal defence responses during pathogenesis and resistance. The Plant Journal *46*, 14–33.

van Doorn, W.G., Beers, E.P., Dangl, J.L., Franklin-Tong, V.E., Gallois, P., Hara-Nishimura, I., Jones, A.M., Kawai-Yamada, M., Lam, E., Mundy, J., et al. (2011). Morphological classification of plant cell deaths. Cell Death Differ *18*, 1241–1246.

Van Loon, L.C., and Van Strien, E.A. (1999). The families of pathogenesis-related proteins, their activities, and comparative analysis of PR-1 type proteins. Physiological and molecular plant pathology *55(2)*, 85-97.

Vandenbroucke, K., Robbens, S., Vandepoele, K., Inzé, D., Van de Peer, Y., and Van Breusegem, F. (2008). Hydrogen Peroxide–Induced Gene Expression across Kingdoms: A Comparative Analysis. Mol Biol Evol *25*, 507–516.

Vanderauwera, S., Zimmermann, P., Rombauts, S., Vandenabeele, S., Langebartels, C., Gruissem, W., Inzé, D., and Van Breusegem, F. (2005). Genome-wide analysis of hydrogen peroxide-regulated gene expression in *Arabidopsis* reveals a high light-induced transcriptional cluster involved in anthocyanin biosynthesis. Plant Physiology *139*, 806–821.

Vercammen, D., van de Cotte, B., De Jaeger, G., Eeckhout, D., Casteels, P., Vandepoele, K., Vandenberghe, I., Van Beeumen, J., Inzé, D., and Van Breusegem, F. (2004). Type II metacaspases Atmc4 and Atmc9 of *Arabidopsis* thaliana cleave substrates after arginine and lysine. J. Biol. Chem. *279*, 45329–45336.

Verslues, P.E., Batelli, G., Grillo, S., Agius, F., Kim, Y.S., Zhu, J., Agarwal, M., Katiyar-Agarwal, S., and Zhu, J.K. (2007). Interaction of SOS2 with Nucleoside Diphosphate Kinase

2 and Catalases Reveals a Point of Connection between Salt Stress and H2O2 Signaling in *Arabidopsis* thaliana. Molecular and Cellular Biology *27*, 7771–7780.

Vlot, A.C., Dempsey, D.A., and Klessig, D.F. (2009). Salicylic Acid, a Multifaceted Hormone to Combat Disease. Annual review of phytopathology *47*, 177-206.

Wan, D., Li, R., Zou, B., Zhang, X., Cong, J., Wang, R., Xia, Y., and Li, G. (2012). Calmodulin-binding protein CBP60g is a positive regulator of both disease resistance and drought tolerance in *Arabidopsis*. Plant Cell Rep *31*, 1269–1281.

Wang, B.L., Tang, X.Y., Cheng, L.Y., Zhang, A.Z., Zhang, W.H., Zhang, F.S., Liu, J.Q., Cao, Y., Allan, D.L., Vance, C.P., et al. (2010). Nitric oxide is involved in phosphorus deficiency-induced cluster-root development and citrate exudation in white lupin. New Phytologist *187*, 1112–1123.

Wasternack, C., and Hause, B. (2013). Jasmonates: biosynthesis, perception, signal transduction and action in plant stress response, growth and development. An update to the 2007 review in Annals of Botany. Ann. Bot. *111*, 1021–1058.

Wasternack, C., and Parthier, B. (1997). Jasmonate-signalled plant gene expression. Trends in Plant Science *2*, 302–307.

Wheeler, G.L., Jones, M.A., and Smirnoff, N. (1998). The biosynthetic pathway of vitamin C in higher plants. Nature *393*, 365–369.

Willekens, H., Chamnongpol, S., Davey, M., Schraudner, M., Langebartels, C., Van Montagu, M., Inzé, D., and Van Camp, W. (1997). Catalase is a sink for H2O2 and is indispensable for stress defence in C3 plants. The EMBO Journal *16*, 4806–4816.

Yamasaki, H. and Sakihama, Y. (2000). Simultaneous production of nitric oxide and peroxynitrite by plant nitrate reductase: *in vitro* evidence for the NR-dependent formation of active nitrogen species. FEBS Lett *468*, 89–92.

Yang, H., Mu, J., Chen, L., Feng, J., Hu, J., Li, L., Zhou, J.-M., and Zuo, J. (2015). S-nitrosylation positively regulates ascorbate peroxidase activity during plant stress responses. Plant Physiology *167*, 1604–1615.

Yang, T., and Poovaiah, B.W. (2002). Hydrogen peroxide homeostasis: activation of plant catalase by calcium/calmodulin. Proc. Natl. Acad. Sci. Usa. *99*, 4097–4102.

Yao, D., Gu, Z., Nakamura, T., Shi, Z.-Q., Ma, Y., Gaston, B., Palmer, L.A., Rockenstein, E.M., Zhang, Z., Masliah, E., et al. (2004). Nitrosative stress linked to sporadic Parkinson's disease: S-nitrosylation of parkin regulates its E3 ubiquitin ligase activity. Proc. Natl. Acad. Sci. Usa. *101*, 10810–10814.

Yi, Y., and Guerinot, M.L. (1996). Genetic evidence that induction of root Fe(III) chelate reductase activity is necessary for iron uptake under iron deficiency. Plant J. *10*, 835–844.

Yu, M., Lamattina, L., Spoel, S.H., and Loake, G.J. (2014). Nitric oxide function in plant biology: a redox cue in deconvolution. New Phytologist *202*, 1142–1156.

Yu, M., Yun, B.-W., Spoel, S.H., and Loake, G.J. (2012). A sleigh ride through the SNO:

regulation of plant immune function by protein S-nitrosylation. Current Opinion in Plant Biology *15*, 1–7.

Yun, B.-W., Feechan, A., Yin, M., Saidi, N.B.B., Le Bihan, T., Yu, M., Moore, J.W., Kang, J.-G., Kwon, E., Spoel, S.H., et al. (2011). S-nitrosylation of NADPH oxidase regulates cell death in plant immunity. Nature *478*, 264–267.

Zaffagnini, M., De Mia, M., Morisse, S., Di Giacinto, N., Marchand, C.H., Maes, A., Lemaire, S.D., and Trost, P. (2016). Protein S-nitrosylation in photosynthetic organisms: A comprehensive overview with future perspectives. Biochimica Et Biophysica Acta (BBA) - Proteins and Proteomics *1864*, 952–966.

Zaffagnini, M., Morisse, S., Bedhomme, M., Marchand, C.H., Festa, M., Rouhier, N., Lemaire, S.D., and Trost, P. (2013). Mechanisms of nitrosylation and denitrosylation of cytoplasmic glyceraldehyde-3-phosphate dehydrogenase from *Arabidopsis* thaliana. J. Biol. Chem. *288*, 22777–22789.

Zago, E., Morsa, S., Dat, J.F., Alard, P., Ferrarini, A., Inzé, D., Delledonne, M., and Van Breusegem, F. (2006). Nitric oxide- and hydrogen peroxide-responsive gene regulation during cell death induction in tobacco. Plant Physiology *141*, 404–411.

Zamocky, M., Furtmüller, P.G., and Obinger, C. (2008). Evolution of Catalases from Bacteria to Humans. Antioxidants & redox signaling *10(9)*, 1527-1548.

Zaninotto, F., La Camera, S., Polverari, A., and Delledonne, M. (2006). Cross talk between reactive nitrogen and oxygen species during the hypersensitive disease resistance response. Plant Physiology *141*, 379–383.

Zaveri, N.T. (2006). Green tea and its polyphenolic catechins: medicinal uses in cancer and noncancer applications. Life Sciences *78*, 2073–2080.

Zeidler, D., Zähringer, U., Gerber, I., Dubery, I., Hartung, T., Bors, W., Hutzler, P., and Durner, J. (2004). Innate immunity in *Arabidopsis* thaliana: lipopolysaccharides activate nitric oxide synthase (NOS) and induce defense genes. Proc. Natl. Acad. Sci. Usa. *101*, 15811–15816.

Zhang, S., and Klessig, D.F. (2001). MAPK cascades in plant defense signaling. Trends in Plant Science *6*, 520–527.

Zheng, M., Aslund, F., and Storz, G. (1998). Activation of the OxyR transcription factor by reversible disulfide bond formation. Science *279*, 1718–1721.

Zhong, H.H., and McClung, C.R. (1996). The circadian clock gates expression of two *Arabidopsis* catalase genes to distinct and opposite circadian phases. Molec. Gen. Genet. *251*, 196–203.

Zimmermann, P., Heinlein, C., Orendi, G., and Zentgraf, U. (2006). Senescence-specific regulation of catalases in *Arabidopsis thaliana* (L.) Heynh. Plant Cell Environ *29*, 1049–1060.

Zipfel, C., Robatzek, S., Navarro, L., Oakeley, E.J., Jones, J.D.G., Felix, G., and Boller, T. (2004). Bacterial disease resistance in *Arabidopsis* through flagellin perception. Nature *428*,

764–767.

Zou, J.-J., Li, X.-D., Ratnasekera, D., Wang, C., Liu, W.-X., Song, L.-F., Zhang, W.-Z., and Wu, W.-H. (2015). *Arabidopsis* CALCIUM-DEPENDENT PROTEIN KINASE8 and CATALASE3 Function in Abscisic Acid-Mediated Signaling and H 2O 2Homeostasis in Stomatal Guard Cells under Drought Stress. The Plant Cell *27*, 1445–1460.